January 2015

Manganese Toxicity: Accumulation in Bone, Effect on Brain Neurochemistry, and Impact on Adult Neurogenesis

Stefanie O'Neal
Purdue University

Graduate School Form 30
Updated 1/15/2015

PURDUE UNIVERSITY
GRADUATE SCHOOL
Thesis/Dissertation Acceptance

This is to certify that the thesis/dissertation prepared

By Stefanie L O'Neal

Entitled

MANGANESE TOXICITY: ACCUMULATION IN BONE, EFFECT ON BRAIN NEUROCHEMISTRY, AND IMAPCT ON ADULT NEUROGENESIS

For the degree of Doctor of Philosophy

Is approved by the final examining committee:

Wei Zheng
Chair

Jason Cannon

Ulrike Dydak

Yansheng Du

To the best of my knowledge and as understood by the student in the Thesis/Dissertation Agreement, Publication Delay, and Certification Disclaimer (Graduate School Form 32), this thesis/dissertation adheres to the provisions of Purdue University's "Policy of Integrity in Research" and the use of copyright material.

Approved by Major Professor(s): Wei Zheng

Approved by: Wei Zheng 9/30/2015

Head of the Departmental Graduate Program Date

MANGANESE TOXICITY: ACCUMULATION IN BONE, EFFECT ON BRAIN NEUROCHEMISTRY, AND IMPACT ON ADULT NEUROGENESIS

A Dissertation

Submitted to the Faculty

of

Purdue University

by

Stefanie L O'Neal

In Partial Fulfillment of the

Requirements for the Degree

of

Doctor of Philosophy

December 2015

Purdue University

West Lafayette, Indiana

This dissertation, and the effort leading to its completion, is dedicated to my husband, for taking this journey with me, and supporting me always.

ACKNOWLEDGEMENTS

This dissertation would not have been possible without the help of many people who contributed their time and effort to my education, progress as a scientist, and professional development. I would like to express my sincere gratitude and appreciation to my advisor, Dr. Wei Zheng, for who pushed me, but gave me exceptional freedom. I am also grateful to my graduate committee members for their support and encouragement. Dr. Jason Cannon, who never discouraged my ideas but helped me find ways to make them successful, thank you. Dr. Ulrike Dydak, who always told me to do what I thought was right and offered encouragement at every step, thank you. Dr. Yansheng Du, whose valuable advice and suggestions were always available, thank you. Thank you also to my lab mates, Dr. Lan Hong, Dr. Sherleen Fu, and Dr. Christopher Bates for getting hands-on and teaching me the skills necessary to complete my work. Finally, thank you to Sara Wirbisky and Sena Agim for being my local support system and for your friendship.

TABLE OF CONTENTS

Page

Page

Page

Page

LIST OF TABLES

LIST OF FIGURES

Figure Page

LIST OF ABBREVIATIONS

5-HIAA, 5-hydroxyphenylalanine

5-HT, 5-hydroxytryptamine (serotonin)

AAS, atomic absorption spectroscopy

ASC, astrocytic stem cell

BBB, blood-brain barrier

CSF, cerebrospinal fluid

CTR1, copper transporter-1

Cu, copper

DA, dopamine

DOPAC, 3,4-dihydroxyphenylacetic acid

DMT1, divalent metal transporter-1

EDTA, ethylenediaminetetraacetic acid

Fe, iron

GABA, gamma aminobutyric acid

Glu, glutamate

Hippocampus, HP

HPLC, high performance liquid chromatography

HVA, homovanillic acid

IHC, immunohistochemistry

IN, intranasal instillation

MMT, methylcyclopentadienyl manganese tricarbonyl

Mn, manganese

MnBn, manganese concentrations in bone

MRI, magnetic resonance imaging

MRS, magnetic resonance spectroscopy

NAA, neutron activated analysis

NE, norepinephrine

OB, olfactory bulb

PAS, para-aminosalicylic acid

PD, Parkinson's disease

PI, pallidal index

RMS, rostral migratory stream

SGZ, subgranular zone

SN, substantia nigra

STR, striatum

SVZ, subventricular zone

Tf, transferrin

TfR, transferrin receptor

TH, tyrosine hydroxylase

T_{ss}, steady state concentration

$t_{1/2}$, half life

ABSTRACT

O'Neal, Stefanie L. Ph.D., Purdue University, December 2015. Manganese Toxicity: Accumulation in Bone, Effect on Neurochemistry, Impact on Adult Neurogenesis. Major Professor: Wei Zheng.

Manganese (Mn) exposure is a growing public health concern as new evidence continues to show that high level exposure to this essential metal is toxic. Chiefly toxic to the central nervous system, it produces signs and symptoms resembling, but not identical to idiopathic Parkinson's disease. The hypothesis tested in this dissertation is that Mn accumulation in body tissues produces subclinical changes in the central nervous system altering neuronal repair mechanisms and leading to neurodegenerative damage. The studies in this dissertation evaluated the extent of these changes in the central nervous system. Changes in the toxicokinetic properties of Mn in bone affecting the parameters of accumulation, distribution, and elimination were also identified. Importantly, the half-life of Mn in bone was estimated to be approximately 8.6 years in humans, a finding which will be essential in developing a biomonitoring system for Mn exposure. Significant accumulation of Mn in brain and body tissues was observed along with significant metal dyshomeostasis following Mn exposure. Several brain regions had altered

neurochemistry, and as a consequence, impaired motor function was observed. The subventricular zone (SVZ), one of two neurogenic niches in the adult brain, had the largest magnitude of change. Therefore, effects of Mn exposure on cell proliferation and differentiation in this region were investigated further. The processes involved in adult neurogenesis were significantly altered following Mn exposure, particularly with regard to cell proliferation. The full extent of the consequences resulting from Mn exposure in the pathology of neurodegenerative disease remains unknown, but the results of these studies demonstrate that although Mn exposure undoubtedly leads to several changes observed early in neurodegenerative disease pathology, no overt neurodegeneration was observed. The results of this work will help researchers studying the effect of metal exposure on adult neurogenesis and will also help researchers studying neurodegenerative disease and other disorders of the central nervous system.

CHAPTER 1: INTRODUCTION AND BACKGROUND

1.1 Abstract

Exposure to manganese (Mn) causes clinical signs and symptoms resembling, but not identical to, Parkinson's disease. Since the last review on this subject by this group in 2004, the past decade has been a thriving period in the history of Mn research. This chapter provides a comprehensive review on new knowledge gained in the Mn research field. Emerging data suggest that beyond traditionally recognized occupational manganism, Mn exposures and the ensuing toxicities occur in a variety of environmental settings, nutritional sources, contaminated foods, infant formulas, and water, soil and air with natural or man-made contaminations. Upon fast-absorption into the body via oral and inhalation exposures, Mn has a relatively short half-life in blood, yet fairly long half-lives in tissues. Recent data suggest Mn accumulates substantially in bone, with a half-life of about 8-9 years expected in human bones. Mn toxicity has been associated with dopaminergic dysfunction by recent neurochemical analyses and synchrotron X-ray fluorescence imaging studies. Evidence from humans indicates that individual factors such as age, gender, ethnicity, genetics, and pre-existing medical conditions can have profound impacts on Mn toxicities. In addition to body fluid-based biomarkers, other biomarkers are now being considered, including Mn levels in finger and toenails,

noninvasive measurement of Mn in bone, and functional alteration assessments. The information provided in this chapter is intended to establish the importance of this research. More specific background for research presented in each chapter will be provided in the introduction sections of respective chapters.

1.2 Introduction

Manganese (Mn) is the 12th most abundant element on the earth (Nadaska et al., 2012). As a transition metal, Mn exists in more than five valence states, with a majority as Mn^{2+} or Mn^{3+} (Aschner et al., 1999). In the environment, it is found mainly in its oxidized chemical forms, as MnO_2 or Mn_3O_4 (Post, 1999). Mn is essential to human health, acting as a co-factor in the active centers of various enzymes, and is required for normal development, maintenance of nerve and immune cell functions, and regulation of blood sugar and vitamins, among other functions (Aschner et al., 2007; Crossgrove and Zheng, 2004; Guilarte, 2010). Overexposure to this metal, however, causes toxicity to many organ systems and across different life stages. Clinically, this toxicity is termed manganism.

In 2004, this group summarized the impact of Mn exposure on general human health (Crossgrove and Zheng, 2004). At the time, a majority of evidence on Mn intoxication came from occupational settings, because of high exposure levels. Over the past decade, much progress has been made in the Mn research field, from toxicokinetics to exposure assessment and from the mode of action to clinical therapeutic intervention. Recent studies from this and other laboratories have indicated that low-level occupational

exposure, with air Mn concentrations at or below occupational standards can also be detrimental. Neurochemical, neurobehavioral, and neuroendocrine changes may occur before structural damage occurs, and are linked to pathogenic conditions (Alessio et al., 1989; Cowan et al., 2009a,b; Dydak et al., 2011; Lucchini and Zimmerman, 2009; Mutti et al, 1996). In addition to the exposure level and duration, there are other unique factors, such as age, gender, ethnicity, genetics, location, and pre-existing medical conditions that may contribute to Mn toxicity.

This chapter seeks to provide a comprehensive review of the new insights into environmental Mn exposure gained in the last decade. The current understanding of Mn toxicokinetics and its distribution in brain by using advanced synchrotron X-ray fluorescence imaging technique will be first introduced. The advantage and disadvantage of using bone Mn levels as a potential indicator for Mn body burden will be addressed. This will be followed by a general review of the updated knowledge on Mn systemic toxicities including effects on brain, liver, and the cardiovascular system. Finally, comments and recommendations will be made with regard to the diagnosis of Mn intoxication and clinical intervention.

1.3 Absorption, Distribution, and Elimination

The highest concentrations of Mn are present in bone, liver, kidney, pancreas, adrenal and pituitary glands (Rahil-Khazen et al., 2002). The normal concentration of Mn in human tissues is 1 mg/kg in bone (Liu et al., 2014), 1.04 mg/kg in pancreas, and 0.98 mg/kg in kidney cortex (Rahil-Khazen et al., 2002). The normal blood Mn concentrations range from 4-15 μg/L in humans (ATSDR, 2012). A recent survey among

the general Chinese population suggests that women have a higher blood Mn level than men (~28.6%) (Zhang et al., 2015). Mn is transported and regulated by several macromolecules summarized in **Table 1**.

Table 1. Proteins Involved in Maintaining Mn Homeostasis. Proteins required for regulating Mn are shown in conjunction with the particular species bound and the corresponding function.

Name and abbreviation	Mn species bound	Function	References
Divalent metal transporter (DMT1/SLC11A2)	Mn^{2+}	Mn uptake	Au et al., 2008
Transferrin (Tf)	Mn^{3+}	Mn uptake	Aschner and Gannon, 1994
Tf Receptor (TfR)	Mn^{3+}	Mn uptake	Baker et al., 2015
Citrate	Mn^{2+}	Mn transport in blood brain barrier	Crossgrove et al., 2003
ZIP8 (SLC39A8)	Mn^{2+}	Mn uptake	He et al., 2006
ZIP14 (SLC39A14)	Mn^{2+}	Mn uptake	Fujishiro et al., 2012
Voltage regulated calcium channels	Mn^{2+}	Mn uptake	Lucaciu et al., 1997
Ionotropic glutamate receptor calcium channels	?	Mn uptake	Kannurpatti et al., 2000
Store-operated calcium channels	Mn^{2+}	Mn uptake	Crossgrove and Yokel, 2005
SLC30A10	?	Mn efflux	DeWitt et al., 2013
Ferroportin (SLC40A1)	Mn^{2+}	Mn efflux	Madejczyk and Ballatori, 2012
Metallothionein	?	storage protein	Kobayashi et al., 2007
Iron-responsive element-binding protein (IRP1)	Mn^{2+}	Mn can replace the 4th Fe in the 4Fe-4S active center.	Wang et al., 2006
Ceruloplasmin	Mn^{2+}	potentially oxidizes Mn(II) to Mn(III)	Gibbons et al., 1976
superoxide dismutase		oscillates between Mn(II) and Mn(III) species	Sheng et al., 2012

Note: ? indicates uncertainty.

1.3.1 Chemical Species of Mn in Body Fluids

In the human body, Mn exists primarily in two oxidized states, i.e., Mn^{2+} and Mn^{3+}. Mn^{2+} species in the blood are bound to high molecular mass fractions, such as albumin and β-globulin as hydrated ions, and also in complexes with bicarbonate, citrate, and other low molecular mass species (Harris and Chen, 1994; Reaney et al., 2002). Nearly 100% of Mn^{3+} species are bound to transferrin (Tf), to form a more stable complex (Michalke and Fernsebner, 2014). Mn molecules in tissues such as liver, kidney, pancreas, bone, and brain exist primarily as Mn^{2+} (Crossgrove and Zheng, 2004).

In the cerebrospinal fluid (CSF), Mn^{2+} ions are bound to low molecular weight compounds, such as Mn-citrate (Michalke and Fernsebner, 2014). This form is thus thought to be transported by a citrate transporter (Yokel, 2009). More evidence, however, suggests that Mn^{2+} species are transported mainly by the divalent metal transporter-1 (DMT1) as the primary influx route to brain, although the other transporting proteins such as ZIP8 are suggested to mediate Mn transport into brain (Aschner et al., 2007; Chua and Morgan, 1997). Evidence in literature has also suggested that Mn^{2+} can enter the brain by store-operated calcium channels; but the extent of this route is much less than that of transporter-mediated transports (Yokel, 2009). The other Mn species entering the brain is Mn^{3+}, which is complexed with transferrin and via the transferrin receptor (TfR)-mediated process (Zheng, 2005, **Table 1**).

1.3.2 Absorption

The main route of Mn absorption is through the gastrointestinal tract; but the absorption also occurs in the lungs following inhalation exposure (Nadaska et al., 2012).

The intravenous injection of illegal narcotics containing Mn has recently provided a third route of exposure (Sikk et al., 2011).

Inhalation exposure to airborne Mn is common among welders and smelters (Jiang et al., 2006; Korczynski, 2000; Leavens et al., 2007). Inhaled Mn can by-pass the liver to enter the blood stream; from there it can enter the brain via the olfactory tract bypassing the blood brain barrier (Lucchini et al., 2012; Zoni et al., 2012). Studies in rats demonstrate that Mn is rapidly transported along the evolutionarily conserved olfactory pathway and is present within the olfactory bulb 8-48 hours after exposure. It is believed that the trigeminal nerve may also play a role in delivering Mn from the nasal cavity to the brain (Kanayama et al., 2005; Leavens et al, 2007; Zoni et al., 2012).

Oral exposure is another common route of exposure. Mn is required in small quantities obtained through dietary intake. The average daily intake for many Western diets is between 2.3 and 8.8 mg (EPA, IRIS); but this can be much higher. Consumption of food or water contaminated with high levels of Mn has toxic consequences (Kondakis et al., 1989). For example, the water supply in Bangladesh is contaminated with Mn up to 2.0 mg/L (Frisbie et al., 2002), which is 4-fold higher than the WHO standard for drinking water of 400 µg/L (Khan et al., 2012). Studies among school children suggest that increased levels of Mn in the drinking water in Bangladesh area are inversely associated with students' achievement scores in mathematics (Khan et al., 2013). High levels of Mn in drinking water in Canada have been found to lead to significantly higher levels of Mn in hair samples in school-age children. The increased hair Mn concentrations are significantly associated with increased hyperactive behaviors (Bouchard et al., 2007), impaired cognitive development (Khan et al., 2012), and a

decrease in IQ points (Bouchard et al., 2011). In Italy, school-age children living near a ferroalloy plant have been found to have significant impairment of motor coordination, hand dexterity, and odor identification after exposure to excess levels of Mn in soils (Lucchini et al., 2012). It is alarming that the high Mn concentration in drinking water is not solely a public health issue unique to developing countries; approximately 5.2% of the 2,167 wells surveyed across the United States exceeded the health benchmark of 300 µg/L (DeSimone et al., 2009).

Another potential source of oral exposure is from consuming milk- or soy- based infant formulas, which contain high levels of Mn. The FDA sets a minimum nutritional requirement of 5 µg/100 kcal for the amount of Mn infant formulas must contain; yet there is no maximum established. According to the Institute of Medicine's recommendation, infants can consume about 3 µg Mn/day for 0-6 months. Infants can drink up to a liter of formula a day. When formula is prepared according to the manufacturer's instructions, infants could consume from 32-51 µg of Mn per day, far exceeding the aforementioned recommendation. Soy-based formulas contain more Mn than cow-based formulas, and both contain much more Mn than does human breast milk (Tran et al., 2002). Since only a small percentage of Mn is eliminated in human breastmilk and because breastfed babies consume smaller volumes of milk than do bottle-fed babies at each feeding (Stastny et al., 1984), feeding breastmilk is considered much safer than feeding formulas to infants. It is also known that the concentrations of Mn in a mother's milk decrease as lactation progresses. Laboratory testing has shown that babies who drink formulas had higher concentrations of Mn in hair samples than those who were breast-fed (Collipp et al., 1983). The higher level of dietary Mn intake has been

suggested to be associated with the risk of developing the attention deficit hyperactivity disorder (Aschner and Aschner, 2005).

Recently, cases of Mn-induced Parkinsonism have been reported among intravenous ephedrone abusers in Estonia, Turkey, Eastern Europe, the Baltic States and Canada (Tuschl et al., 2013; Zheng, 2005). Mn is added to the drug cocktail as the oxidizing agent potassium permanganate; the final Mn concentration can be as high as 0.6 g/L. Multiple injections per day can result in doses ranging from 60-180 mg/day by intravenous administration. This amount far exceeds the 0.1 mg Mn/day recommended as an intravenous supplement. Continued uses can lead to elevated Mn concentrations in blood and urine, and patients have signs and symptoms such as impaired speech, cockwalk, bradykinesia and ataxia (Sikk et al., 2011) Even after cessation of ephedrone use, some of the motor symptoms continue to progress (Sikk et al., 2011; Tuschl et al., 2013).

1.3.3 Distribution

Once Mn enters systemic circulation from either the small intestine or lung, it mainly accumulates in liver (1.2-1.3 mg/kg), brain (0.15-0.46 mg/kg) and bone (1 mg/kg up to 43%) (Krebs et al., 2014; Liu et al., 2014; Rahil-Khazen et al., 2002; Subramanian and Meranger, 1985). Mn is detectable in the CSF before it is detectable in the brain parenchyma, suggesting that it is transported through the choroid plexus (Schmitt et al., 2011).

The brain is the target organ of Mn toxicity. In human subjects exposed to Mn in the work place, MRI studies have established higher levels of Mn accumulation in the

globus pallidus than in other brain structures (Dydak et al., 2011; Jiang et al., 207). Rapid advancement in synchrotron X-ray fluorescence (XRF) imaging technique has made it possible to illustrate the Mn distribution pattern in the brain. In rat brains, Mn accumulates with the highest concentration in the globus pallidus, followed by substantia nigra pars compacta, thalamus, caudate putamen, axon bundles, and cortex (Robison et al., 2012). While the hippocampus does not contain more Mn than other brain regions in control animals, Mn exposure in fact increases hippocampal Mn to the same level as those in substantia nigra pars compacta and thalamus. Thus, it appears that the hippocampus is susceptible to Mn toxicity. Moreover, the XRF data show that Mn tends to accumulate in brain regions that also have a high iron (Fe) concentration (Robison et al., 2013).

Mn concentrations are thought to be greater in astrocytes than in neurons (Tuschl et al., 2013). However, the XRF data from single cells show a diffuse Mn distribution pattern within cells of hippocampus CA3, which are likely neurons. Since only 30% of astrocytes are saturated after Mn exposure, it seems unlikely that astrocytes serve as the primary target of Mn accumulation in the rodent model (Robison et al., 2013).

In addition to brain and liver, Mn accumulates extensively in human bone under normal physiological conditions (Pejovic-Milic et al., 2009). By examining the human bone collected during autopsy, it is estimated that bone contains about 40% of the total body burden of Mn (Schroeder et al., 1966). Our recent study in rats has shown that after subchronic oral exposure to Mn, Mn accumulates in femur, tibia, humerus, and parietal bone with accumulation reaching steady state concentrations after 6 weeks of dose administration (O'Neal et al., 2014a).

Mn is intracellularly distributed in red blood cells due to the presence of transferrin receptor (TfR) and divalent metal transporter-1 (DMT1) in this cell type (Crossgrove and Zheng, 2004; Jiang et al., 2007). Inside the cell, Mn acts on mitochondrial complex I and disrupts energy production (Chen et al., 2001; Jiang and Zheng, 2005; Zheng et al., 1998). But mitochondria may not be the major intracellular organelles where Mn ions accumulate. Morello and colleagues (2008) used electron spectroscopy imaging and demonstrated that the highest concentrations of Mn were present in the heterochromatin and the nucleolus, followed by a lower concentration of Mn in the cytoplasm, with the lowest levels in mitochondria. After chronic Mn exposure, the highest levels of Mn were observed in the mitochondria (Morello et al., 2008).

In a comparative *in vitro* study utilizing choroidal epithelial Z310 cells, rat brain endothelial RBE4 cells, dopaminergic N27 and PC12 cell lines, cells were fractionated to separate nuclei and mitochondria. After Mn exposure, the highest levels of accumulation were found in the PC12 and N27 neuronal cell types compared with the non-neuronal brain barrier Z310 and RBE4 cell types. Most Mn was present within the nuclei, which was true for all four cell lines; only limited accumulation was observed in mitochondria (<0.5%) and microsomes (<2.5%) (Kalia et al., 2008). Nonetheless, the profound Mn toxicity on mitochondrial function should not be underestimated.

1.3.4 Elimination

The primary route of Mn elimination is via the fecal hepatobiliary excretion with limited urinary excretion (Klaassen, 1976). Some Mn-containing molecules such as Mn-DPDP and Mn nanoparticles show different elimination patterns from the metal Mn

(Bellusci et al., 2014; Marchal et al., 1993; Zhu et al., 2014). Mn is also eliminated in milk as mentioned above. However, this route of elimination does not constitute a major route of Mn excretion. Similarly, very low levels of Mn are excreted in sweat (Omokhodion and Howard, 1994).

In the brain parenchyma, Mn rapidly accumulates in brain structures such as the superior and inferior colliculi, amygdala, stria terminalis, hippocampus, and globus pallidus. The half-lives of Mn in these tissues are about 5-7 days, with the longest retention in the periaqueductal gray, amygdala, and entorhinal cortex (Grunecker et al., 2013). The elimination rate from brain tissue is expected to be slower than from either liver or kidney. In the rat, the half-lives of 16 brain regions are between 52 and 74 days (Crossgrove and Zheng, 2004).

In a study described in Chapter 2, we administered Mn by oral gavage at 50 mg/kg for 10 weeks. It was interesting to observe that by the fourth week of dose administration, Mn in blood reached the steady-state concentration, which was maintained for the duration of the study. Mn concentrations in the CSF, however, continued to increase even at the 8^{th} week. It is possible that a slow elimination of Mn from the CSF may contribute to the high level of Mn in the brain (O'Neal et al., 2014a). It is also possible that a redistribution of Mn from the bone compartment to the central nervous system may account, at least partially, for the high level of Mn in the CSF. By studying the elimination rate constant and half-lives, our data revealed that the half-lives of Mn in various rat bones were between 77 and 690 days with an average of 143 days for the whole skeleton (O'Neal et al., 2014a). A comparative study between human and rat estimates that every 16.7 days of a rat's life is equivalent to one human year

(Sengupta, 2011). By using this figure, the range of Mn half-lives in the rat skeleton is estimated approximately 4.6 – 41.3 years in humans with an average half-life of 8.6 years for humans (O'Neal et al., 2014a).

1.4 Human Exposure to Mn

The primary source of clinically identified Mn intoxication is due to occupational exposure. Neurotoxicity due to inhalation exposure to airborne Mn has been reported in miners in Mn dioxide mines (Couper, 1837), workers in dry-cell battery factories (Keen and Lönnerdal, 1995), smelters (Cowan et al., 2009a,b; Huang et al., 1989; Jiang et al., 2006; Jiang et al., 2007), steel manufacturing workers or welders (Bowler et al., 2011; Lu et al., 2005; Ono et al., 2002; Racette et al., 2012; Wang et al., 1989). Our own studies on 3,200 welders in 142 factories in the metropolitan area of Beijing reveal a significant correlation between airborne Mn level and manganism among welders with an estimated exposure dosages (calculated by the weight of welding rods) of 5-20 kg (containing 0.3-6% Mn) per working day per person (Crossgrove and Zheng, 2004; Want et al., 1998).

There are many environmental sources of Mn, which include eroded rocks, soils and decomposed plants. Human activities expose individuals to additional sources containing Mn, including the fungicides, Maneb and Mancozeb, medical imaging contrast agents, and water purification agents. Additionally, several countries including the United States, Canada, Argentina, Australia, Bulgaria, France, Russia, New Zealand, China, and the European Union have approved use of the fuel additive methylcyclopentadienyl manganese tricarbonyl (MMT) (Michalke and Fernsebner, 2014; Nadaska et al., 2012). Combustion of gasoline containing MMT releases Mn

phosphates, sulphates and oxides into the air, especially where there is high traffic density releasing particles within the respirable size range (Frumkin and Solomon, 1997; Nadaska et al., 2012). Mn-containing emissions contaminate soil, dust and plants near roadways, which introduces additional Mn to the environment (Lytle et al., 1995). Recent projections of MMT use indicates the average person's Mn absorption may increase by several percent. It should be noted that this is an estimated average level of exposure; therefore some people may be exposed more substantially than others (Frumkin and Solomon, 1997).

Ultimately, Mn from these various sources ends up in the water supply. As Mn filters down through the soil, it is reduced to the more soluble Mn^{2+} form where it can easily make its way into ground and surface waters. Ground water has the highest concentration of Mn; but surface water and water near mining operations contain high levels of Mn as well (Nadaska et al., 2012).

1.5 Manganese-Induced Toxicities

Mn can be stored in organs such as the liver and bone with limited local effects, but Mn targets multiple organ systems with severe consequences including the cardiovascular, reproductive, and respiratory; the main target of Mn toxicity is the central nervous system.

1.5.1 Mn-Induced Neurotoxicity

Cumulative evidence has established that Mn exposure induces signs and symptoms similar but not identical to Parkinson's Disease (Jiang et al., 2006; Racette et

al., 2001; Racette et al., 2005; Rutchik et al., 2012a,b; Tuschl et al., 2013). Early symptoms of Mn toxicity include cognitive deficits and psychiatric disturbances, followed by motor symptoms including rigidity, postural impairment, and tremors (Guilarte and Gonzales, 2015). A study on six manganism patients who were occupationally exposed to Mn as welders or smelters in Guangxi, China suggested that Mn exposure led to clinical manifestations of Parkinsonian syndromes with considerable variations. One patient who had a classic presynaptic syndrome and responded to L-DOPA was clearly Mn-intoxicated. Moreover, a case with 25-year Mn exposure showed a syndrome of Parkinsonism at an early age with magnetic resonance imaging (MRI) abnormalities bilaterally in the globus pallidus (Rutchik et al., 2012a,b). Thus, these observations support an overlap in syndromes between Mn-induced movement disorder and Parkinson's disease (Racette et al., 2001; Racette et al., 2005; Rutchik et al. 2012a,b).

While the linkage between manganism and Parkinson's disease is noteworthy, animal studies suggest that dopaminergic neurons in the substantia nigra and their terminals in the striatum, which are selectively lesioned in Parkinson's disease, remain intact after Mn intoxication (Guilarte, 2010). Additionally, following Mn toxicity, patients are typically unresponsive to levodopa, the dopamine precursor (Guilarte and Gonzales, 2015). Thus, changes in neurotransmission, rather than a massive dopamine neuronal cell loss, likely underlie behavioral observations.

Reports of Mn exposure altering neurotransmitter and metabolite levels have been published in literature (Gwiazda et al., 2007; Racette et al., 2012a). In Chapter 3, we investigated changes in dopamine, dopamine metabolites, including 3,4-dihydroxyphenylacetic acid (DOPAC) and homovanillic acid (HVA), as well as GABA,

in rat brain after Mn exposure. Our data showed a significantly increased dopamine level in the striatum; this increase was accompanied by increased levels of DOPAC and HVA in the same region. In agreement with our report, Vorhees and colleagues (2015) recently showed that Mn exposure increased striatal dopamine and HVA concentrations compared to controls. They also observed an increased norepinephrine in the striatum and increased dopamine, norepinephrine, and serotonin levels in the hippocampus. By utilizing various ages of animals, these investigators reported that Mn exposure altered monoamines as a function of age (Vorhees et al., 2015).

In a human study utilizing magnetic resonance imaging and spectroscopy (MRI/S) to investigate changes in neurochemistry of smelting workers, increases in GABA and decreases in myo-inositol were seen in the thalamus. Changes in thalamic GABA were associated with reduced fine motor performance as assessed by the Purdue pegboard test (Long et al., 2014).

Recent investigation of Mn neurotoxicity has also extended to the field of adult neurogenesis, which takes place in two critical niche areas in brain, i.e., the subventricular zone (SVZ) and the subgranular zone (SGZ). Application of the synchrotron XRF imaging technique to study brain distribution of copper (Cu) and Fe with or without Mn exposure has led to the unexpected discovery that Cu concentrations in the SVZ are considerably higher than in any other brain regions (Pushkar et al., 2013). Further *in vivo* studies revealed that subchronic Mn exposure in rats greatly increased the cell proliferation in the SVZ and the associated RMS, but significantly reduced the Cu levels in the SVZ (Fu et al., 2015). These observations raised the interesting question as to what the role of Cu in adult neurogenesis may be. It is unknown how Mn transport,

intracellular storage and trafficking may affect Cu homeostasis and ultimately alter normal neuronal repair processes, which may contribute to the non-motor symptoms characteristic of Mn-induced Parkinsonian disorder. The research presented in Chapter 4 was designed to study the effect of Mn toxicity on adult neurogenesis following intranasal exposure.

Kikuchihara and colleagues (2015) further confirmed that oral Mn exposure resulted in reduced numbers of local $Pvalb^{+}$ GABAergic interneurons in the other neurogenic niche, the SGZ of the dentate gyrus in the HP of mice (Kikuchihara et al., 2015). Similar to the data published by our group, Kikuchihara's group also observed a reduced Cu level in the subgranular zone after Mn exposure, although differences in animal species, exposure route, and duration between these two studies are evident. Since Mn exposure results in reduced Cu levels in both neurogenic niches, these two independent studies may suggest a similar molecular mechanism underlying Mn neuropathology.

1.5.2 Mn-Induced Cardiovascular Toxicity

Despite a lack of epidemiological evidence, animal and human evidences support the view that Mn exposure significantly alters cardiovascular function. Intravenous injection of Mn at high dose (5-10 mg Mn/kg) caused a decreased heart rate and blood pressure and increased P-R and QRS intervals (Charash et al., 1982). In perfused rat hearts, an MRI contrast agent Mn-DPDP had similar, but reduced effects on cardiac function as compared with Mn^{2+} (Vander et al., 1997). Limited data from human populations are available; but it somewhat contradicts the data from animal studies. As

opposed to the decreased blood pressure and heart rate observed in animal studies, smelters showed significantly faster heart rates than control subjects. Additionally, while animal studies showed increased P-R intervals, the reverse was true for the smelters, although the QRS and T waves were wider and elevated in both male and female smelters compared to controls (Jiang and Zheng, 2005).

Overexposure to the MRI enhancer Mn-DPDP causes flushed face and the head and ears feeling hot. Postural hypotension has also been observed in Mn-DPDP-overdosed patients (Jiang and Zheng, 2005). Even when cardiac function is not significantly altered, the mean diastolic blood pressure can be significantly lower, while and diastolic hypotension can be significantly higher, in Mn-exposed workers as compared to control subjects. Workers with the highest level of exposure to Mn exhibit the lowest systolic blood pressure (Jiang and Zheng, 2005).

Despite differences in levels of exposure between human and animal studies, it appears that Mn exposure inhibits myocardial contraction, dilates blood vessels and induces hypotension, suggesting that Mn exposure has a significant effect on cardiac function. The exact mechanism of cardiac toxicity remains unknown; it has been shown that Mn has a direct effect on mitochondrial function resulting in a reduced myocardial contraction, and causes vasodilation, leading to a decreased blood pressure following acute exposure (Jiang and Zheng, 2005). However, the research evidence on whether and how chronic low level Mn exposure causes cardiovascular toxicities from both human and animal studies remains sparse. Future work to evaluate these effects is well warranted.

1.5.3 Mn Exposure and Infant Mortality

Increased Mn levels in water sources have been linked to increased infant mortality. An analysis of groundwater concentrations in North Carolina reveals that infant mortality increases by a factor of 2 per 1,000 live births for every log increase in groundwater Mn concentration (Spangler and Spangler, 2009). Hafeman et al. (2007) also report an increased mortality in the first year of life in infants in Bangladesh exposed to Mn concentrations at or above the WHO's standard of 400 µg Mn/L compared to unexposed infants (Hafeman et al., 2007).

1.5.4 Mn Toxicity and Liver Function

Since the original report by Klaassen in 1976 describing the hepatobiliary excretion of Mn from the liver (Klaassen, 1976) not much work has been done to describe Mn-induced hepatotoxicity. The liver is a known storage organ for Mn; the highest Mn uptake occurs in the liver, only second to brain uptake (Chua and Morgan, 1997). Hepatic Mn accumulation in mice intravenously injected with Mn nanoparticles persisted significantly longer than other highly perfused tissues such as kidney and spleen; however, no histopathological damage was observed (Bellusci et al., 2014).

Hepatobiliary excretion of Mn represents a primary route of Mn clearance from the body, accounting for 80% of Mn elimination. Thus, severe liver damage, owing to various chronic liver diseases, can result in an excessive accumulation of Mn in brain with ensuing signs and symptoms clinically called Mn hepatic encephalopathy (Long et al., 2009). With weakened liver function, there is also an increased risk of neurodegeneration with continued Mn exposure (Squitti et al., 2009). In those patients

with chronic hepatic encephalopathy, liver transplant has proven to be effective in reducing brain Mn concentrations. When patients were re-examined 5 months after transplant, the T1-weighted MRI signals in the basal ganglia were absent (Long et al., 2009). These data suggest that the normal liver function is essential to maintain homeostasis of Mn in the body, including the central nervous system (CNS).

1.5.5 Mn Toxicity and Individual Susceptibility

There are many factors that may predispose one individual to Mn toxicity over another. These individual factors include age, gender, ethnicity, genetics, and pre-existing medical conditions, such as chronic liver disease.

Age is a common factor which may influence an individual's susceptibility to Mn toxicity. Very young animals as well as humans have increased intestinal Mn absorption (Vorhees et al., 2015) and also have increased accumulations of Mn in the CNS (Cahill et al., 1980), due to increased permeability of neuronal barriers to Mn (Michalke and Fernsebner, 2014). The young also have a reduced biliary excretion capacity (Aschner and Aschner, 2005). The 2011-2012 National Health and Nutrition Examination Survey (NHANES), a study of US residents, found higher Mn levels in the younger population, with the highest levels in one year old infants (Oulhote et al., 2014). These age-related factors can increase the risk of neurotoxicity following exposure.

Alternatively, the very old are a population of special concern, because of the large number of people who develop idiopathic Parkinsonism. Brain regions such as the globus pallidus, substantia nigra and striatum are involved in both Mn neurotoxicity and Parkinsonism; thus it is possible that the elderly may have a subclinical pathology and

could be “pushed over the edge” by increased doses of Mn (Mena et al., 1969). For example, in one of our occupational exposure studies, we found that smelters without clinical symptoms performed significantly worse on the Purdue Pegboard test, which is a measure of fine motor coordination, than control subjects. The scores got worse with age, which was not unexpected as fine motor coordination declines with age. However, Mn exposure appears to exacerbate this decline (Cowan et al., 2009b).

Gender is another common factor which may influence an individual’s susceptibility to Mn toxicity. The 2011-2012 NHANES study of U.S. residents reported significantly higher blood Mn levels in women of all ethnicities than men. The authors suggest metabolic differences in the regulation of Mn between men and women may underlie the difference (Oulhote et al., 2014). A recent study among the Chinese general population also indicates that women’s blood Mn levels are about 29% higher than men’s (Zhang et al., 2015), consistent with reports in the literature that Korean and Italian women’s Mn levels are 25% higher (Bocca et al., 2011; Lee et al., 2012) and Canadian women have about 23% higher levels (Clark et al., 2007) than the respective men’s population.

Gender may also be a contributing factor to developing cardiovascular toxicity after Mn exposure. In a study of male and female smelters exposed to Mn, female smelters had significantly shorter P-R intervals compared to controls and there was no difference in males. QRS and T waves were also significantly different for female smelters (Jiang and Zheng, 2005). Ethnicity could potentially be a factor that could influence susceptibility to Mn toxicity. In NHANES 2011-2012, the Asian population

tended to accumulate significantly more Mn than either non-Hispanic Caucasians or non-Hispanic black individuals (Oulhote et al., 2014).

Persons with iron deficiency are of special concern, because animal evidence indicates that gastrointestinal absorption of manganese is enhanced by iron deficiency (Mena et al., 1969).

While pregnancy is not a pre-existing condition, it is a condition during which the susceptibility to Mn toxicity may be increased. Again, the 2011-2012 NHANES demonstrates that pregnant women accumulate higher levels of Mn than do other persons (Oulhote et al., 2014). In a recent study of maternal blood Mn levels and neurodevelopment of infants at 6 months of age, researchers discovered significant associations between the mother blood Mn levels and their children's scores on mental and psychomotor developmental indexes. Interestingly, both high and low Mn blood levels were associated with lower scores (Chung et al., 2015). Maternal blood Mn levels have also been shown to be associated with inhibited enzyme activity of newborn erythrocyte Ca-pump at both low and high levels of maternal Mn (Yazbeck et al., 2006). A study conducted among pregnant women from Paris suggests that environmental exposure to Mn may increase the risk of preeclampsia. Mn cord blood concentrations in that study were significantly higher in women with preeclampsia (Vigeh et al., 2006).

From a mechanistic point of view, SLC30A10, a solute carrier (family 30 and member 10), has been suggested to regulate Mn export from the cells. This protein is highly expressed in the liver with a higher specificity for Mn than Zn. Genetic alterations in the SLC30A10 enzyme have recently been discovered. An autosomal recessive mutation in this transport protein leads to an inherited Mn-hypermanganesemia (DeWitt

et al., 2013; Tuschl et al., 2013) and results in a pleomorphic phenotype, including dystonia and adult-onset Parkinsonism (Leyva-Illades et al., 2014).

1.6 Diagnosis and Clinical Intervention

1.6.1 Biomarkers of Mn exposure

In Mn occupational exposures, the symptoms often develop quickly because the exposure levels are relatively high. In comparison, symptoms resulting from environmental exposures may be much more subtle and thus difficult to detect because they develop slowly, over a lifetime. Thus, it is crucial to detect these changes with a reliable biomarker in order to prevent the irreversible damage or the loss of function resulting from Mn toxicity. The biomarkers associated with monitoring Mn exposure in animal and human studies are summarized in **Table 2**.

Table 2. Possible Biomarkers of Mn Exposure. Body tissues and fluids previously used as biomarkers to assess Mn accumulation are summarized with the method of analysis and predicted utility in epidemiological studies.

Potential Biomarkers	Measured by	Interpretation	Usefulness in epidemiological studies	Reference(s)
Blood (whole)	ICP-MS; AAS	Most commonly studied; reflects recent exposure; large variation	Limited	ATSDR, 2012; Baker et al., 2015
Blood (plasma)	AAS	Short half-life may miss periods of peak exposure; large variation	No	Baker et al., 2015
Blood (serum)	AAS	Low concentration; large variation	No	Wang et al., 2008
Plasma Mn/Fe ratio	AAS	Good correlation to neurobehavioral changes	Possible	Cowan et al., 2009a; Cowan et al., 2009b
Erythrocyte Mn/Fe ratio		Same as above	Possible	Cowan et al., 2009a; Cowan et al., 2009b
Mn-citrate		Difficult to measure; never tested in humans	unknown	Crossgrove et al., 2003
Urine		No association between Mn inhalation and urinary Mn levels	No	Smith et al., 2007; Laohaudomchok et al., 2011
Saliva	ICP-MS	Partly changes in response to airborne Mn concentrations; large variation	No	Wang et al., 2008
Hair	ICP-MS	Susceptible to external contamination; cleaning methods affect accuracy of measurement	Limited	Riojas-Rodriguez et al., 2010; Menezes-Filho et al., 2009; Eastman et al., 2013
Nails	ICP-MS	Correlated with brain Mn levels; large variation; external contamination issue	Possible	Laohaudomchok et al., 2011; Sriram et al., 2012

Table 2 continued.

Teeth (Dentin)	ICP-MS	Characterizes prenatal and early postnatal Mn exposure	Limited	Arora et al., 2012
Teeth (Enamel)	IMS	Predicts exposure	Limited	Ericson et al., 2007
Bone	AAS; NAA	Reflects body burden; technique available	Yes	O'Neal et al., 2014a
CSF	AAS	Correlated with brain and bone Mn levels	Possible	O'Neal et al., 2014a
Breastmilk			No	
Sweat			No	

ICP-MS: Inductively coupled plasma mass spectroscopy; *AAS*: Atomic absorption spectroscopy; *NAA*: Neutron activated analysis; *IMS*: Ion mass spectrometry

Blood and urine are the most commonly used biological matrices for biomonitoring. However, the poor relationships between Mn concentrations in blood and urine and the external exposure levels make it very difficult to determine the internal exposure (Smith et al., 2007; Zheng et al., 2011). For example, the half-life of Mn in blood is less than 2 hours (Zheng et al., 2000). Plasma Mn concentrations measured during the dosing phase of a chronic Mn exposure study began to decline after two weeks, although Mn exposure was still ongoing (O'Neal et al., 2014a) Mn can be detected in human saliva samples. Our human study on Mn-exposed welders found that changes of saliva Mn concentrations mirrored those of serum Mn levels. But, because of a fairly large variation in saliva Mn levels, the authors did not recommend to use saliva Mn to assess Mn exposure (Wang et al., 2008). Because more than 95% of Mn is eliminated in bile to feces, urine Mn levels are expected to be very low (Schroeder et al., 1966). For these reasons, we do not recommend using Mn levels in blood, urine or saliva as the biomarkers of Mn exposure.

Attempts to identify additional non-invasive biomarkers have concluded that using hair and nail samples may be a possibility. In our own studies (Cowan et al., 2009a,b), we collected hair and nail samples from smelters and control subjects. The data showed such vast variation that we believe it would be misleading to report these data. A thorough, yet rapid process must be developed in order to eliminate external contamination before hair and nail samples can be used in research. Regardless, studies of residents living near a ferromanganese refinery in Brazil have shown that significant correlations exist between hair and fingernail Mn levels and the performance on neuropsychological tests (Viana et al., 2014). Grashow and colleagues (2014) have

recently suggested using toenail Mn concentration as a biomarker of occupational welding fume exposure (Grashow et al., 2014); their study, however, did not relate the toenail Mn level to any biological outcomes.

In a study of Mn-exposed smelters, Mn concentrations in plasma and erythrocytes were found to increase with a corresponding decrease of Fe concentrations in plasma and erythrocytes (Cowan et al., 2009a,b). Since Mn concentrations reflect the environmental exposure and Fe concentrations reflect a biological response to Mn exposure, combining both parameters by dividing the Mn concentration by the Fe concentration (i.e., MnC/FeC) would enlarge the difference between groups and therefore increase the sensitivity. This thought process led to the development of a concept of Mn/Fe ratio in plasma (pMIR) or erythrocytes (eMIR) (Cowan et al., 2009a). Because there is a significant correlation between pMIR and eMIR to airborne Mn concentration, both pMIR and eMIR appear to be good candidates as the biomarkers for Mn exposure assessment. Nonetheless, the same study also showed a better correlation between eMIR and low- or high- exposure outcomes (Cowan et al., 2009a). The utility of pMIR in environmental exposure assessment requires more rigorous testing. Additionally, as Mn-citrate in blood rapidly enters brain, elevated levels of plasma or serum Mn-citrate may be a biomarker of elevated risk of Mn-dependent neurological disorders in occupational health (Michalke and Fernsebner, 2014).

A relatively long half-life (about 8-9 years in human) of Mn in the skeletal system (see above) renders bone Mn concentration an ideal indicator to assess the body burden of Mn. The technical challenge has always been the development of equipment with appropriate sensitivity for such a purpose. The good news is that such a technology has

now become a reality. In recently published manuscripts, Nie and colleagues have optimized and verified a neutron activation-based analysis (NAA) technique for noninvasive, real-time quantification of Mn concentrations in bone. The equipment, at this writing, is compact enough to be transportable to the sites for testing human workers and subjects. The method is sensitive and can quantify Mn concentrations as low as 0.5 ppm of Mn in bone (Liu et al., 2014; Liu et al., 2013) and recently even lower to 0.3 ppm (personal communication).

Another non-invasive technique that can be used to analyze Mn exposure *in vivo* is MRI. Mn accumulation in the brain can be visualized as an increased T1-weighted "hyper-intense" MRI signal. By dividing the signal observed in the globus pallidus by the signal observed in the white matter in the frontal cortex and multiplying by 100, a pallidal index (PI) can be calculated to quantify Mn intensity. The PI has been proven to be a reliable marker for Mn exposure (Dydak et al., 2011; Jiang et al., 2007). Workers with more than 5 years' experience showed nearly 100% occurrence of enhanced PI, suggesting that the PI is specific for Mn exposure even when no clinical symptoms are evident (Jiang et al., 2007). One downside for using MRI is that it is only good for recent exposures. In human studies of smelters or intravenous ephedrone users, the signal in the globus pallidus almost completely disappears 5-6 months after cessation of exposure (Jiang et al., 2007; Sikk et al., 2011).

Magnetic resonance spectroscopy (MRS) is another useful technique to quantify neurochemical markers associated with Mn exposure (Jiang et al., 2007). Quantitation of GABA, glutamate, total creatine (tCr), and N-acetyl-aspartate (NAA)/tCr values, along with other macromolecules, has been made available by MRS. In the thalamus and basal

ganglia of Mn-exposed smelters, levels of GABA were nearly doubled, whereas the mean airborne Mn level was only 0.18 mg/m^3, which is below the previous occupational standard (OSHA, 2013). This may indicate an early metabolic or pathological change associated with low-level Mn exposure and MRS appears capable of detecting these biochemical changes before the full-blown symptoms become evident (Dydak et al., 2011).

For animal researchers, recent advancement in the synchrotron XRF imaging technique allows to visualize the concentration and distribution pattern of multiple metals in brain. The technique can now reach the resolution to the single cell level (Robison et al., 2013).

1.6.2 Clinical Intervention

The foremost therapeutic strategy in treatment of Mn toxicity is to remove the patient from the source of the Mn exposure. If the intoxication is life threatening, the procedures to relieve the critical signs and symptoms should first be employed. For a thorough treatment, chelation therapies can help reduce the body burden of Mn; but such treatments may not be able to improve symptoms. Another possible therapy includes Fe supplementation.

Chelation of free Mn with intravenous EDTA has been shown to increase Mn excretion in urine and decrease Mn concentrations in blood; but chelation does not significantly improve patients' clinical symptoms (Crossgrove and Zheng, 2004; Jiang et al., 2006). A recent report by Tuschl et al., (2013) demonstrates that two patients with inherited hyper-manganesemia who received EDTA chelation had a significantly

increased urinary excretion of Mn. Whole blood Mn levels and the MRI signals in the globus pallidus were also reduced (Tuschl et al., 2013). *In vitro* studies have documented that EDTA can effectively block toxic effects of Mn on mitochondrial oxygen consumption when added either before or after Mn exposure (Liu et al., 2013). Thus, for the purpose of reducing Mn in the blood compartment in the initial emergency phase, EDTA has a therapeutic benefit. However, EDTA molecules are highly water soluble and poorly pass across the blood brain barrier. The low brain bioavailability of EDTA limits its effectiveness in treatment of Mn intoxication (Jiang et al., 2006).

Para-aminosalicylic acid (PAS) is an FDA approved drug used for the treatment of tuberculosis. Studies mainly in Chinese patients show the promising effectiveness in treating severe Mn intoxication with promising prognosis (Jiang et al., 2006). Animal studies further verify its chelating effect in removing Mn from the body (Zheng et al., 2009). As a hard Lewis acid, Mn^{3+} can form a stable complex with hard donor atoms such as oxygen donors in PAS structure, while the Mn^{2+} cation prefers relatively softer donors such as nitrogen, which is also present in PAS structure. Thus, it is possible that PAS may form stable complexes with both Mn^{2+} and Mn^{3} species and remove them from where they are stored. Moreover, the salicylate structure in PAS, which has a proven anti-inflammatory effect, may contribute to the therapeutic prognosis of PAS in treatment of manganism (Jiang et al., 2006; Yoon et al., 2009). Our recent studies also demonstrated that the parent PAS was found predominantly in blood and in choroid plexus tissues, whereas its metabolite AcPAS was found in brain parenchyma, CSF, choroid plexus and capillary fractions (Hong et al., 2011). Both PAS and AcPAS were transported in the brain by the multidrug resistance-associated protein 1 (MRP1), a member of the

superfamily of ATP-binding cassette (ABC) transporters. However, the removal or efflux of PAS from brain parenchyma into blood was mediated by the multidrug resistance protein 1 (MDR1), also called P-glycoprotein (Hong et al., 2014).

One additional therapy includes Fe supplementation. In a pilot study with a sample size of one, Tuschl et al. (2013) showed that Fe supplementation, in addition to chelation therapy, led to a marked improvement of neurological symptoms, whereas the chelation therapy alone did little to improve symptoms. The authors proposed that supplementing with Fe may help reduce blood Mn levels and lower Mn body burden (Tuschl et al., 2013).

1.7 Discussion

The past decade is a thriving period in the history of Mn research. The total volume of publications related to “manganese toxicity” by a PubMed search in the last 11 years is 1,619 (from our last published review on 1 April 2004 to this writing on 5 April 2015), which far exceeds the cumulative numbers of 1,199 published papers on Mn toxicity for the past 167 years ever since Couper (Couper, 1837) reported on the first case of manganism in 1837 (~ to 31 March 2004). On a more fundamental level, the essence of what we consider to be a Mn exposure has undergone a significant change, from traditionally recognized occupational manganism to low-level Mn exposures in a variety of environmental settings, nutritional sources, contaminated foods, infant formulas, and water, soil and air with natural or man-made contaminations. Cumulative evidence on Mn toxicities and the vast public interest in this metal speak volumes of its public health importance, calling for a thorough understanding of its risk, the mechanism of its harm,

some forms of effective clinical interventions, and any applicable strategy for prevention. Thus, we predict that the research on Mn toxicity is far from finished and will become even more productive in the coming decade.

1.8 Research Challenges

The research challenges addressed by this dissertation are as follows: i) the lack of knowledge in toxicokinetic behavior of Mn in bone and the association between bone Mn levels and brain Mn levels, ii) the lack of understanding in changes in common neurotransmitters associated with Parkinsonian disorders following subchronic exposure to Mn, iii) the lack of evidence as to whether Mn affects adult neurogenesis, and iv) the lack of research to understand whether and how Cu dyshomeostasis impacts adult neurogenesis.

1.9 Central Hypothesis

The central hypothesis under investigation in this doctoral dissertation is that Mn exposure leads to substantial accumulation of Mn in the body, particularly in bone tissues and produces subclinical effects in the CNS, including alteration of levels of critical neurotransmitters in brain. Mn accumulation may result in diminished neuronal repair capacity, and in this way, may ultimately contribute to neurodegenerative damage.

1.10 Specific Aims to Test Central Hypothesis

To test the central hypothesis in this doctoral dissertation, we have designed and accomplished the following specific aims:

1. **Determine the toxicokinetic parameters (absorption, distribution, and elimination) of Mn in bone tissue.** The toxicokinetics of Mn in bone were determined by measuring Mn content in bone using atomic absorption spectroscopy (AAS) at various times during the accumulation and elimination phases after oral dosing. The rates with which Mn accumulates and eliminates from bone tissues were also investigated. Several bones with different composition were analyzed to determine if bone-specific differences existed. Lastly, correlations between brain and bone Mn levels were evaluated to identify if bone Mn concentrations accurately represent brain Mn concentrations. **Rationale:** Approximately 40% of the body burden of Mn is stored in bone. This is an important first step to determining if and how Mn stored in bone may be released over time, serving as an endogenous source of continued Mn exposure, particularly with regard to the central nervous system.

2. **Characterize Mn accumulation in rat brain after exposure and investigate the effects on regional neurochemistry.** In this aim, we quantified Mn concentrations and neurotransmitter levels in the central nervous system using AAS and high performance liquid chromatography (HPLC). We further investigated the resulting changes in monoamines using immunohistochemistry to determine if the enzyme responsible for the metabolism of dopamine, tyrosine hydroxylase was altered. Levels of DARPP-32, a marker of striatal medium spiny neurons, were also investigated. Lastly, we determined if cell death occurred as a result of Mn exposure using histology probes for Fluorojade C in

rat brain slices. **Rationale**: Studies in literature have investigated changes in neurochemistry; yet, the results remain inconclusive. Depending on the dose level of Mn used or the duration of exposure, the results, particularly with regard to dopamine, vary considerably. This research utilized several dose levels and examined multiple brain regions to determine if a dose response relationship existed and whether effects were limited to a particular region.

3. **Identify how Mn exposure affects the processes of neurogenesis and gliogenesis in the adult subventricular zone.** In this aim, we investigated differential changes in expression of BrdU, DCX, and GFAP in the SVZ following intranasal instillation of Mn using immunohistochemistry (IHC) techniques and confocal quantification. The cells that reside in this region may migrate to the olfactory bulb where they undergo further changes. Expression of BrdU, DCX, and GFAP were also evaluated in the various cell layers of the olfactory bulb. A sub-aim of this hypothesis was to characterize the intranasal instillation technique for future use in studies of Mn neurotoxicity and adult neurogenesis by investigating changes in neurochemistry using HPLC and expression of mRNA and protein levels of selected metal transporters. Physiological measurements were also made to determine if overt toxicity or immune response occurs following intranasal Mn exposure. **Rationale**: Recent work from our lab has shown that Mn exposure by intranasal instillation alters adult neurogenesis in the SVZ. This is the first application of the intranasal instillation technique to studies of adult neurogenesis following Mn exposure. These studies are of critical importance given that the primary exposure route following Mn toxicity in humans is direct olfactory transport.

Investigating changes in the SVZ and OB could provide new evidence for the association between Mn exposure and Parkinson's disease.

1.11 Significance of the Research

The interaction between Mn neurotoxicity and Parkinson's disease is complex and not completely understood. Many associations between Mn-induced Parkinsonism and Parkinson's disease have been found in humans but the results have often been contradictory. Additionally, recent evidence from our lab has suggested that Mn exposure alters processes of neuronal repair and adult neurogenesis in the SVZ known to be active in Parkinson's disease. It is well-warranted to further investigate changes in this region as well as changes in neurochemistry following Mn exposure because alterations in these processes could lead to dysregulation of a variety of other processes in the body. An understanding of how Mn exposure influences adult neurogenesis and how Cu levels are regulated in the SVZ are critical for the development of effective therapeutic strategies in neurodegenerative diseases which implicate Cu dysregulation in their pathologies.

The contribution of our research is expected to be a detailed understanding of how Mn exposure affects neurochemistry and adult neurogenesis. Specifically, we expect to 1) elucidate toxicokinetic parameters of Mn in bone which will help in the search for a suitable biomarker of Mn exposure and determine if Mn stored in bone can serve as an internal depot of Mn for extended durations, 2) determine how Mn exposure regionally affects brain neurochemistry and potentially uncover dose-response relationships, 3) demonstrate that the intranasal route of Mn exposure is a suitable method for studies of adult neurogenesis and Mn toxicity in general, and 4) discover how Mn interacts with

brain repair mechanisms, specifically the proliferation and differentiation of neural progenitor stem cells.

The experimental methodologies to be used are rigorous and diverse, including atomic absorption spectroscopy, high performance liquid chromatography, immunohistochemistry, Western blotting, quantitative polymerase chain reaction (qPCR), and behavioral assays to pursue important new information about Mn toxicity in the mammalian system. Understanding how brain and bone Mn levels correlate after Mn exposure will help discover a novel biomarker suitable for the assessment of Mn exposure in humans. Importantly, the primary route of Mn exposure in the human population is inhalation; so utilizing an intranasal route of exposure could more closely mirror what occurs in the human population. No other researchers have used this technique to investigate metal toxicity and neurogenesis. By this pathway, environmental contaminants, including Mn, directly interact with the central nervous system and therefore further investigation of this exposure route is well warranted.

Completion of this work will provide evidence of Mn interaction with neuronal repair mechanisms and lead to a new area of toxicology research, specifically metals toxicology. A better understanding of these processes may present novel pathways and target strategies for regulating the processes of adult neurogenesis in the SVZ and SGZ by guiding and encouraging the existing processes. This work will assist future researchers investigating Parkinson's disease, Alzheimer's disease, Amyotrophic Lateral Sclerosis, Wilson's and Menke's diseases as well as stroke, and traumatic brain injury, among many other applications, making our work in the field of adult neurogenesis highly significant and of great interest. Additionally, these findings in the SVZ can be

applied to the analysis of other regions with more limited neurogenic capabilities, including the hypothalamus, further extending the scope of the research.

1.12 Structure of the Dissertation

This dissertation is organized in the following sequence: the introduction and background are presented in Chapter 1, which provides an in-depth analysis of the new findings from the last 10 years. Chapter 2 is devoted to the toxicokinetic understanding of Mn in bone and its relationship to Mn accumulation in brain. This is followed by a thorough analysis of neurotransmitter concentrations in brain as a result of Mn exposure in Chapter 3. Chapter 4 details the changes to neurogenic function that occur in the subventricular zone and olfactory bulb following intranasal Mn exposure. Finally, Chapter 5 summarizes the findings and discusses the future directions of this work. Notably, most of the research data have been published (i.e., data in Chapters 2 and 3) or are prepared for publication (i.e., data in Chapter 4). Thus, the presentation in these chapters follows the structure of published papers. To maintain the flow of each individual chapter, some repetitive background information is expected in the introduction sections.

CHAPTER 2: MANGANESE ACCUMULATION IN BONE FOLLOWING CHRONIC EXPOSURE IN RATS: RELATIONSHIP TO MANGANESE LEVELS IN BRAIN

2.1 Abstract

Literature data indicate that bone is a major storage organ for manganese (Mn), accounting for 43% of total body Mn. However, the kinetic nature of Mn in bone, especially the half-life ($t_{1/2}$), remained unknown. The study presented in this chapter was designed to understand the time-dependence of Mn distribution in rat bone after chronic oral exposure. Adult male rats received 50 mg Mn/kg (as $MnCl_2$) by oral gavage, 5 days per week, for up to 10 weeks. Animals were euthanized every two weeks during Mn administration for the uptake study, and on day 1, week 2, 4, 8, or 12 after the cessation at 6-week Mn exposure for the $t_{1/2}$ study. Mn concentrations in bone (MnBn) were determined by AAS analysis. By the end of 6-week's treatment, MnBn appeared to reach the steady state (T_{ss}) level, about 2-3.2 fold higher than MnBn at day 0. Kinetic calculation revealed $t_{1/2}$s of Mn in femur, tibia, and humerus bone of 77 (r=0.978), 263 (r=0.988), and 429 (r=0.994) days, respectively; the average $t_{1/2}$ in rat skeleton was about 143 days, equivalent to 8.5 years in human bone. Moreover, MnBn were correlated with

Mn levels in striatum, hippocampus, and CSF. These data support MnBn as a useful biomarker of Mn exposure.

2.2 Introduction

Occupational exposure to manganese (Mn), such as in mining, smelting, welding or dry-cell battery production, has been associated with a neurodegenerative parkinsonian disorder clinically called manganism (Barbeau et al., 1976; Chandra et al., 1981; Crossgrove and Zheng, 2004; Jiang et al., 2006). Environmental exposure to this toxic metal has also been linked to the consumption of Mn-containing pesticides and contamination in drinking water and food (Bouchard et al., 2011). Addition of Mn to gasoline as the anti-knocking reagent, methylcyclopentadienyl Mn tricarbonyl (MMT) further raises concerns about health risks associated with a potential increase in environmental levels of Mn (Butcher et al., 1999; Sierra et al., 1995). Recently, increasing numbers of cases of Mn-induced Parkinsonism have been observed among drug addicts using ephedrone (Sikk et al., 2011). It is because of rising public health concerns that a thorough understanding of Mn neurotoxicity, including its distribution in the body and mechanism of action, is well justified.

Patients suffering from manganism have signs and symptoms closely resembling, but not identical to, Parkinson's disease (PD) (Aschner et al., 2007; Jiang et al., 2006; Racette et al., 2012). Recent data also show that Mn may play a role in PD etiology (DeWitt et al., 2013; Lucchini et al., 2007). Since clinically manifested Mn neurotoxicity is usually progressive and irreversible, early diagnosis becomes critical to treatment and prevention of Mn intoxication. Historically, searches for biomarker(s) of Mn exposure

and health risk have focused on Mn concentrations in blood, urine, and/or nail. These biomarkers, however, are of limited use for exposure assessment in that primarily intracellular accumulation of Mn renders blood, urine, or nail Mn levels inaccurate in reflecting the true body burden of Mn (Apostoli et al., 2000; Zheng and Monnot, 2012). For example, in group comparisons among active workers, blood Mn has some utility for distinguishing exposed from unexposed subjects; yet a large variability in mean values renders it insensitive for discriminating one individual from the rest of the study population. Human studies using magnetic resonance imaging (MRI), in combination with non-invasive assessment of γ-aminobutyric acid (GABA) by magnetic resonance spectroscopy (MRS), have provided evidence of Mn exposure in patients devoid of clinical symptoms of Mn intoxication (Dydak et al., 2011; Jiang et al., 2007). These methods, however, do not provide an adequate estimation of Mn body burden in a long-term, low-dose Mn exposure scenario (Zheng and Monnot, 2012). Thus, to date, a reliable biomarker to accurately reflect Mn exposure or body burden remains unavailable.

Data in literature suggest that, at normal physiological conditions, Mn accumulates extensively in human bone tissues (Pejovic-Milic et al., 2009; Schroeder et al., 1966; Zaichick et al., 2011). Schroeder et al. (1966) observed an average concentration of 2 mg/kg of Mn in bone ash, which gives rise to about 32.5% of body Mn in bone, according to our recent calculation (Liu et al., 2013). The International Commission on Radiological Protection (ICRP) has reported approximately 40% of body Mn accumulates in bone (ICRP, 1972). Information from animal studies of Mn accumulation in bone can be found in literature, albeit is very limited (Dorman et al., 2005; Seaborn and Nielsen, 2002). Using a physiologically-based pharmacokinetic

modeling approach, Andersen et al. (1999) reported that Mn stored in bone tissues contributed to over 40% of body Mn; the estimate is closer to the aforementioned human data. Studies by Furchner et al. (1966) using radioactive ^{54}Mn administered orally to rats at a normal physiological dose have found that the radioisotope in bone had a half-life of more than 50 days, which was much longer than the ^{54}Mn half-life in other rat tissues. Another study by Newland et al. (1987) in primates using ^{54}Mn reported that Mn had a relatively long half-life of about 220 days in the whole head after inhalation exposure. In the same study, the researchers found that the half-life of ^{54}Mn in brain tissues from the same animals was much shorter; hence they ascribed a long half-life of ^{54}Mn in the head to ^{54}Mn present in the skull or to replenishment from other depots (Newland et al., 1987). These data have clearly established that bone is one of the major organs for long-term storage of Mn in the body. Thus, a reliable assessment of Mn health benefits or risks should take into account the extensive Mn deposition in bone. However, knowledge on the rate of Mn accumulation in human or animal bone, and the pertinent biological half-life of Mn in bone was incomplete.

Recent advances in neutron activation-based detection technology has made it possible to develop a portable neutron activation analysis (NAA) system for quantifying MnBn (Aslam et al., 2008; Liu et al., 2013; Pejovic-Milic et al., 2009). This highly innovative technique uses a portable deuterium–deuterium neutron generator (as the neutron source) to detect Mn in bone, non-invasively and in real time, in human subjects. To support this technical innovation, there was a need to understand the toxicokinetics of Mn in bone under a long-term, low-dose exposure condition.

The purposes of the current study were to (1) characterize the time-dependent accumulation of Mn in rat bone following chronic oral administration of Mn to animals; (2) determine the elimination $t_{1/2}$ of Mn in bone tissues; (3) investigate if bone samples collected from different body parts had similar or different kinetic characteristics; and (4) seek the correlations between MnBn and Mn concentrations in select brain regions known to be targets of Mn neurotoxicity. Understanding the time-dependent changes of tissue distribution of Mn within bone, central nervous system (CNS), and other tissues will help understand Mn neurotoxicity described in the following chapters.

2.3 Materials and Methods

2.3.1 Chemicals

Chemical reagents were purchased from the following sources: Mn chloride tetrahydrate ($MnCl_2 \cdot 4H_2O$) from Fisher Scientific (Pittsburgh, PA); Mn and Cu standard solutions were from SCP Science (Champlain, NY); ketamine from Fort Dodge (Fort Dodge, IA); xylazine from Vedco (St. Joseph, MO). All reagents were analytical grade, HPLC grade, or the best available pharmaceutical grade.

2.3.2 Experimental design

The overall experimental design is illustrated below (**Figure 1**):

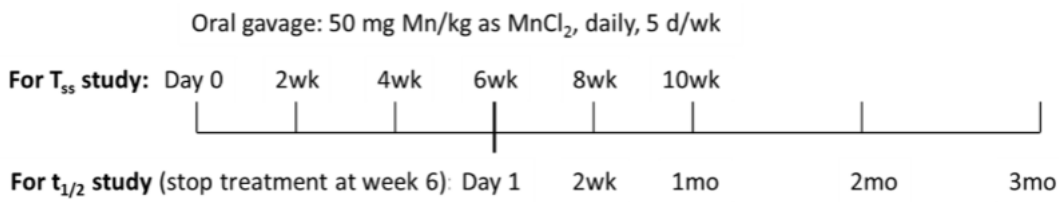

Figure 1. Chapter 2 Experimental Design. Bones were collected and analyzed at each time point shown. The top row indicates ongoing dose administration. The bottom row collection days begin once dosing has ceased.

Phase 1 studies were designed to determine the time course of Mn accumulation in bone. Rats received daily administration of 50 mg Mn/kg as $MnCl_2$ by oral gavage, 5 days per week for the period of time specified in the above illustration. In this phase, dose administration lasted up to 10 weeks with cohorts of animals euthanized every two weeks to determine the steady state Mn concentrations (T_{ss}) in bone following oral exposure.

Phase 2 studies were designed to determine the elimination $t_{1/2}$ of Mn from bone tissues. The results from phase 1 suggest a T_{ss} was reached by 6 weeks of continuous Mn exposure. After the last dose of the week-6 dose administration, animals were euthanized at 24 hours, 2 weeks, 1, 2 and 3 months to determine $t_{1/2}$ of MnBn.

2.3.3 Animals and Mn Administration

Male Sprague Dawley rats were purchased from Harlan Laboratories, Inc. (Indianapolis, IN). Upon arrival, animals were housed in a temperature-controlled, 12-h light/dark cycle room and allowed to acclimate for one week prior to experimentation. At the time of use, rats were 8 weeks old and weighed 220-250 g. Animals had ad libitum access to filtered tap water and pelleted rat chow (Harlan Teklad 2018 Diet, Harlan Laboratories). The studies were approved by the Institutional Animal Care and Use Committee at Purdue University.

$MnCl_2 \cdot 4H_2O$ dissolved in sterile saline was administrated to rats by oral gavage of 50 mg Mn/kg, once per day, 5 days per week, for up to 10 weeks. This dose regimen was selected based on our preliminary study showing plasma Mn concentration of ~25 μg/L after 2-week oral doses, which is comparable to blood Mn levels in Mn-exposed human subjects. Earlier human studies indicate that Mn-poisoned workers usually have

blood Mn concentrations between 4-15 μg/L (Inoue and Makita, 1996; Vezér et al., 2007). Our own human study among 39 Mn-poisoned welders in Beijing reveals that the welders with a distinct manganism have a blood Mn level in the range of 8.2-36 μg/L (Crossgrove and Zheng, 2004). Thus, a continuous daily oral gavage at 50 mg/kg would likely result in a steady-state blood concentration similar to chronic occupational exposure in humans. The daily equivalent volume (4 ml/kg) of sterile saline was given to control animals. Twenty-four hours after the last injection, rats were anesthetized with ketamine/xylazine (75:10 mg/kg; 1 mg/kg, ip). Cerebrospinal fluid (CSF) samples, free of blood, were collected using a 26G butterfly needle inserted between the protuberance and the spine of the atlas, and blood samples were obtained from the descending aorta and processed for plasma. Rat brains were dissected to harvest choroid plexus from lateral and third ventricles, hippocampus, striatum, and frontal cortex. Samples were stored at -80°C for later analysis.

2.3.4 Determination of Mn, Fe, Cu and Zn Concentrations by AAS

All brain and bone samples were digested with concentrated ultrapure nitric acid in a MARSXpress microwave-accelerated reaction system. Plasma and CSF samples were digested overnight with nitric acid in a drying oven at 55°C. An Agilent Technologies 200 Series SpectrAA with a GTA 120 graphite tube atomizer was used to quantify Mn, Fe, Cu and Zn concentrations. Digested samples were diluted 50, 500, or 1000 times with 1.0% (v/v) HNO_3 in order to keep the readings within the concentration range of the standard curves. Ranges of calibration standards were 0-5 μg/l for Mn, 0-10 μg/l for Fe, and 0-25 μg/l for Cu and Zn. Detection limits for Mn, Fe, Cu and Zn were

0.09 ng/ml, 0.18 ng/ml, 0.9 ng/ml, and 0.28 ng/ml, respectively, of the final assay solution (Zheng et al., 1998, 1999, 2009).

2.3.5 Toxicokinetic and Statistics Analysis

Values of MnBn from various body parts were plotted as a function of time. Calculation of the terminal-phase elimination rate constant (K_e) was based on the assumption of first-order elimination kinetics (Gibaldi and Perrier, 1982; Zheng et al., 2001). A linear regression analysis was used to estimate the K_e of individual curves obtained from different body bones, from which the $t_{1/2}$ was obtained using the following equation:

$$t1/2 = \frac{0.693}{K_e}$$

All data are expressed as mean ± S.D.; statistical analyses of the differences between groups were carried out by one-way ANOVA with post hoc comparisons by Dunnett's test or Student's t-test using SPSS for Windows (version 20.0). The differences between the two means were considered significant if *p* values were equal to or less than 0.05.

2.4 Results

2.4.1 Increased Mn concentrations in body fluids after Mn exposure

Following oral chronic Mn exposure, the plasma concentrations of Mn were significantly increased compared to baseline (week 0) after only two weeks of Mn

exposure (**Fig. 2**). After 4 weeks of Mn dosing, plasma Mn concentration remained significantly higher compared to the baseline, but it declined from the 2 week value (**Fig. 2**). Plasma Mn concentrations were not significantly different after 6, 8, or 10 weeks of Mn exposure as compared to the baseline. Similarly, Mn concentration in CSF was significantly increased compared to baseline after 2 weeks of Mn exposure ($p < 0.05$; **Fig. 2**). Interestingly, Mn concentrations in CSF samples remained significantly higher at 4, 6, 8, and 10 weeks of dosing in comparison to the baseline value ($p < 0.01$; **Fig. 2**). Between the sixth and eighth weeks of Mn exposure, Mn levels in the CSF appeared to plateau.

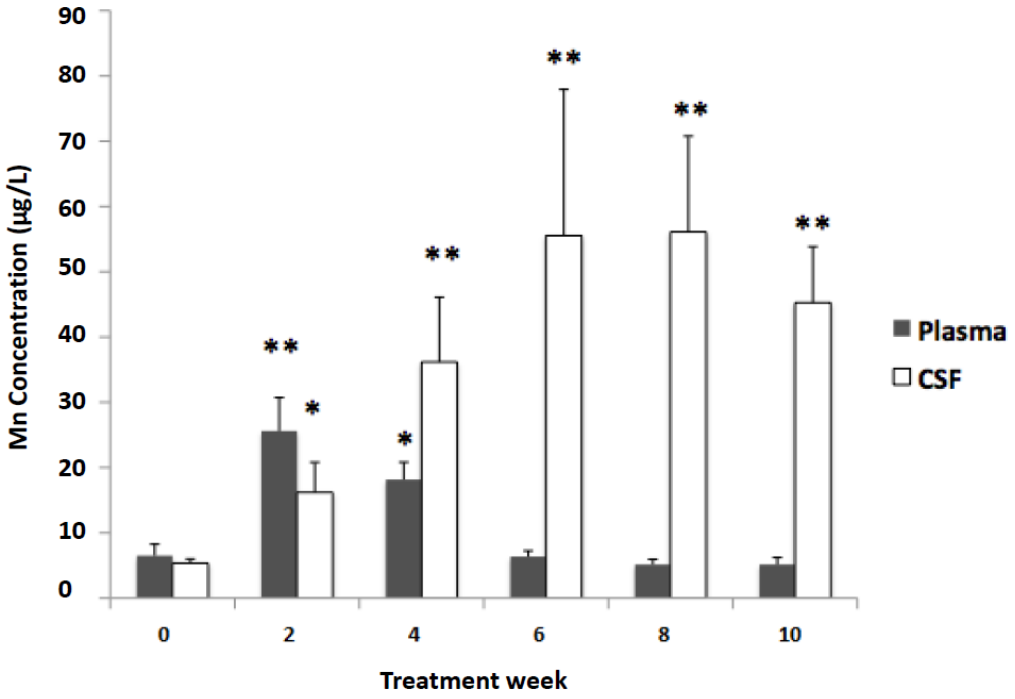

Figure 2. Time Course of Mn Concentrations in Plasma and Cerebrospinal Fluid. Rats received 50 mg Mn/kg as $MnCl_2$ by oral gavage once daily, five days per week for the time indicated. Mn concentrations in plasma and CSF were determined by AAS. Data represent mean ± S.D., n = 5-6; *$p < 0.05$, ** $p < 0.01$.

2.4.2 Increased Mn Concentrations in Bones after Mn Exposure

Mn accumulation in bone was investigated in bone samples including femur, tibia, humerus, and parietal bones. While chronic Mn oral exposure did not significantly affect animals' body weights after 6 weeks exposure, the weight of femur bones was significantly reduced compared to controls (-8.5%, $p < 0.01$; **Table 3**). Concentrations of Mn in bone appeared to be elevated after only two-weeks of exposure, although the values were not statistically significant (**Fig. 3**). After 4-weeks of exposure, a significant accumulation of Mn in bone was observed in all bone samples ($p < 0.05$; **Fig. 3**). This increase in Mn accumulation in all bone samples continued until the 8^{th} week of Mn exposure. Since there were no statistically significant differences between the data points from the 6^{th}-, 8^{th}- or 10^{th}-week bone samples, MnBn appeared to reach the steady state (T_{ss}) concentration after 6-weeks of Mn exposure (**Fig. 3**).

Table 3. Changes of Total Body Weight and Femur Bone Weight s after Chronic Oral Mn Exposure in Rats. Rats received 50 mg Mn/kg as MnCl2 by oral gavage once daily, five days per week, for 6 weeks. Mn concentrations were determined by AAS. Data represent mean ± S.D., n = 5-6; * $p < 0.05$.

	Body Weight		Bone Weight	
	Day 0	18 Weeks	Day 0	18 Weeks
Control	261.6 ± 5.22	354.9 ± 16.24	1.07 ± 0.13	1.30 ± 0.02
Mn-treated	268.4 ± 8.65	352.13 ± 9.96	1.21 ± 0.38	1.19 ± 0.01*

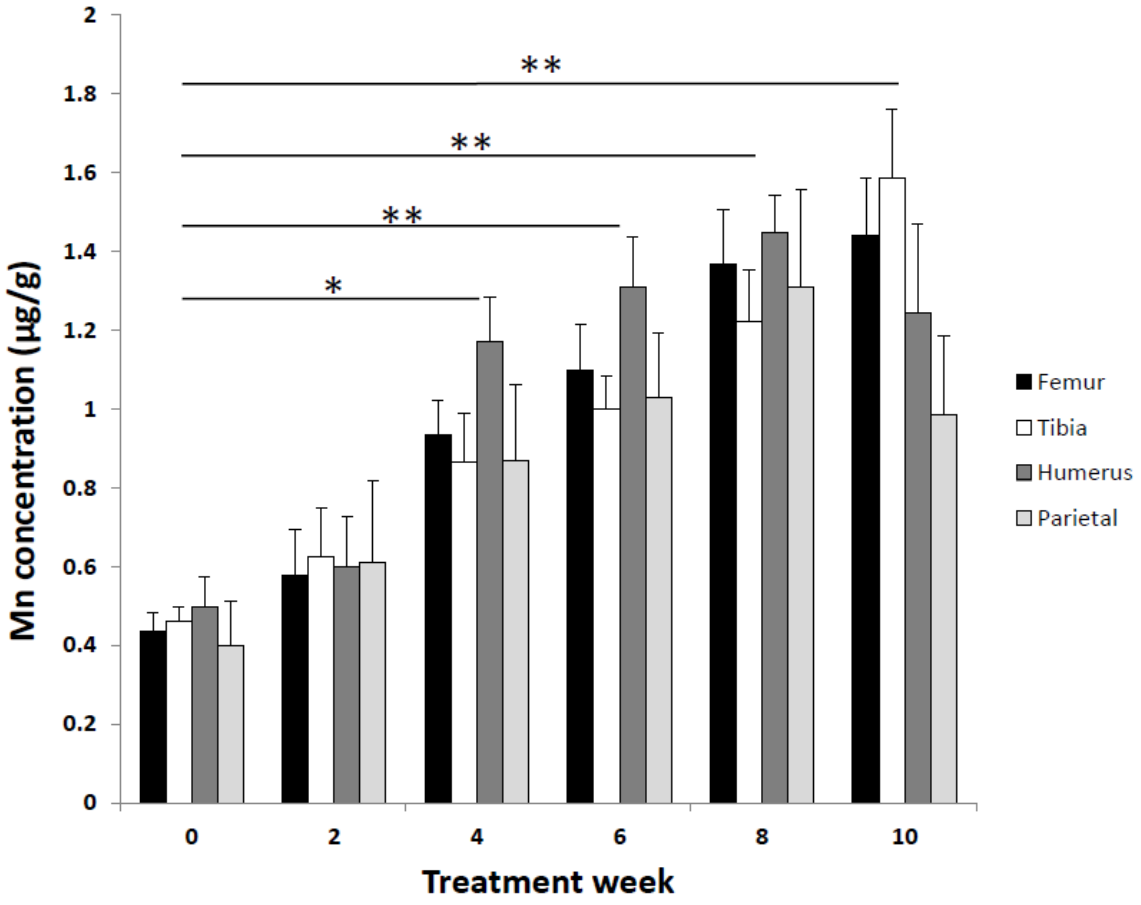

Figure 3. Time-Dependent Accumulation of Mn in Rat Bones. The animal treatment regimen is described in the legend to Fig. 1. Mn concentrations in various bone samples were determined by AAS. Data represent mean ± S.D., n = 5-6; * $p < 0.05$, ** $p < 0.01$ indicating group comparisons made between samples collected at times after Mn exposure and samples at time 0.

2.4.3 Mn $t_{1/2}$ in Rat Bones

To determine the elimination $t_{1/2}$, animals were exposed to Mn for 6 weeks until the T_{ss} was reached. Bone tissues were then dissected at 24 hours, 2 weeks, 1, 2 and 3 months following exposure cessation for AAS quantification of Mn concentrations in femur, tibia, humerus, and parietal bone. Average values for each type of bone were plotted on a semi-log scale over time to yield four separate regression lines. The slopes of these regression lines were taken as the individual elimination rate constant K_e and used to calculate the MnBn $t_{1/2}$ for each bone type. Our calculations result in $t_{1/2}$s of 77, 263, 429, and 690 days for femur, tibia, humerus, and parietal bones, respectively. To estimate the Mn $t_{1/2}$ in the whole rat skeleton, the values for all bones at each time point were averaged. Following the same procedure used to calculate the $t_{1/2}$ in individual bones, the average MnBn $t_{1/2}$ was estimated to be approximately 143 days (**Fig. 4**).

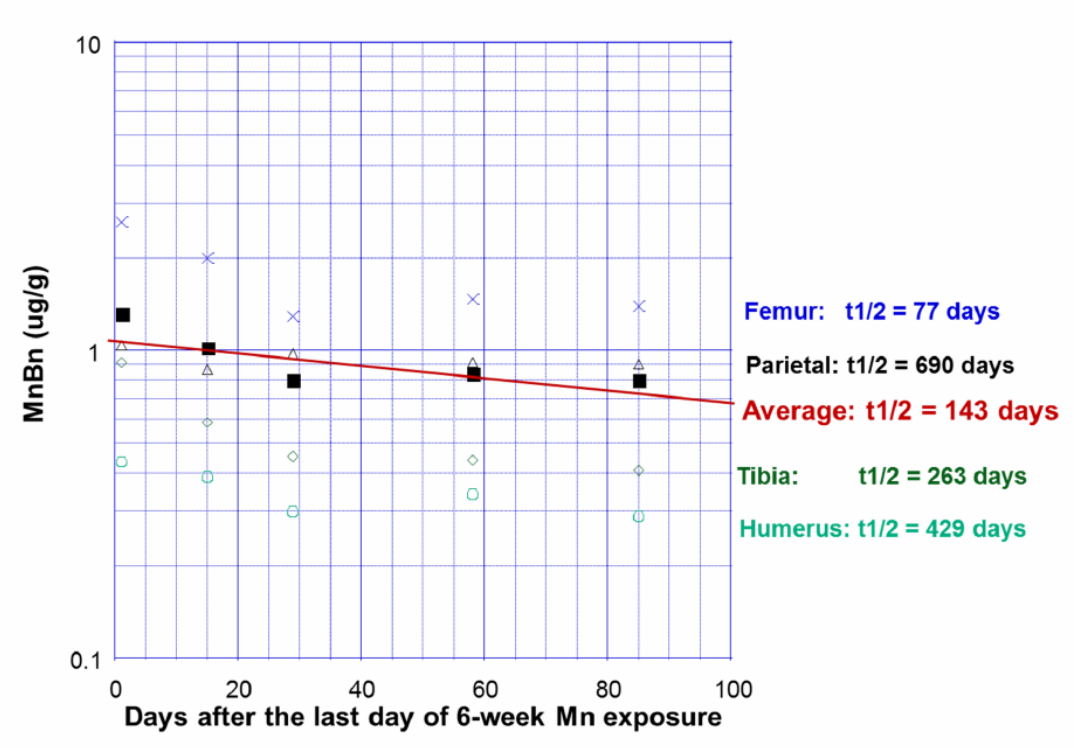

Figure 4. Terminal Phase Elimination Half-Life ($t_{1/2}$) of Mn in bones. Rats received 50 mg Mn/kg as $MnCl_2$ by oral gavage once daily, five days per week for 6 weeks. Groups of animals were euthanized at the times indicated. The values of MnBn were plotted as a function of time; the elimination rate constants were estimated by linear regression analysis, and used to calculate the elimination $t_{1/2}$. To estimate average $t_{1/2}$ in rat skeleton, all values at each time point were averaged and the linear regression method was then used.

2.4.4 Correlations between Mn Concentrations in Bone and Mn Concentrations in Selected Brain Regions

To test the hypothesis that Mn stored in bone tissues may serve as the internal source of Mn in brain, a linear regression method was used to correlate Mn concentrations in the striatum and hippocampus with MnBn from the same animals. Since the choroid plexus in brain ventricles transports metals and secretes the CSF, which provides the internal milieu of the CNS (Zheng et al., 2003), correlations between MnBn and Mn concentration in choroid plexus and CSF collected from the same animals were also investigated. The results showed that there were strong correlations between MnBn and Mn levels in striatum (correlation coefficient r=0.7549, $p < 0.001$) and hippocampus (r=0.7823, $p < 0.001$). Interestingly, the Mn concentration in the choroid plexus was also strongly associated with MnBn (r=0.6519, $p < 0.001$), so was the correlation between MnBn and CSF (r=0.7204, $p < 0.001$), suggesting that bone could potentially serve as an endogenous source of Mn to the body and CNS (**Fig. 5**).

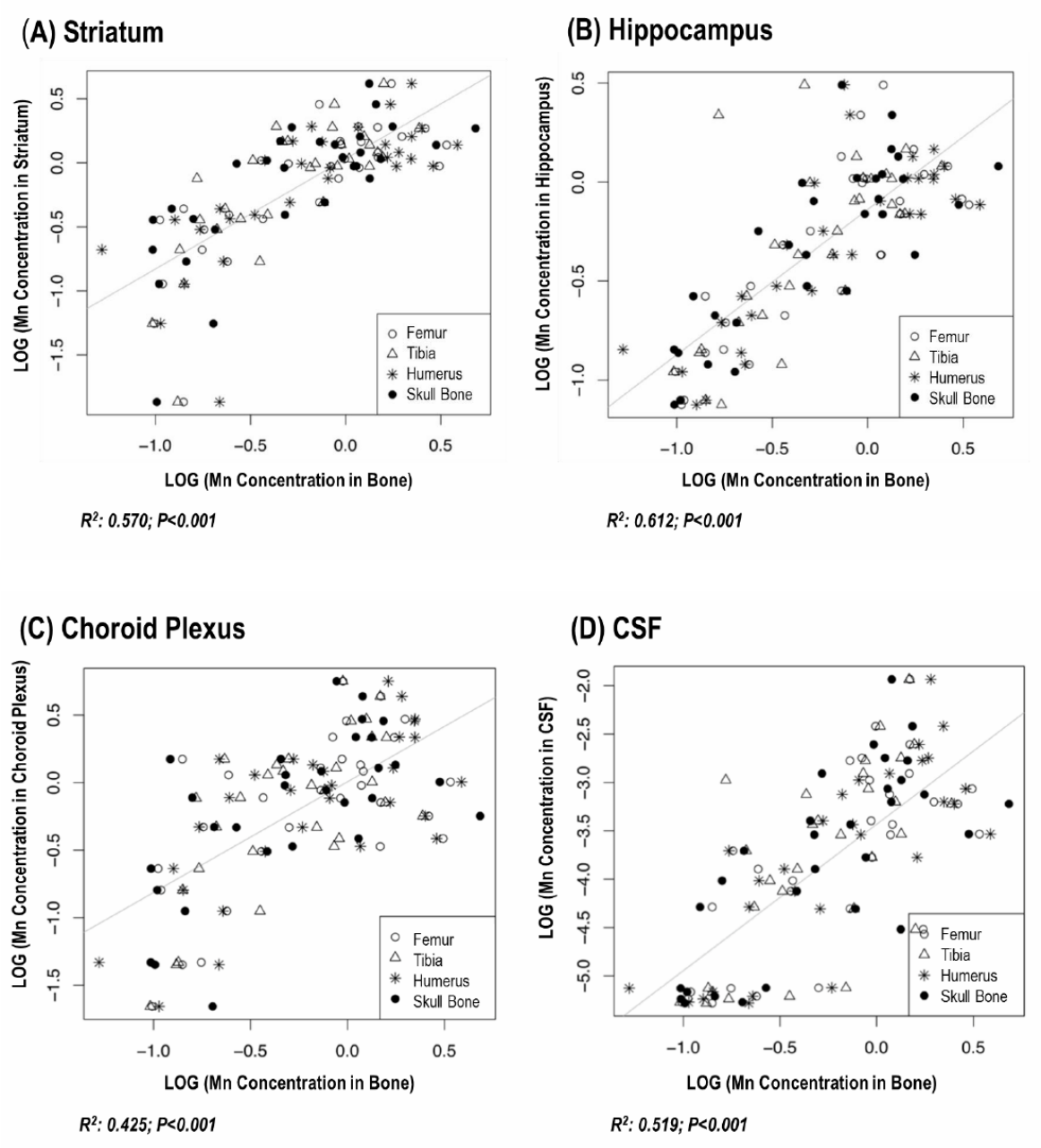

Figure 5. Changes of Mn Concentrations in Brain, Choroid Plexus and CSF as a Function of Mn Concentration in Bone. Mn concentrations in all tissues were determined by AAS. Liner regression was used to estimate the correlation coefficients.

2.4.5 Correlation of Mn in Bone with Concentrations of Fe, Cu, and Zn in Rat Skeleton

To understand how Mn accumulation in bone affects accumulation of other metals, such as Fe, Cu, and Zn in the rat skeleton, the linear regression method was again used to correlate MnBn with concentrations of Fe, Cu, and Zn in femur, tibia, and humerus bones from the same animals. The results showed there were strong positive correlations between MnBn and Fe levels in the rat bones ($r=0.8509$; $p < 0.001$), and MnBn and Zn ($r=0.7510$; $p < 0.001$), but an inverse correlation between MnBn and Cu ($r=-0.7259$; $p < 0.001$; **Fig. 6**). The results suggested that Mn accumulation in bone likely affected other essential metals in bone.

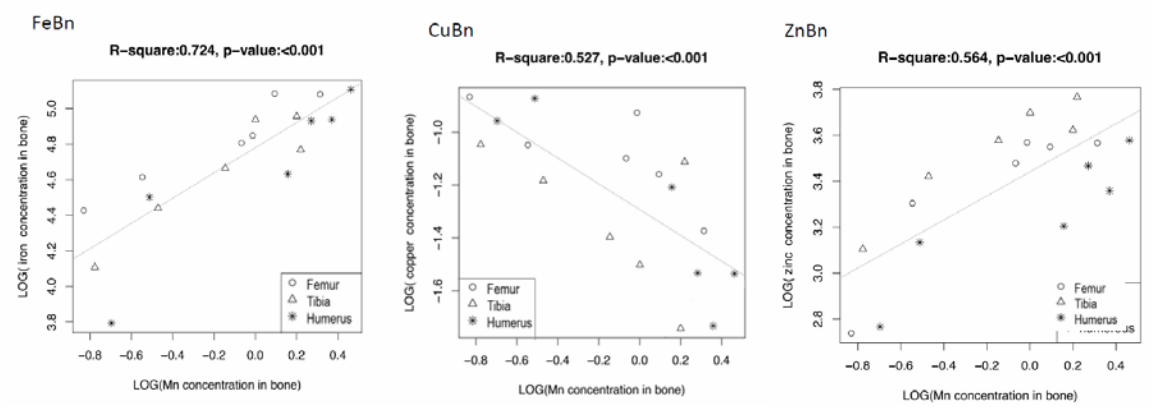

Figure 6. Changes of Fe, Cu and Zn Concentrations in Bone as a Function of Mn Concentration in Bone. Concentrations of Mn, Fe, Cu and Zn were determined by AAS. Liner regression was used to estimate the correlation coefficients.

2.4.6 MnBn in Rats with Other Mn Exposure Paradigm

A rapid time-dependent Mn accumulation in bone observed in Phase 1 of this study raised the question as to whether alternative Mn dose regimens and routes of exposure may lead to similar Mn accumulation in bone. In our previous studies, we have used a subchronic Mn exposure model by administering rats 6 mg Mn/kg (low dose) or 15 mg Mn/kg (high dose) as $MnCl_2$, 5 days per week for 4 weeks by intraperitoneal injection, and found significant alterations in neurochemical profiles (O'Neal et al., 2014b). To investigate bone Mn accumulation in this animal model, rats received ip injections of Mn with the same dose regimen. Following 4-weeks ip dose administration, MnBn was significantly increased in both exposure groups as compared to controls (49.3 ± 9.3 for low dose, 172.9 ± 35.3 for high dose vs. 13.0 ± 7.8 for control; mean ± S.D. μg/g; $p < 0.01$; **Fig. 7**). It was apparent that Mn accumulated in bone tissues was in a dose-dependent manner after ip Mn exposure.

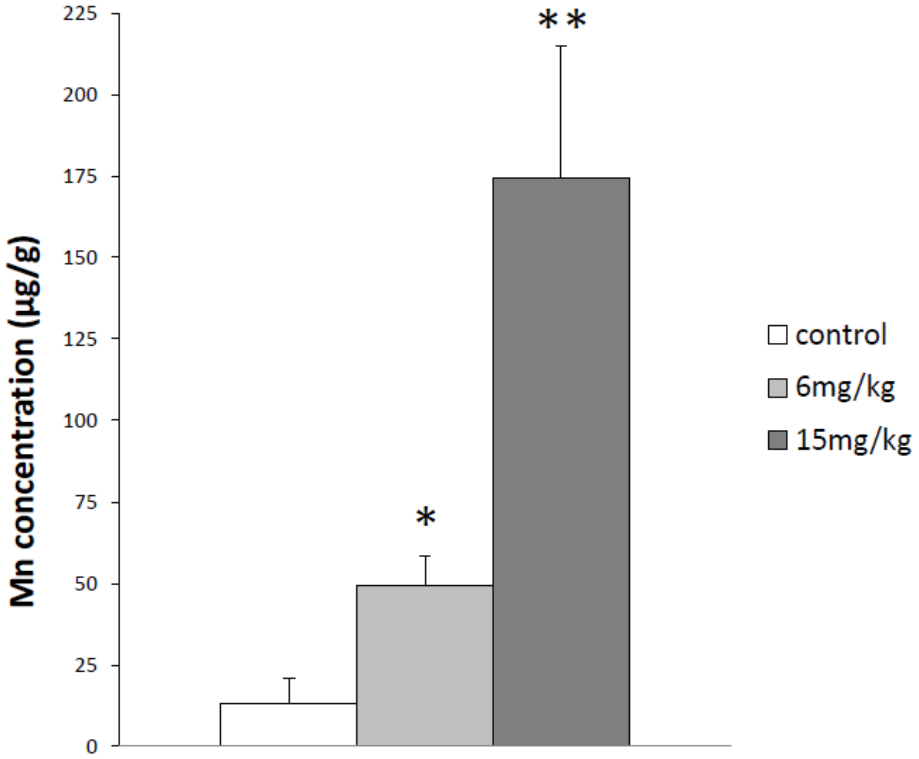

Figure 7. Mn Concentration in Rat Bone after Chronic IP Injection Exposure. Rats received 6 mg Mn/kg as $MnCl_2$ by ip. injections once daily, five days per week, for 4 weeks. Data represent mean ± S.D., n = 5-6; *$p < 0.05$, ** $p < 0.01$

2.4.7 Mn Concentration in Muscle

In vivo noninvasive measurements of MnBn (Liu et al., 2013) will likely include some contribution of Mn present in skeletal muscle. We determined Mn concentrations in muscle in animals receiving oral doses of Mn. The soleus muscle was selected because of its proximity to the tibia, one of the bones commonly measured *in vivo*. This proximity makes soleus muscle the ideal candidate for examination because it will directly impact measurements of MnBn in humans. The results showed an initial increase of Mn in the soleus muscle, which reached a statistical significance after only 4 weeks of dose administration ($p < 0.05$; **Fig. 8**). However, similar to the Mn concentrations in plasma and CSF, the levels of Mn began to decrease despite continued administration of Mn, and stayed relatively unchanged in comparison to controls at time 0 (~0.35-0.40 µg/L). Thus, it seems likely that under long-term, chronic exposure conditions, the Mn concentration in muscle tissues would remain at a relatively constant level.

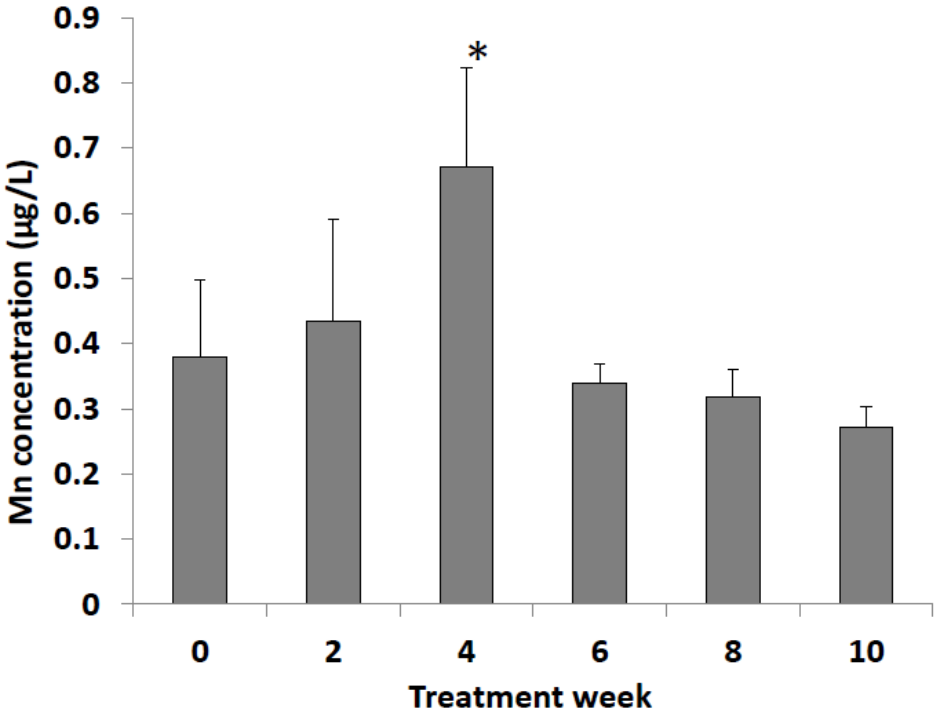

Figure 8. Mn Concentration in Muscle after Chronic Oral Mn Exposure. Mn concentrations in soleus muscle were determined by AAS. Data represent mean ± S.D., n = 5-6; * $p < 0.05$. Figure 17. Time-dependent accumulation of Mn in selected brain regions following chronic oral Mn exposure. Rats received 50 mg Mn/kg as $MnCl_2$ by oral gavage once daily, five days per week for the time indicated. Mn concentrations in brain were determined by AAS. Data represent mean ± S.D., n = 5-6; *$p < 0.05$, ** $p < 0.01$.

2.5 Discussion

This study is the first to report estimations of the $t_{1/2}$ of Mn in bone after a chronic oral Mn exposure. Other reports in literature have described extensive Mn accumulation in bone (Pejovic-Milic et al., 2009; Schroeder et al., 1966; Zaichick et al., 2011); yet none has calculated the half-life of Mn in the rat skeleton.

Occupational exposure to Mn in the air at concentrations from 0.1-1.27 mg/m^3 shows levels of Mn in the blood to be 10.3-12.5 µg/l (Vezér et al., 2007). Among patients with clinical signs and symptoms of manganism, the blood Mn concentration varies between 4-40 µg/L (Crossgrove and Zheng, 2004; Inoue and Makita, 1996; Jiang, et al., 2007). Interestingly, the plasma Mn concentration in rats at day 30 following this oral dose regimen is ~20 µg/L; the level is highly comparable to human Mn blood level at poisoning. Interestingly, the steady-state concentrations of Mn in rat striatum under this dose regimen are about 1-1.2 µg/g between four and six weeks of dose administration; under this brain concentration range, a significant striatal neurodegenerative injury has been observed (Fujioka et al., 2003). Noticeably, environmental exposure to Mn has been known to occur through eating foods and drinking water contaminated with Mn (ATSDR, 2012). Studies of humans drinking contaminated water in Bangladesh and Greece show that levels of Mn between 50 µg/l and 8.61 mg/l can cause adverse health effects (Hafeman et al., 2007; Kondakis et al., 1989). The LD_{50} of oral $MnCl_2$ exposure in rats is 338 mg/kg (McMillian, 1999). Our dose of 50 mg/kg is approximately 15% of this value. Although rats were exposed orally in the current study, the ATSDR (2012) reports that health effects observed after an oral exposure are similar to those observed after an inhalation exposure. Thus, the current oral Mn administration appears to be an

appropriate animal model for chronic Mn intoxication study including Mn accumulation and elimination from bone tissues.

It is interesting to know that in the first 4 weeks of Mn dose administration MnBn continued to increase, while the blood Mn concentration started to decline by the end of the 4^{th} week of dosing. Although the blood Mn concentration returned to nearly baseline level after 10 weeks of exposure, MnBn remained significantly higher than in controls. This observation supports the view that a short blood $t_{1/2}$ of Mn is due primarily to its intracellular distribution (Zheng et al., 2000) and thus, Mn blood concentration is deemed insufficient for assessment of Mn exposure or health risk (Zheng et al., 2011). Data from the current study clearly demonstrate that the bone tissue serves as a storage site upon Mn chronic exposure. Indeed, the average $t_{1/2}$ of MnBn was estimated to be about 143 days. In a comparative study of human and rat developmental time points and associated body weights, Sengupta (2011) proposes that every 16.7 days throughout the life of the rat is equivalent to one human year. Using this analogy, we estimate the half-life of Mn in the rat femur to be 4.61 years, tibia 15.75 years, humerus 25.69 years, and parietal bone would be an astounding 41.32 years. To estimate the value for the entire skeleton, it is more appropriate to take the half-lives of bone sampled from different body parts. Thus, by using the average half-life in in the current study, we estimate that the average half-life of Mn in the rat skeleton corresponds to 8.6 years for humans.

The current study also reveals an interesting observation, i.e., the shortest half-lives of Mn are observed in the weight-bearing bones. Specifically, we observed the shortest half-lives in femur and tibia bones and the longest in parietal bone. Regarding animal locomotor behavior, rats are a generalist species, with skeletal structures

developed for burrowing, running, jumping, and walking. Although not bipedal, rats do spend time standing on their hind limbs while exploring or searching for food. This potentially puts more pressure on the femur and tibia bones when compared with their humerus or parietal bones. This leads to another interesting question as to why the weight-bearing bones have a shorter storage time for Mn.

In both adult humans and rats, the main function of the skeleton is remodeling. Bone remodeling consists of both bone formation and resorption. Between the different types of bones, there are anatomical and functional differences. For example, the perfusion rate within tubular long bones differs between areas of cortical bone such as the diaphysis, and areas of trabecular bone, including the femoral head and neck. Tøndevold and Eliasen (1982) have found that the perfusion rate is highest in areas with more trabecular bone and lowest in the diaphysis with more cortical bone. They also show that the perfusion rate is similar between the femur and tibia (Tøndevold and Eliasen, 1982), although the differences between these and other bone types, such as parietal bone, remain unknown. Serrat et al. (2007) indicate that some bones, such as the humerus, have different ossification patterns than does the femur. Bancroft et al. (2002) also suggest that the differences in fluid perfusion rates among bone tissues could alter the levels of nutrients including intracellular calcium and other biochemical factors, such as prostaglandin E2 and cyclooxygenase-2 in bone *in vitro*. Further, they observe that the fluid flow in these tissues mechanically stimulates pressure gradients so to move fluid outward into the cortical bone (Bancroft et al., 2002). Taking into account these literature data, we postulate that differences in anatomical structure, perfusion rate of bone tissues,

and hydrostatic pressure or compression may explain the observed differences in Mn half-lives in different bones.

In the present study, we do not see significant changes in animals' body weights after chronic Mn oral exposure. However, we did observe the weight of femur bone to be significantly reduced after 18 weeks of Mn exposure. This observation suggests that in addition to simple storage, Mn ions accumulated in bone may have a direct detrimental effect on bone's normal structure and function. In addition, we found that MnBn was positively associated with Fe and Zn in bone but inversely related to Cu. The implications of these relationships are currently unknown. Thus, Mn-induced osteotoxicity as a result of chronic Mn exposure in humans as well as animals deserves further in-depth investigation.

To understand whether MnBn could be used as a potential biomarker for Mn-induced neurotoxicity, we correlated MnBn with Mn levels in selected brain regions, including striatum, hippocampus, and choroid plexus from the same animals. It was evident that the values of MnBn were well correlated with each of these brain regions. These relationships are important for studies of Mn neurotoxicity in humans, for striatum is known to accumulate Mn to a great extent in humans (Dydak et al., 2011; Jiang et al., 2007), hippocampus is a potential target of Mn toxicity (Wang et al., 2012), and Mn accumulation in the choroid plexus is known to cause the dysregulation of the homeostasis of iron and copper in the central milieu (Zheng et al., 2003; 2012).

One of the purposes of this study was to build a theoretical foundation for human noninvasive quantitation of MnBn by using a novel deuterium-deuterium (DD) neutron generator–based neutron activated analysis (NAA) system (Liu et al., 2013). A

transportable version of this system, which has been developed recently at Purdue University, has a detection limit of 0.7 ppm (μg/g). Schroeder et al. (1966) report that normal human subjects have a MnBn of 2 μg/g, which was determined using postmortem human bone tissues. Based on our current data, MnBn at the steady-state exceeds 1 μg/g. Thus, this transportable AAS device shall be of practical value in human study. The concentration of Mn in muscle was also determined in order to understand the kinetic changes of Mn levels in this tissue. Our results demonstrated that the Mn concentration in muscle remained constant after chronic exposure. Taken together, we feel that because MnBn has a long half-life, is well correlated with levels of Mn in brain and is not interfered by Mn in muscle, the MnBn measured *in vivo* by the transportable NAA system would serve as an excellent biomarker of Mn exposure in occupational and environmental research.

This study has limitations. First, the study as designed does not allow us to investigate the regional distribution and deposition of Mn within bone. Current studies in the lab are investigating the differences in distribution of Mn between cortical and trabecular bone. At the time of writing, our preliminary data from animals exposed to 6 mg Mn/kg as $MnCl_2$ via ip injection five days per week for four weeks suggests that Mn accumulates in the trabecular bone of control animals, but in the cortical bone of Mn-exposed animals. Further work by synchrotron XR technique to depict regional distribution of Mn in bone is desirable. Second, our current study does not address how Mn ions gain access to bone tissues, what subcellular ligands in bone tissues Mn ions are bound with, and whether Mn transporters, such as divalent metal transporter-1 (DMT1) and transferrin receptor (TfR), play any roles in Mn deposition and its toxicity to other

metals. Finally, due to the limited budget, the current study was not able to investigate the percentage of Mn in bone with regards to the total body burden, although such percentages have been reported in literature (see Introduction).

In summary, the data presented in this report suggest that a 4-week Mn oral exposure can lead to a significant accumulation of Mn in bone tissues. The half-lives of Mn in rat bone are in the range of 77-690 days with an average of 143 days. Moreover, the weight-bearing bones such as femur appear to have a shorter $t_{1/2}$ than non-weight bearing bones. Since brain Mn levels change as a function of MnBn, we propose that the MnBn may be an effective biomarker for assessment of Mn exposure and health risk.

CHAPTER 3: SUBCHRONIC MANGANESE EXPOSURE ALTERS NEUROCHEMISTRY IN A RAT MODEL

3.1 Abstract

High levels of manganese (Mn) in the brain are neurotoxic and result in a progressive, irreversible disorder known as manganism which includes both psychological and motor disturbances. Evidence suggests that Mn exposure impacts neurotransmitter levels in the brain. However, it remained unclear if subchronic, low-level Mn exposure resulted in alterations in neurotransmitter systems with concomitant behavioral deficits. The study in this chapter used high performance liquid chromatography (HPLC) to quantify neurotransmitter levels in rat striatum, substantia nigra, and hippocampus. Subchronic Mn exposure via i.p. injection of 15 mg Mn/kg as $MnCl_2$ caused significantly increased dopamine levels in the striatum. The enhancement was accompanied by significantly elevated levels of the dopamine metabolites, DOPAC and HVA, in the striatum. In addition, levels of HVA were significantly increased in the substantia nigra and hippocampus. Mn toxicity on neurochemical concentrations in brain could be the consequences of Mn accumulation in bones (Chapter 2). These data indicate that subchronic, low-level Mn exposure disrupts multiple neurotransmitter

systems in the rat brain which may be responsible, in part, for observed locomotor deficits. The data presented in this chapter may provide clues to understanding the effects of Mn exposure on adult neurogenesis (investigated in Chapter 4).

3.2 Introduction

Manganese (Mn) is an essential trace element required for normal function and development of many physiological processes. In the central nervous system, Mn functions as a cofactor for enzymes necessary for neuronal function and neurotransmitter biosynthesis, such as superoxide dismutase 2, pyruvate decarboxylase, and glutamine synthetase (Aschner et al., 2009; Bowman et al., 2011; Schneider et al., 2009). Normally, regulatory mechanisms carefully maintain homeostatic levels of Mn in the body by controlling absorption and elimination of excess metal via hepatobiliary excretion (Klaassen, 1976). However, excess Mn exposure can overload these mechanisms (Schneider et al., 2009), leading to Mn accumulation in body tissues, including bone (Chapter 2), liver, kidney, and pancreas (Dobson et al., 2004). Mn in the 2^+ and 3^+ states readily crosses the blood-brain barrier (BBB) (Aschner et al., 1999) and preferentially accumulates in specific brain regions, such as striatum (STR), globus pallidus, cerebellum, and hippocampus (HP) (Andersen et al., 2010; Fitsanakis et al., 2008; O'Neal and Zheng, 2015).

Adequate levels of Mn are obtained from food, such as nuts, tea, and legumes, and water intake (Bowman et al., 2011). Mn dusts in the air, Mn-containing pesticides in

soil, contaminated water, and occupational exposure during mining and agricultural processes, are potential sources of toxic exposure (Mergler, 1999). The highest levels of exposure are observed in the workplace, where workers chronically exposed to levels < 5 mg/m^3 have reported symptoms of Mn toxicity (Crossgrove & Zheng, 2004). These symptoms result from toxic Mn accumulation in the caudate putamen, globus pallidus, STR, and substantia nigra (SN) (Aschner et al., 1999) and are clinically diagnosed as manganese intoxication or manganism. Manganism is a severe, progressive and largely irreversible disorder that resembles, but is distinguishable from idiopathic Parkinson's disease (PD) and other extrapyramidal motor disorders (Racette et al., 2012a).

The prevailing symptoms of manganism include poor hand-eye coordination, bradykinesia, changes in mood and memory deficits, abnormal gait, muscle and joint pain or weakness, bent posture, and a kinetic tremor (Mergler, 1999; Racette et al., 2012a). These symptoms exist as a slowly progressing biphasic continuum, with psychiatric symptoms appearing first in the "prodromal period" or early phase of the disease, while motor symptoms dominate the later, "established" phase (Racette et al., 2012a; Rodier, 1955) and persist even after the person is no longer exposed to Mn (Aschner et al., 2009; McMillian, 1999).

Mn accumulation in the basal ganglia may alter levels of neurotransmitters, such as dopamine (DA) and GABA, in the striatum and in pathways postsynaptic to the nigrostriatal system (McMillian, 1999; Racette et al., 2012a) which produce the observed motor symptoms. Data from rodent studies generally offer conflicting reports on how Mn exposure affects neurochemistry and motor function. A general consensus regarding

the effects of Mn on motor function is that hyperactivity is observed early in Mn toxicity, in both human and animal studies, and as the disease progresses, patients and animals both tend to become hypoactive.

There is evidence that Mn exposure results in a Parkinson's phenotype, with decreased dopamine in the striatum. However, dopaminergic neurons in the substantia nigra and their terminals in the striatum, which are selectively lesioned in Parkinson's disease, remain intact after Mn intoxication (Guilarte, 2010). Thus, changes in neurotransmission, as opposed to frank cell-loss, likely underlie behavioral observations. Most studies to date have focused on striatal dopamine levels and not regional differences in other monoamines and their metabolites, or GABA. Additionally, few studies have aimed to investigate changes in motor function in animals, particularly rodents, despite many of the prominent symptoms of manganism being motor deficits, including abnormal gait and postural impairment. Therefore, the present study was undertaken to identify alterations in multiple neurotransmitter systems resulting from subchronic, low-level Mn exposure in rats. We have previously used a Mn exposure dose regimen, i.e., 6 mg/kg i.p. injection for 4-6 weeks to study Mn toxicity on iron (Fe) and copper (Cu) transport properties in brain barrier systems (Zheng et al., 1999; Zheng et al., 2009). To ensure a dose-related response, the current study used two dose levels, 6 mg/kg and 15 mg/kg, which bracket the commonly used doses to investigate changes in Mn levels with concomitant changes in regional neurochemistry, motor function, and changes at the cellular level. Neurotransmitter levels were assessed in the striatum, substantia nigra, and hippocampus, an area implicated in learning and memory. It was necessary to study the

hippocampus because many of the earliest symptoms of manganism are due to impaired memory. Thus, examination of changes in 4 neurotransmitter (dopamine, norepinephrine, serotonin, and GABA) systems in multiple brain regions was expected to provide significant data on the complex neurochemical changes that result from Mn intoxication.

3.3 Materials & Methods

3.3.1 Chemicals

All chemicals were of analytical grade, HPLC grade or the highest available pharmaceutical grade. HPLC grade water was obtained from a NANOpure Diamond Ultrapure Water System (Barnstead International, Dubuque, IA); Mn chloride tetrahydrate ($MnCl_2 \cdot 4H_2O$) from Fisher Chemical (Fair Lawn, NJ); nitric acid, tripotassium phosphate (K_3PO_4) and DPX mountant from VWR International (Radnor or West Chester, PA); Mn, Cu, Zn, and Fe stock solutions from SCP Science (Champlain, NY); perchloric acid from RICCA (Arlington, TX); dopamine, 3,4-dihydroxyphenylacetic acid (DOPAC), homovanillic acid (HVA), 5-hydroxytryptamine (5-HT), 5-hydroxyindolacetic acid (5-HIAA), noradrenaline (NE), γ-aminobutyric acid (GABA) standards, disodium hydrogen phosphate, anhydrous (Na_2HPO_4) triethylamine (TEA), octanesulfonicacid (OSA), acetonitrile, paraformaldehyde (PFA), sodium phosphate monobasic (NaH_2PO_4), Triton X-100, and porcine skin gelatin from Sigma (St. Louis, MO). Bovine serum albumin (BSA) was purchased from Thermo Scientific

(Rockford, IL); methanol, ethylenediaminetetraacetic acid (EDTA), and sucrose from Macron Fine Chemicals (Center Valley, PA); *o*-phthalaldehyde (OPA) from Pickering Laboratories (Mountain View, CA); and BCA protein assay kit from BioRad (Hercules, CA). Normal donkey serum was purchased from Jackson ImmunoResearch (West Grove, PA); mouse monoclonal anti-TH and rabbit polyclonal anti-DARPP-32 antibodies from Millipore (Temecula, CA); secondary donkey anti-mouse IR800 and donkey anti-rabbit IR800 antibodies from LICOR (Lincoln, NE); histoclear from National Diagnostics (Atlanta, GA); potassium permanganate from Amresco (Solon, OH); Fluorojade C from Histochem (Jefferson, AR); and glacial acetic acid from Mallinckrodt Chemicals (Phillipsburg, NJ).

3.3.2 Animals

Male Sprague Dawley rats were obtained from Harlan Laboratories, Inc. (Indianapolis, IN) and allowed to acclimate to the holding room for 7 days after arrival. Rats at time of experimentation were 8 weeks of age, weighing approximately 240-260g at study initiation. Animals were randomized by drawing numbers for treatment designation. Rats were group housed in a temperature- (72 ± 4 °C) and humidity- (30-70%) controlled room on a 12 hour light/dark cycle (lights on at 0600). Rats had ad libitum access to food (Harlan 2018 rodent diet) and reverse osmosis water.

All animal studies were approved by the Institutional Animal Care and Use Committee at Purdue University.

3.3.3 Mn Administration and Experimental Design

According to Cooper (1984), doses of 5-20 mg/kg/d have not been shown to be very toxic in animal studies and therefore, our selected doses should not cause acute toxicity. The dose of 6 mg/kg was selected because it has been administered previously in our lab by multiple dose routes, including intravenous, oral, and intraperitoneal. With this dose, our lab has shown a significant reduction in both succinate dehydrogenase and aconitase (Zheng et al., 1999).

Stock solutions of 6 mg Mn/ml (low dose) and 15 mg Mn/kg (high dose) were prepared by dissolving $MnCl_2 \cdot 4H_2O$ in saline and passing through a 0.2 μm syringe filter. Mn-exposed rats received ip injections of either 6 mg Mn/kg or 15 mg Mn/kg in a volume of 1 ml/kg once per day, 5 days per week, for 4 consecutive weeks. Control animals were administered the same volume of sterile saline.

3.3.4 Sample Collection

Animals were euthanized by decapitation 24 h after the last dose. Brains were quickly removed from the skull and bisected midsagittally. The left hemispheres were stored in 4% paraformaldehyde for histological evaluation. The right hemispheres reserved for neurochemistry were placed in a coronal rat brain matrix and 2 mm slices containing the desired brain regions were obtained. The samples were then further dissected on ice to obtain striatum, substantia nigra, and hippocampal samples, which were then flash-frozen in liquid nitrogen. Liver and femur tissues were collected for

determination of metal concentrations using atomic absorption spectroscopy (AAS). Samples were stored at -80°C until processing.

3.3.5 Behavioral Testing

On days 8, 11, and 18 of dosing, animal's locomotor activity was evaluated using an open field behavioral test. Animals were transferred to the behavioral testing room and placed inside an open field chamber. The chambers were constructed of solid opaque Plexiglas measuring 40 cm × 40 cm. Top Scan Lite computer software (version 2.0; Clever Sys Inc. Copyright 2000-2011) was used to generate a model of the open field chamber with accurate perimeter measurements and a center field comprising 60% of the total area. Animals were placed in the open field chambers for 5 min and their positions were recorded by a camera mounted on the ceiling. Behavioral testing conditions were simulated on two separate occasions during the first week of dosing to acclimate the animals to the testing environment. Animals' average velocities and distances traveled during the experiment were quantified using the Top Scan Lite software.

3.3.6 Atomic Absorption Spectroscopy

Liver and femur samples collected at necropsy were weighed on an analytical balance (AB204-S; Mettler Toledo, Columbus, OH) and transferred to a digestion vial. A total volume of 2 ml nitric acid (HNO_3) was added to each sample. Tissues were digested in a high pressure MarsXpress microwave (CEM Corporation, Matthews, NC) for 15 min at 200°C. Each digestion was transferred to a volumetric flask and diluted

with ddiH_2O to 5 ml. Each digestion solution was mixed thoroughly, transferred to a 15 ml conical tube, sealed with parafilm, and stored at 4°C until analysis. Hepatic and femur Mn, copper (Cu), zinc (Zn), and iron (Fe) concentrations were quantified using an Agilent Technologies 200 Series SpectraAA with GTA 120 graphite furnace (Santa Clara, CA). Concentration ranges of standard solutions were between 1-10 ppb for Mn, 1-50 ppb for Cu, 1-1.05 ppb for Zn, and 1-20 ppb for Fe. A 0.1% HNO_3 blank was prepared and used to dilute metal standards at 1000 mg /l to appropriate working standards. Samples were further diluted with ddiH_2O to keep the readings within the concentration range of the standard curves. The detection limit for Mn was 0.038 µg/l of the assay solution. Metal content was expressed as µg/g of tissue.

3.3.7 Neurochemical Analysis

Neurotransmitter analysis was conducted similarly as previously described (Wang et al., 2013). Briefly, STR, SN, and HP samples were frozen in liquid nitrogen at necropsy and stored at -80°C until processing. Samples were sonicated in 0.5 ml 0.4N perchloric acid ($HClO_4$) on ice, at 40% power, pulsing for 45 s to precipitate proteins. Samples were then centrifuged at 16,400 *g* for 35 min at 4°C. Supernatant was transferred to 0.22 µm Spin-X tube with nylon filter (Corning, Corning, NY) and centrifuged at 1000 *g* for 15 min at 4°C. Samples were then stored at -80°C until HPLC analysis. A Dionex UltiMate 3000 (ThermoScientific; Germering, Germany) system with a built in autosampler and a Coulochem III (Thermo Scientific) electrochemical detector were used for HPLC analysis of DA, its metabolites DOPAC and HVA, as well

as 5-HT and its metabolite 5-HIAA, NE, and GABA. The optimized method used an isocratic monoamine mobile phase (consisting of 0.08 M NaH_2PO_4, 10% methanol, 2% acetonitrile, 2.0 mM OSA, 0.025 mM EDTA, and 0.2 mM TEA, in 13 mΩ purified water, pH 2.4). Samples were injected and monoamines separated on a reverse phase C18 column (150 x 3.2mm, 3.0 μm particle size, MD-150, Thermo Scientific, Bannockburn, IL) protected by a guard column. Separation occurred at 32 °C at a flow rate of 0.6 ml/min. For GABA detection, samples were derivatized with OPA (*o*-phthalaldehyde, methanol, and 2-mercaptoethanol) before injection onto the column. The isocratic mobile phase (pH 6.75) consisted of Na_2HPO_4 in 13 mΩ purified water with 22% methanol and 3.5% acetonitrile. Separation occurred at 35°C with a flow rate of 0.5 ml/min. For monoamine neurotransmitter and metabolite detection, the electrochemical potential of the detector was set at 250 mV, with a conditioning cell at -150 mV. For GABA detection, the electrochemical potential of the detector was set at 550 mV, with a conditioning cell at -150 mV. Neurotransmitter and metabolite levels in each sample were quantified by comparing sample values to a reference curve prepared by adding standards of a known concentration to perchloric acid. Chromeleon 7.0 software was used for data acquisition and analysis. Neurotransmitter concentrations were expressed as ng/mg of protein as assessed by BCA protein assay (Smith et al., 1985) using BSA as the standard (Bradford, 1976).

3.3.8 Immunohistochemistry

At necropsy, the left hemisphere was immersed in 4% paraformaldehyde (PFA, catalog # P6148-500G; Sigma, St. Louis, MO) and post-fixed for 7 days at 4°C. Then, hemispheres were stored in a 30% (w/v) sucrose (catalog # 8360-06; Macron Fine Chemicals, Center Valley, PA) solution until sinking. The hemispheres were coronally sectioned in 30µm increments on a microtome (Microm HM450, Thermo Scientific; Walldorf, Germany) and sections were placed in cryoprotectant solution and stored at -20°C until labeling. Free-floating slices were rinsed 6 times with phosphate buffered saline (PBS), 10 min per rinse. Sections were blocked in 10% normal donkey serum in PBST containing 0.3% Triton X-100 for 1 h. Sections were incubated in primary antibody, either mouse monoclonal anti-TH (1:2000; cat. #MAB318; Millipore; Temecula, CA) or rabbit polyclonal anti-DARPP32 (1:500; cat.#AB10518; Millipore; Temecula, CA) diluted in PBST with 1% donkey serum for 72 h at 4°C. Sections were rinsed 3 times with PBS and incubated with either donkey anti-mouse IR800 (1:500; cat.#926-32212; Li-Cor; Lincoln, NE) or donkey anti-rabbit IR800 (1:500; cat.#926-32213; Li-Cor; Lincoln, NE) diluted in PBST with 1% donkey serum for 2 h at room temperature. After 3 washes with PBS, sections were mounted on slides and air-dried overnight at room temperature. After immersion in Histoclear for 10 min, slides were blotted dry and coverslipped with DPX mountant. Immunofluorescence quantification was performed similar to previously described (Cannon et al., 2013; Tapias et al., 2014). Briefly, immunofluorescence was detected with the Odyssey infrared imaging system

(Li-Cor; Lincoln, NE) at 21µm resolution. Regions of interest were selected and intensity of each region determined using Image Studio software (version 3.1).

Another set of slices was processed for Fluorojade C staining to identify degenerating neurons. Slices were removed from cryoprotectant and rinsed 6 times in PBS for 10 min per rinse. Slices were mounted on slides coated with 0.5% porcine skin gelatin and dried overnight at room temperature. Slides were then immersed for 5 min in 0.03M tripotassium phosphate (K_3PO_4,) in 70% ethanol, diluted from 200% ethanol in water, and then rinsed in 70% ethanol and water for 2 min each. Followed by immersion in a 0.06% potassium permanganate solution for 10 min and rinsed in water for 2 min. Slides were immersed in a 0.0001% Fluorojade C solution, diluted in 0.1% glacial acetic acid for 10 min followed by 3 rinses in water for 2 min each. Slides were dried on a 50°C heating block (Lab Line Instruments, Inc.; Melrose Park, IL) for 5 min and cleared in Histoclear for 1 min. At this point, slides were blotted dry and coverslipped with DPX mountant. All Fluorojade C staining steps were performed at room temperature. Negative control slices were treated in the same manner as all other slices, but primary antibody was omitted. Slices from animals treated with kainic acid were used as a positive control (Sarkar & Schmued, 2011). Fluorescence was assessed on an Olympus (BX53F; Tokyo, Japan) microscope using a FITC filter and 50 ms pixel dwell time. The microscope was equipped with an Olympus (U-HGLGPS; Tokyo, Japan) light source.

3.3.9 Statistical Analysis

All data are expressed as mean ± S.D. Statistical analyses of the differences between groups were carried out by one-way ANOVA. Where ANOVA analysis indicated that significant differences between groups occurred, specific differences were identified by post hoc analysis using Tukey's test. Statistical analysis of the behavioral data was done by one-way ANOVA with repeated measures. A *p*-value less than 0.05 was considered statistically significant. All analyses were conducted using Graph Pad Prism (Version 3.0, Graph Pad Prism; San Diego, CA).

3.4 Results

3.4.1 Mn Exposure Reduces Body Weight

Animals were weighed daily prior to dose administration and weights recorded to the nearest 0.1 g (**Fig. 9**). At the beginning of the study, there was no significant difference in body weights between groups (n=5 in all groups). All animals weighed 252 ± 8 g. Mn treatment reduced animal's body weight in a dose dependent manner. Animals in the group receiving 6 mg Mn/kg lost an average of 10 g during the first three days of dosing and began to regain weight by the fourth day. Animals in the group receiving 15 mg Mn/kg lost an average of 40 g during the first five days of dosing and began to regain weight by the sixth day. Although Mn-treated animals regained weight to some extent, average body weights were significantly lower than control beginning on the second day of dosing, an effect that persisted for the duration of the study.

Noticeably, Mn dose administration by oral gavage at 50 mg/kg once daily, five days per week, for 6 weeks did not significantly reduce the body weight of Mn-treated animals compared with control animals; group averages at the end of the study were within 3g of one another (**Table 3**).

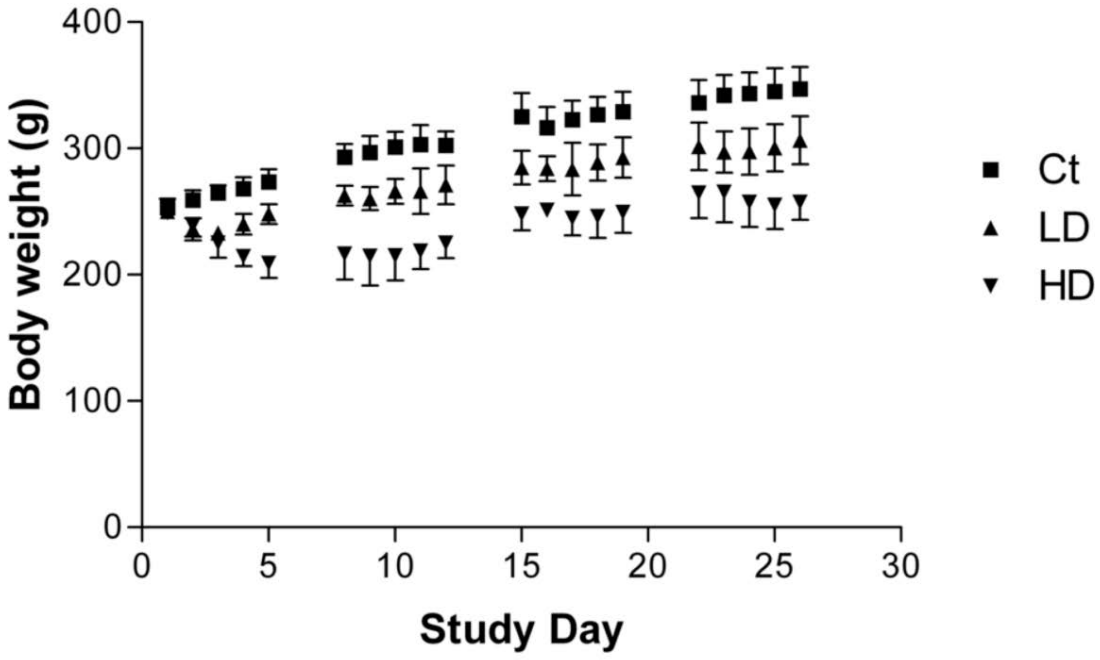

Figure 9. Daily Intraperitoneal Injections of $MnCl_2$ Resulted in Reduced Weight Gain among Mn-Exposed Animals. Rats were weighed prior to daily dose administration and weights were averaged for each group. Mn exposure resulted in significant changes in body weights in a dose-dependent manner. Control rats (square) consistently gained weight over the course of the study while animals in the low (6 mg/kg; triangle) and high (15 mg/kg; inverted triangle) dose groups showed an initial decrease in body weight but began to gain weight after 3 and 5 days, respectively. Rats in the Mn-exposed groups continued to gain weight, but at significantly reduced rate compared with controls for the duration of the study. Error bars indicate S.D.

3.4.2 Mn Accumulates in the STR and HP

AAS analysis was completed to determine if and to what extent Mn accumulated in brain tissue following Mn exposure. The levels of Mn in the STR and HP from both Mn-exposed groups were significantly higher than in controls ($p < 0.001$; **Table 4**).

Table 4. Concentration of Metal in Select Rat Brain Regions Following Subacute Mn Exposure. Atomic absorption spectroscopic analysis of Mn content in rat brain samples. Animals received i.p. injection of 6 or 15 mg/kg Mn once daily for 5 days per week for 4 weeks. Metal concentrations were quantified and are expressed as ug/g wet weight. Mn concentrations were significantly increased in the STR and HP of both Mn-treated groups compared with controls. Data represent mean ± S.D., n-7-10; $^{\#}p < 0.001$.

	6 mg Mn/kg as $MnCl_2$		15 mg Mn/kg as $MnCl_2$	
	STR	HP	STR	HP
Control	0.785 ± 0.229	0.642 ± 0.082	0.426 ± 0.164	0.337 ± 0.048
Treated	2.904 ± 0.483$^{\#}$	1.924 ± 0.313$^{\#}$	2.636 ± 0.745$^{\#}$	1.505 ± 0.458$^{\#}$

3.4.3 Mn Exposure Resulted in Hypoactivity

The average distance traveled decreased for animals in all groups between the first and the last training sessions (**Fig. 10A**). The average velocities correspondingly decreased for each group (**Fig. 10B**). However, these changes did not reach statistical significance. During the later training sessions, some animals exhibited long periods of inactivity in the testing chambers. Examination of these two related behavioral parameters at each time point revealed significant decreases in distance traveled during the second and third behavioral testing sessions for the high dose group as compared with the control group (10.4 ± 2.42 vs. 19.4 ± 6.71, 7.6 ± 2.70 vs. 16.2 ± 1.30 m, respectively; mean ± S.D.; high dose vs. control; $p < 0.05$). Additionally, the average velocity of the high dose group was significantly decreased compared to that of the control group during the third behavioral testing session (0.027 ± 0.011vs. 0.058 ± 0.002 m/s; mean ± S.D.; high dose vs. control; $p < 0.05$). No significant differences were observed during the first behavioral training session, which occurred during the second week of dose administration.

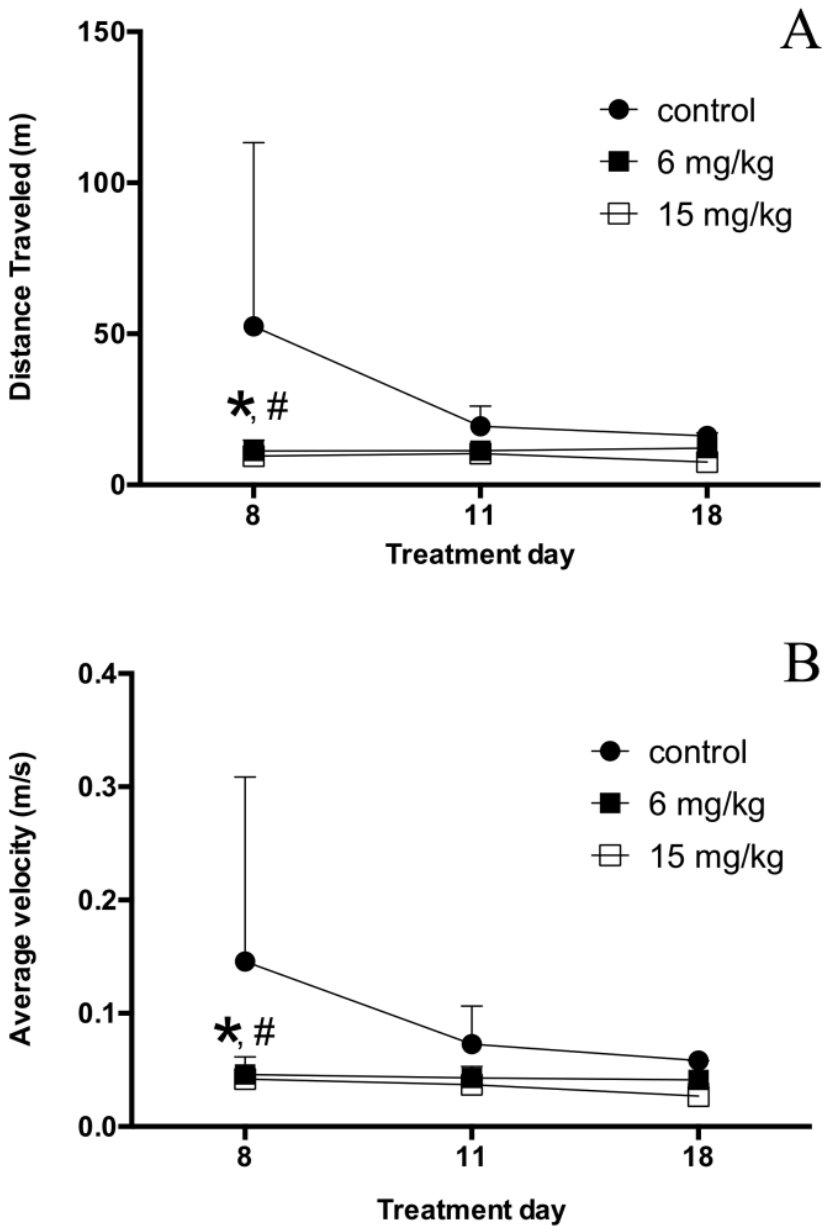

Figure 10. Open Field Analysis of Locomotor Activity. Distance traveled (**A**) and average velocity (**B**) were measured in an open field test on study days 8, 11, and 18. Animals were placed in the testing apparatus and behaviors measured for five minutes on each testing day. Values for each group were averaged and are shown. Distance traveled and average velocity were significantly reduced in both treatment groups compared with controls 8 days after Mn exposure began. These effects disappeared when animals were evaluated on study days 11 and 18. ANOVA with Tukey's post hoc test. Error bars represent S.D. (n = 3-5). *: $p < 0.05$ for 6 mg/kg group compared with control; #: $p < 0.05$ for 15 mg/kg group compared with control.

3.4.4 Levels of Biogenic Amines and Metabolites in Brain Tissue Following Mn Exposure

The DA level in the STR was significantly higher in the high-dose group than the control group (157.0 ± 15.73 vs. 99.8 ± 42.10 ng/mg protein; mean ± S.D.; high vs. control; $p < 0.05$; **Fig. 11A**). DA levels in the SN and HP displayed a non-monotonic curve, with no statistical significances, where levels were decreased following 4 weeks of low-dose Mn treatment and were slightly higher in the high dose group, but not quite reaching the same levels as the control group (**Fig. 11E,I**).

Levels of the DA metabolite, DOPAC, in the STR of the high-dose group was significantly higher than those of the low-dose and control groups *(*10.7 ± 2.16, 16.9 ± 1.68 vs. 10.6 ± 4.87 ng/mg protein; mean ± S.D.; low, high vs. control; $p < 0.05$ for both; **Fig. 11B**). Levels of DA and DOPAC were similarly elevated in both the SN and HP, but these changes did not reach statistical significance (**Fig. 11F,J**).

Following 4 weeks of high-dose Mn exposure, levels of the secondary DA metabolite, HVA, were significantly higher in the STR compared with the low-dose and control groups (5.4 ± 1.58, 10.5 ± 1.79 vs. 2.7 ± 3.63 ng/mg protein; mean ± S.D.; low dose, high dose vs. control; $p < 0.05$ and < 0.001, respectively; **Fig. 11C**). HVA levels in the SN and HP were also significantly higher in the high-dose group than in the control group (in SN, 0.6 ± 0.29 vs. 0.3 ± 0.06 ng/mg protein; in HP, 0.2 ± 0.04 vs. 0.1 ± 0.02 ng/mg protein; high dose vs. control; $p < 0.05$ and 0.01 respectively; **Fig. 11G,K**).

The DA turnover ratio was defined as the sum of the DA metabolites, DOPAC and HVA, divided by DA in each brain region. While DA turnover in the STR appeared to be increased, differences were not significant (**Fig. 11D**). In the SN, DA turnover was significantly increased for both Mn-treatment groups when compared with the control (1.5 ± 0.37, 1.6 ± 0.27 vs. 0.9 ± 0.22; mean ± S.D.; low, high vs. control; $p < 0.05$ for both; **Fig. 11H**). There was no difference between the turnover ratios of the low- and high-dose groups. In the HP, differences in DA turnover did not reach statistical significance (**Fig. 11L**).

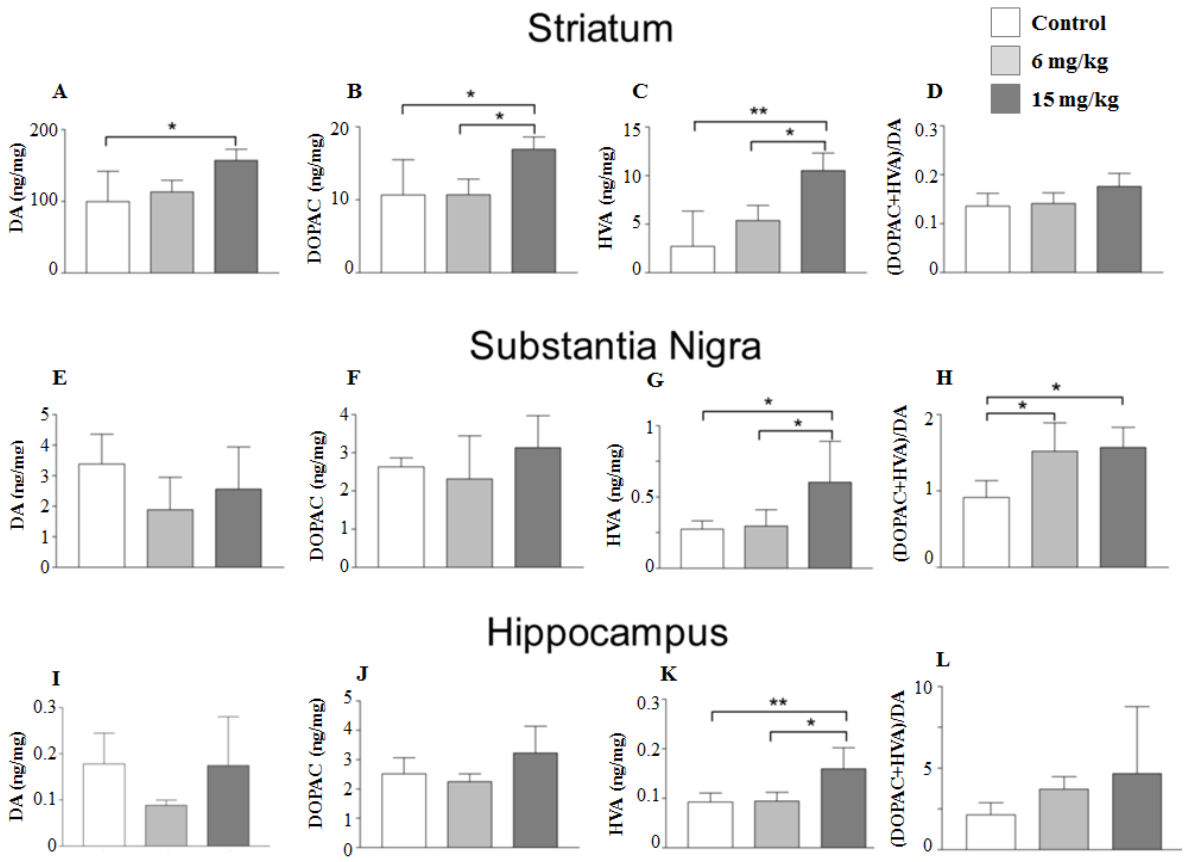

Figure 11. HPLC Analysis of Dopamine, its Metabolites, and Turnover. DA (**A,E,I**), and its metabolites 3,4-dihydrophenylacetic acid (DOPAC; **B,F,J**), and homovanillic acid (HVA; **C,G,K**) were quantified in STR (**A-C**), SN (**E-G**), and HP (**I-K**) by HPLC with electrochemical detection. DA turnover in each region was calculated as the sum of the metabolites divided by DA concentration (**D,H,L**). ANOVA with Tukey's post hoc test. Data represent mean ± S.D. (ng/mg protein; n = 3-5). *: $p < 0.05$, **: $p < 0.01$.

5-HT levels in the STR and SN were not significantly changed following either Mn-treatment as compared with the control (**Fig. 12A,D**). In the HP, levels of 5-HT revealed a non-monotonic curve, decreasing in the low-dose but increasing in the high-dose group, in comparison with the control group. The level of 5-HT in the HP was significantly higher in the high-dose treatment group than in the low-dose group (3.2 ± 0.80 vs. 1.9 ± 0.20 ng/mg protein; mean ± S.D.; high dose vs. low dose; $p < 0.01$; **Fig. 12G**).

Significantly elevated levels of the 5-HT metabolite, 5-HIAA, were observed in the STR of the high-dose group, when compared with the low-dose group (4.7 ± 0.58 vs. 3.3 ± 0.47 ng/mg protein; mean ± S.D.; high dose vs. low dose; $p < 0.05$; **Fig. 12B**). Mn exposure did not affect the level of 5-HIAA in the SN or HP (**Fig. 12E,H**).

The 5-HT turnover ratio is defined as the amount of 5-HIAA divided by 5-HT in each brain region. 5-HT turnover was not statistically changed in the three brain regions studied. (**Fig. 12C,F,I**).

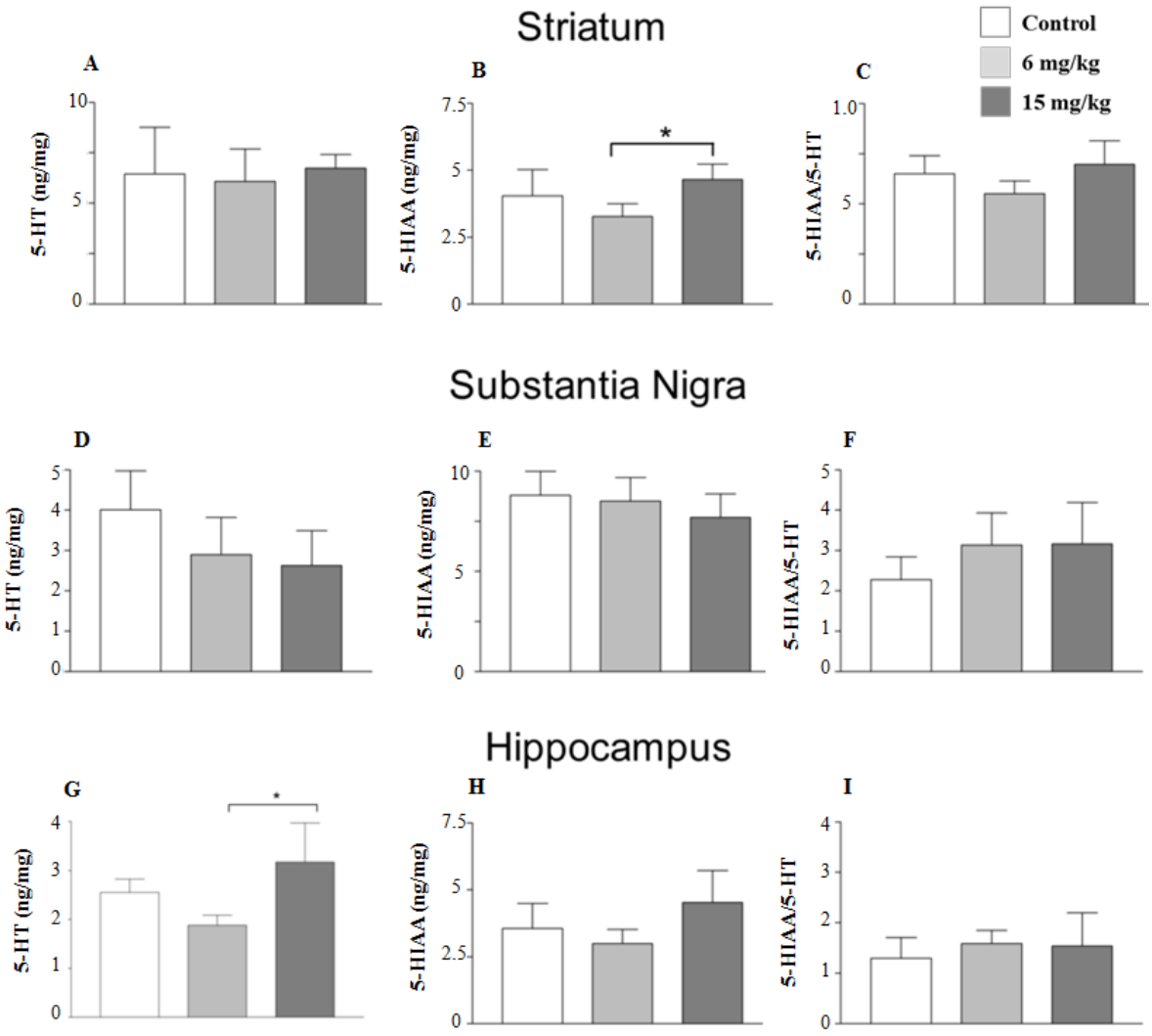

Figure 12. HPLC Analysis of Serotonin, its Metabolite, and Turnover. 5-HT (**A,D,G**) and its metabolite 5-HIAA (**B,E,H**) were quantified using HPLC with electrochemical detection. 5-HT turnover was calculated by dividing the concentration of 5-HIAA by 5-HT (**C,F,I**). ANOVA with Tukey's post hoc test. Data represent mean ± S.D. (ng/mg protein; n = 3-5). *: $p < 0.05$.

NE levels in the STR and SN were not significantly different between Mn exposed and control animals (**Fig. 13A-B**). In the HP, significantly higher NE levels were observed in the high-dose exposure group compared with the low-dose group (6.4 ± 1.29 vs. 4.1 ± 0.81 ng/mg protein; mean ± S.D.; high dose vs. low dose; $p < 0.05$; **Fig. 13C**).

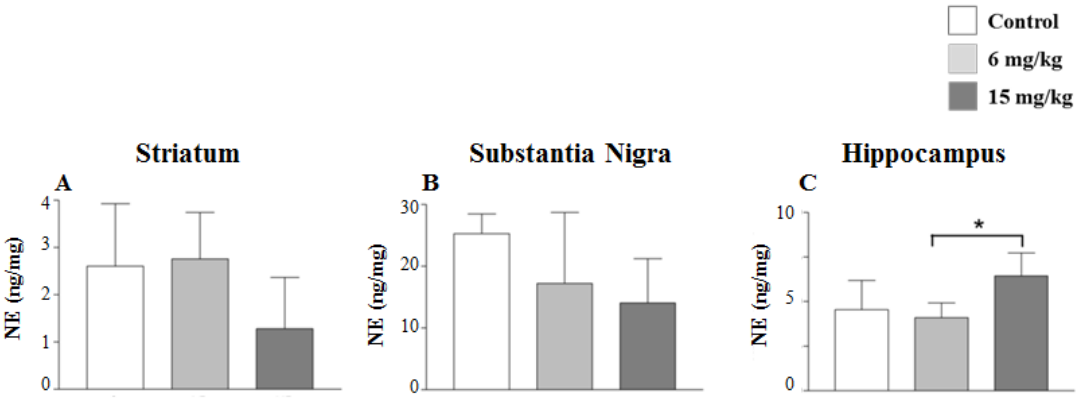

Figure 13. HPLC Analysis of Norepinephrine Levels. NE levels in striatum (STR) (**A**), substantia nigra (SN) (**B**), and hippocampus (HP) (**C**) were quantified using HPLC with electrochemical detection. ANOVA with Tukey's post hoc test for multiple comparisons. Data represent mean ± S.D. (ng/mg protein; n = 3-5). *: $p < 0.05$.

Levels of GABA, the main inhibitory neurotransmitter, were not statistically different in the STR or SN (**Fig. 14A-B**). A significant increase in the HP GABA level was observed in high-dose Mn exposed animals compared with controls (2,221 ± 310.4 vs. 1,441 ± 524.5 ng/mg protein; mean ± S.D.; high dose vs. control; $p < 0.05$; **Fig. 14C**).

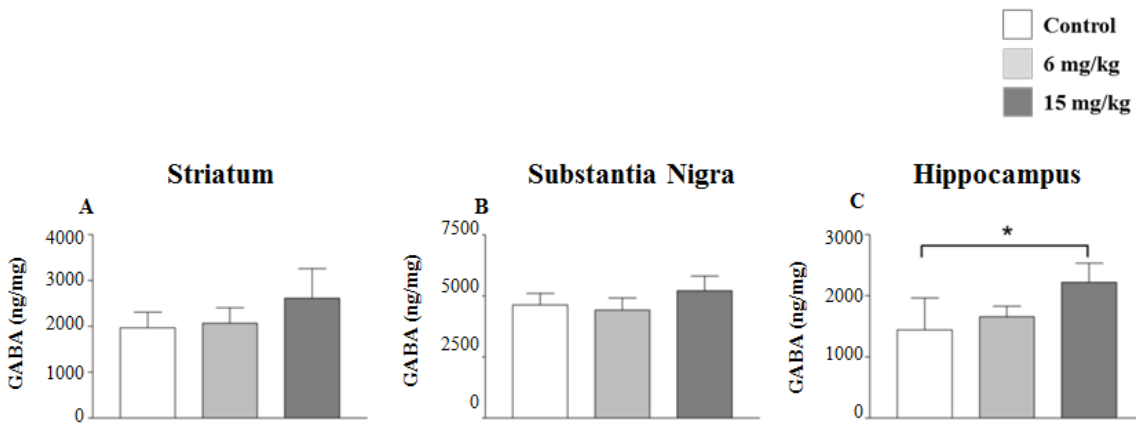

Figure 14. HPLC Analysis of GABA Levels. GABA levels in striatum (STR) (**A**), substantia nigra (SN) (**B**), and hippocampus (HP) (**C**) were quantified using HPLC with electrochemical detection. ANOVA with Tukey's post hoc test for multiple comparisons. Data represent mean ± S.D. (ng/mg protein; n = 3-5). *: $p < 0.05$.

3.4.5 Immunohistochemistry of Striatum Following Mn Exposure

Fluorescence intensities of TH and DARPP-32 were not statistically different in the STR of Mn-exposed animals in comparison with those of control animals (**Fig. 15C** and **16C**). Fluorojade C staining did not identify degenerating neurons in any group (data not shown).

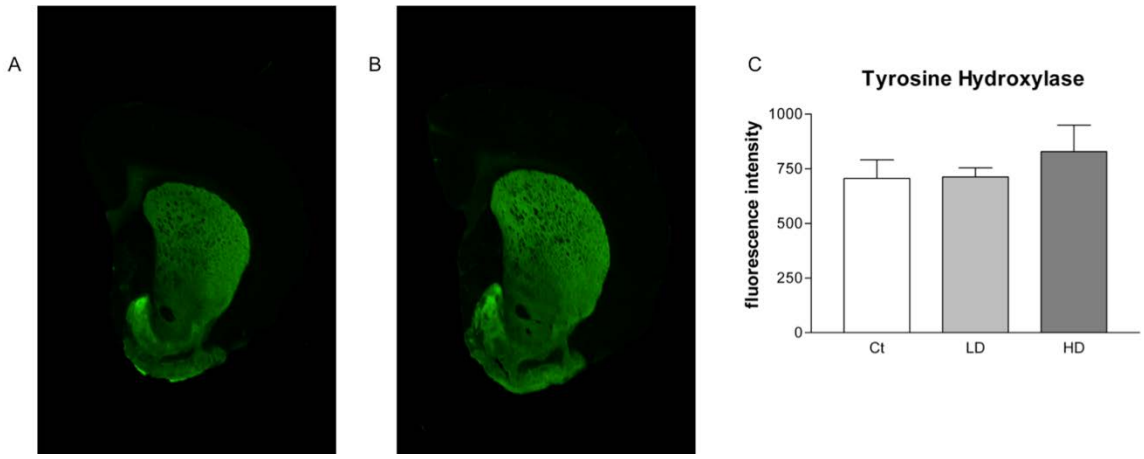

Figure 15. Quantitative Infrared Immunofluorescence Analysis of Striatal TH. Coronal slices from rat striatum (STR) were probed for antibodies against TH. Secondary antibodies were tagged with an infrared fluorescent marker. Depicted are representative scans showing fluorescence intensity in STR slices from control animals (**A**) and Mn treated animals (**B**). Manually selected ROIs are shown as dashed lines. A minimum of three slices were quantified from each animal and the resulting values were averaged. Group values were averaged and are shown (**C**). No difference was observed between control and either low or high dose groups. Mn treatment did not affect STR TH signal intensity. ANOVA with Tukey's post hoc test for multiple comparisons. Data represent mean ± S.D. (n = 4-5).

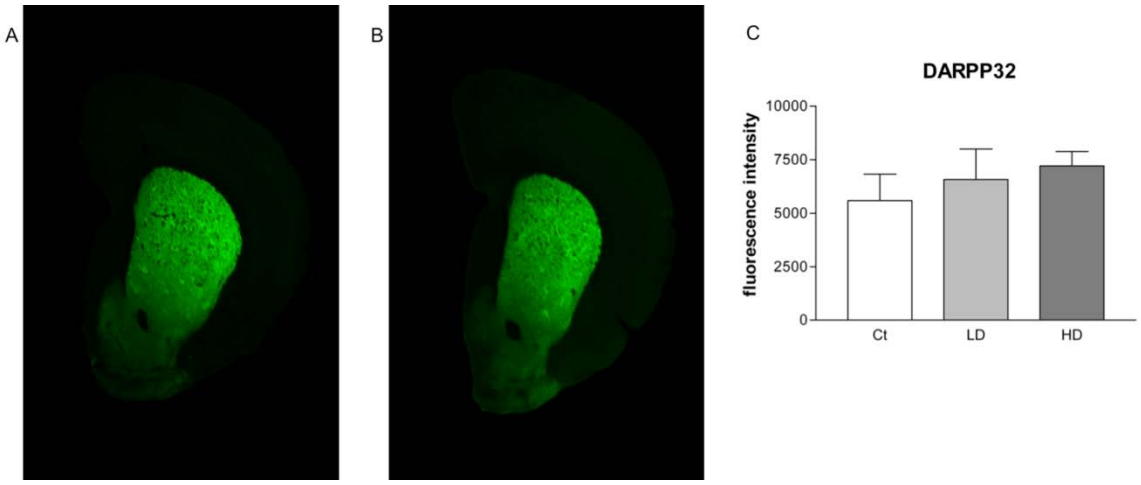

Figure 16. Quantitative Infrared Immunofluorescence Analysis of Striatal DARPP32. Coronal slices from rat striatum (STR) were probed for antibodies against DARPP32. Secondary antibodies were tagged with an infrared fluorescent marker. Depicted are representative scans showing fluorescence intensity in striatal slices from control animals (**A**) and Mn treated animals (**B**). A minimum of three slices were quantified from each animal and the resulting values were averaged. Group values were averaged and are shown (**C**). No difference was observed between control and either low or high dose groups. Mn treatment did not affect striatal DARPP32 signal intensity. ANOVA with Tukey's post hoc test for multiple comparisons. Data represent mean ± S.D. (n = 4-5).

3.5 Discussion

The data presented in the current study have established that subchronic, low-doses of $MnCl_2$ significantly altered levels of neurotransmitters in rats and produces a dose-dependent decrease in locomotor behaviors.

The low dose Mn treatment used in this study has been detailed in a previous report from our laboratory and others (Lebda et al., 2012; Zheng et al., 2009). The high dose level of Mn used in this paper has been used by several other laboratories (Ou et al., 2011; Hong et al., 1984; Husain et al., 2001). Under these dose regimens, Mn exposure significantly reduced animals' body weights. Additionally, Mn treatment at the high dose markedly reduced motor activity.

In a review of Mn exposed animal models, McMillian (1999) noted that behavioral results from many studies show a "slowly developing biphasic response to Mn exposure," with an initial increase in the observed behavior followed by a subsequent decline in behavior. This is true for multiple species, including rats and monkeys (Nachtman et al., 1986; Vezér et al., 2007). However, in the current study, we did not observe the initial increase in motor activity. This could be due to a late first time point that may miss the early behavioral changes. An alternative hypothesis is that our animals were at the tail end of the early, prodromal phase. As such, the observed hypoactivity may have resulted from altered neurochemistry and progression of the treatments' effects.

Our HPLC results clearly demonstrated that DA levels in STR, but not in SN, were significantly increased after Mn treatment. The elevated level of DA in the STR

observed in our study is consistent with reports in the literature that at lower internal cumulative doses of Mn exposure, there is a trend towards increasing DA levels in the STR (reviewed by Gwiazda et al., 2007). Our dose levels were within the range they reviewed and our findings were in agreement with their conclusions.

We have also observed significantly increased levels of HVA in the STR; but increases in NE were limited to the HP. Increased levels of HVA and NE in the STR have been observed in studies with dose duration from 90-120 days (Chandra et al., 1979). Species differences between the two studies (i.e. mice vs. rats) may account for the discrepancy noted. While there is a report to suggest increased GABA in the STR for a wide range of Mn doses (Gwiazda et al., 2007), we did not observe significant changes in striatal GABA, but did find significantly increased levels of GABA in the HP of Mn-treated rats. In the SN, GABA levels were unchanged.

Several reports have demonstrated that Mn treatment initially causes an increase in DA, HVA, and NE, but as the exposure increases, the neurotransmitter levels are decreased (Chandra et al., 1979; Chandra & Shukla, 1981; Cotzias et al., 1974). It was proposed that DA and NE are increased due to increased synthesis of biogenic amines early in manganism (Chandra et al., 1979). Our data are in close agreement with this hypothesis. Several mechanisms may potentially explain the findings in this study. First, the increased levels of the enzyme MAO-B may metabolize DA to DOPAC. Gwizada et al. (2007) noted increased MAO-B levels after low doses of Mn and they also showed increased striatal DA, in agreement with our results. Our DA turnover results further support this possible mechanism. Second, Guilarte et al. (2006) proposed that DA

neurons may have an impaired ability release DA into the synapse after Mn exposure, which could cause intracellular DA levels to increase. Calabresi et al. (2001) postulated that altered release characteristics may alter the life-time of DA within the STR. Finally, it is plausible that Mn may stimulate TH activity to increase DA production (Chandra et al., 1979). In this study, we have assessed levels of TH in the STR of all groups of rats by immunofluorescence; however, the striatal TH expression was not affected by Mn exposure. Thus, it is unlikely that the increases in DA levels were attributable to Mn action on TH. In future studies, it may be prudent to investigate changes of TH levels in SN, because DA is primarily synthesized in the SN and axons project to the STR (Kunar et al., 1999).

It must be noted that differences in Mn species, dose routes, durations and frequencies used may yield different results due to the complex effects of Mn (Ordoñez-Librado et al., 2008). For example, a similar study by Blecharz-Klin, et al. (2012) used an intranasal dose route for two weeks instead of four in slightly older animals; they did not observe a difference in either striatal DA or DOPAC, but noted a decreased level of striatal HVA. Additionally, they observed decreased DA turnover. It is possible that different dose regimens may exert marked differences in neurochemical changes.

Our recent X-ray fluorescence imaging data show that Mn accumulates in the SN (Robison et al., 2012). However, the current neurochemistry study showed that the SN appears to be largely unaffected by Mn treatment. We noted altered levels of HVA in the SN, but the region was unaffected for all other neurotransmitters investigated. These SN neurons are spared, at least in the early stages of the disease (Roth, 2009).

It is worth noting that there has been significant effort devoted to examining a potential role that Mn exposure may play in PD. The observation of increased DA is in contrast to a key feature of PD, which is striatal DA depletion due to loss of nigrostriatal DA neurons. Chronic Mn-induced increases in DA could be deleterious as DA itself is a reactive molecule contributing to oxidative stress (Hastings & Zigmond, 1994). Finally, PD is characterized by complex neurochemical changes, beyond striatal DA depletion alone. Even in a straightforward animal model involving chemical ablation of nigrostriatal DA neurons, complex changes occur in other neurotransmitter systems (Schwarting & Huston, 1996). Thus, elucidating similarities and differences between Mn treatment and prominent PD models will require additional studies.

In summary, our neurochemistry data are in agreement with existing data in the literature, suggesting that this dose regimen produces a model of early manganism. Because the symptoms of manganism are slowly progressive and exist along a continuum, perhaps this model is nearer the end of the first phase. Use of this model of early manganism may allow the study of mechanisms that progress to clinical manganism. Cotzias (1958) noted that the early phase may lack motor disturbances and the disease primarily consists of psychological symptoms. These psychological symptoms are harder to detect and therefore, more sophisticated behavioral analyses to assess the symptoms such as disturbance of sleep, eating and sexual disturbances may be needed.

CHAPTER 4: MANGANESE INTERACTION WITH BRAIN REPAIR MECHANISMS IN THE ADULT SUBVENTRICULAR ZONE FOLLOWING INTRANASAL EXPOSURE

4.1 Abstract

Manganese (Mn) is necessary for normal biological processes; however, overexposure to this metal can lead to toxic accumulation in the body, particularly in the brain. Mn accumulation in the brain can result in altered copper (Cu) homeostasis. Altered Cu levels are implicated in a variety of neurodegenerative disease pathologies. The goal of this study was to test the hypothesis that Mn accumulation in the rat subventricular zone (SVZ) led to altered neurogenesis as a result of altered Cu homeostasis in this region. Adult male rats were intranasally exposed to Mn daily for two weeks. During the last four days of Mn administration, rats also received twice daily injections of BrdU to label actively proliferating cells in the SVZ. Brain slices from these animals were used for immunohistochemistry studies and triple labeled for BrdU and DCX (neuroblasts), and GFAP (stem cells) to distinguish between newly differentiated cell types. Following Mn exposure, Mn concentrations were significantly increased and Cu concentrations were significantly decreased in the SVZ. Following Mn exposure,

BrdU and DCX expression were significantly increased in the SVZ as well as the olfactory bulb while GFAP was only significantly increased in the SVZ. The results of this study demonstrate that Mn exposure affects adult neurogenesis by altering Cu homeostasis in the SVZ. This suggests that Mn exposure may negatively impact those neurodegenerative diseases which implicate Cu in their pathology.

4.2 Introduction

Exposure to high levels of the essential metal manganese (Mn) is neurotoxic, resulting in manganism, an irreversible neurological disease with symptoms similar to, but distinguishable from idiopathic Parkinson's disease. Excess exposure predominantly occurs via inhalation in occupational settings, which is not surprising because Mn is one of the most commonly used metals in industrial processes. It is used both as a pure metal and an alloy to produce a variety of products including dry-cell batteries, glass and ceramics (Nadaska, Lesny, and Michalik, 2012). The median onset of disease is 1 year after exposures begin and includes both motor and behavioral symptoms (Racette et al., 2012a). Motor symptoms are exclusively attributed to accumulation of Mn in the basal ganglia (Newland, 1999).

In our lab, we have confirmed that Mn accumulates in the rodent basal ganglia and other brain regions, with considerable accumulation in the subventricular zone (SVZ) and the hippocampus (HP); the latter has the structure called the subgranular zone (SGZ) in the dentate gyrus. The SVZ and SGZ are important in adult neurogenesis because these are the only two recognized neurogenic niches in the adult mammalian brain. These niches house microenvironments capable of maintaining a population of actively

dividing, undifferentiated neural stem progenitor cells (Garzon-Muvdi and Quinones-Hinojosa, 2010). The neurogenic capability of the SVZ is due in part to its proximity to nutrients and growth factors in the cerebrospinal fluid (CSF) filling the lateral ventricles where the SVZ is located (Curtis, Faull and Eriksson, 2007). In the SVZ, there are four cell types: the ependymal cells "type E" cells, "type B" cells which are astrocytic stem cells (ASCs; $GFAP^+$ astrocytes) and give rise to "type C" ($nestin^+$ transit-amplifying) cells, which finally differentiate into "type A" neuroblasts (DCX^+) (Doetsch et al., 1999; Zaverucha-do-Valle et al., 2013). The neuroblasts migrate anteriorly along the rostral migratory stream (RMS) to the olfactory bulb (OB) where they may mature into local interneurons. Surviving cells are able to functionally integrate, replacing dead cells of the same phenotype. It has been suggested that functionally integrated new neurons participate in neural plasticity, learning and memory, as well as sexual behaviors in mammals, and song production in birds (Alvarez-Buylla and Garcia Verdugo, 2002).

The cells in the SVZ can be stimulated by neurodegenerative diseases, such as Huntington's disease, and also epilepsy and stroke (Curtis, Faull and Eriksson, 2007) or Mn exposure (Fu et al., 2015; Wang et al., 2012). In our lab, we have shown that Mn exposure by subchronic intraperitoneal injection induces cell proliferation in the SVZ. Further, we have investigated changes in cell differentiation after Mn exposure and showed increased production of glial cells.

Mn accumulates in the striatum (STR), hippocampus (HP), and substantia nigra (SN), brain regions implicated in clinical manganism, as well as the SVZ. In the SVZ, we also observed a significant reduction in copper (Cu) levels after Mn treatment (Fu et al., 2015). This is interesting because synchrotron analysis reveals Cu levels in this brain

region are about 20-30 times higher than in other brain structures (Pushkar et al., 2013), a finding our lab has confirmed using atomic absorption spectroscopy (AAS). These findings suggest that high Cu levels in the SVZ are required to maintain the normal status of neurogenesis in adult brains, and that Mn exposure alters Cu homeostasis in the SVZ. Cu dyshomeostasis in the brain is implicated in the pathology of a number of neurodegenerative diseases, including idiopathic Parkinson's disease, Alzheimer's disease, familial amyotrophic lateral sclerosis, prion disease, Wilson's disease and Menkes' disease (Barnham and Bush, 2008, Gaggelli et al., 2006, Mates et al., 2010, Zheng and Monnot, 2012).

Previous *in vivo* studies of adult neurogenesis have investigated the effects of Mn exposure via intraperitoneal, intravenous, or oral gavage administration of Mn-containing solutions (Fu et al., 2015; Kikuchihara et al., 2015). However, the primary route of toxic Mn exposure in the human population is inhalation, which permits a direct pathway from the environment into the central nervous system (CNS). This route is of particular relevance to adult neurogenesis studies because direct transport along the olfactory pathway would ensure the highest concentration of Mn reached the OB. Retrograde transport of Mn from the OB along the RMS would potentially deliver higher concentrations of Mn to the SVZ than any other route of exposure.

The present studies used an intranasal instillation (IN) technique to study the effects of Mn exposure on adult neurogenesis. The goals of this study were: (1) to identify the changes in adult neurogenesis resulting from Mn exposure, (2) to determine the extent of metal dysregulation after Mn exposure, and (3) to establish IN as a valuable route of administration for modeling Mn neurotoxicity and studying neurogenesis in adult

rats. The results of these studies are expected to provide direct evidence of Mn interaction with neuronal repair mechanisms by altering Cu homeostasis. These results are likely to create a new area of toxicology research, specifically metals and neurotoxicological research.

4.3 Materials and Methods

4.3.1 Experimental Design and Animals

Male Sprague Dawley rats were obtained from Harlan Laboratories, Inc. (Indianapolis, IN) and allowed to acclimate to the test facility for 7 days. When the study commenced, animals were 8 weeks old and weighed approximately 180-200 g. Rats were group housed in a temperature- (72 ± 4 °C) and humidity- (30-70%) controlled room on a 12 hour light/dark cycle (lights on at 0600). Rats had ad libitum access to food (Harlan 2018 rodent diet) and reverse osmosis water.

Rats were weighed each day prior to dose administration. At the time of experimentation, rats received an IN of saline (as control), 0.2, or 0.8 mg Mn/kg as $MnCl_2$ daily for 14 days. These doses were chosen based on the work by Blecharz-Klin et al., (2012) who showed altered neurochemistry and behavior following this regimen. During the last 4 days of Mn administration, rats also received twice daily intraperitoneal injections of 50 mg BrdU/kg. BrdU is a thymidine analog that is incorporated into the DNA of actively dividing cells during the S phase of the cell cycle. Animals' final body weights were recorded and rats were euthanized 24 hr after the last Mn administration.

See **Figure 17** for a diagram of the overall experimental design. All animal studies were approved by the Institutional Animal Care and Use Committee at Purdue University.

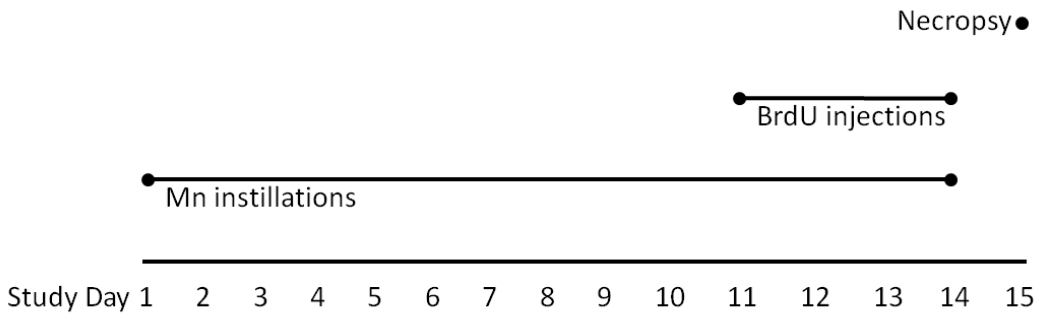

Figure 17: Chapter 4 Experimental Design. Shows daily Mn instillations, BrdU injections, and necropsy schedule.

4.3.2 Intranasal Instillation Technique

Prior to Mn administration, rats were anesthetized using 2% isoflurane gas. A Hamilton syringe coupled to a length of flexible polyethylene tubing (0.18 mm inner diameter) was filled with the dose solution to be instilled. The tubing was inserted approximately 2 cm into the rat's nostril and 10 µL of solution was instilled at the olfactory mucosa (see **Figure 18**). The tubing was removed and the procedure repeated in the other nostril; the starting side alternated each day (Genter et al., 2012). The intranasal instillation method has previously been used to study Mn exposure by many researchers, including Tjälve et al. (1996) and Gianutsos et al. (1997).

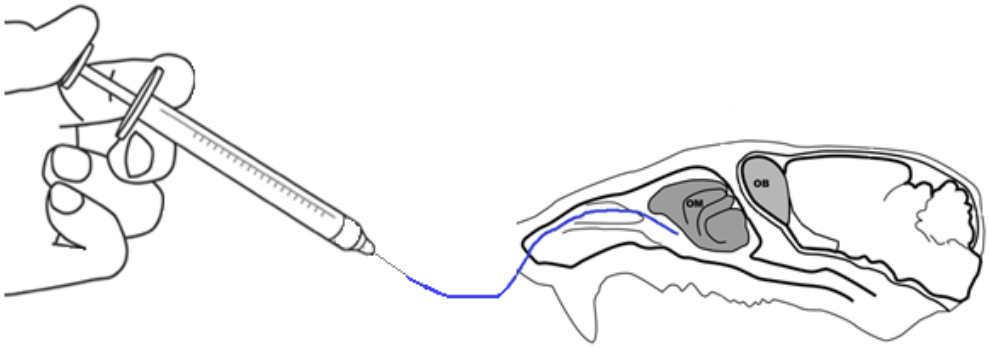

Figure 18: Diagram of Intranasal Instillation Procedure. Blue line indicates path of flexible tubing into rodent nasal passage. Dose solutions are instilled at the olfactory mucosa (OM) and Mn passes primary neurons by retrograde transport directly into the olfactory bulb (OB) within the CNS. Over time, Mn is transported into deeper brain structures.

4.3.3 Euthanasia and Necropsy

Rats were deeply anesthetized by intraperitoneal injection with a ketamine/xylazine cocktail (75/10 mg/kg) and exsanguinated. Rats used for immunohistochemistry studies were perfused with phosphate buffered saline, pH 7.4 (PBS) followed by 4% paraformaldehyde to fix the tissues. The whole brain was removed and postfixed in 4% paraformaldehyde at 4°C. Rats used for all other studies were not perfused. From these animals, blood samples were collected from the descending aorta into heparinized vials. Brains were removed and the SVZ, STR, HP, OB, choroid plexus, pituitary, thalamus and frontal cortex tissues were dissected on ice. Lung tissue and femurs were also collected. All tissues were stored at -80°C until processed. Blood was not stored; it was processed for plasma 20 min after collection.

4.3.4 Atomic Absorption Spectroscopy

Tissue samples collected at necropsy were weighed then digested in enough concentrated nitric acid (HNO_3) to completely cover the tissues. Digestion was facilitated by using a high pressure MarsXpress microwave (CEM Corporation, Matthews, NC) for 15 min at 200°C. SVZ, CP, and pituitary tissues were digested in acid overnight in an oven at 55°C. Each digestion was diluted with ddiH_2O to keep the readings within the ranges of the standard curves: 1-10 ppb for Mn and 1-50 ppb for Cu. Tissue metal concentrations were quantified using an Agilent Technologies 200 Series SpectrAA with GTA 120 graphite furnace and expressed as µg/g of tissue.

4.3.5 Western Blotting

Total protein was isolated from each brain region. Tissues were lysed in RIPA homogenization buffer, minced with spring scissors, and then sonicated. Tissues were incubated on ice for 10 min and centrifuged at 12,000 *x g* for 15 min at 4°C. Supernatant was collected and protein was denatured by boiling for 5 min at 95°C. Pierce BCA Protein Assay (ThermoFisher) was used to quantify protein. Approximately 50 µg of total protein was loaded per lane and separated on a 10-15% SDS-polyacrylamide gel then blotted onto a polyvinylidene membrane using a semi-dry transfer (BioRad).

The membrane was blocked in 5% non-fat dry milk diluted in a solution of Tris-buffered saline solution with 0.01% Tween 20 pH 7.4 (TBST) for 2 hr at room temperature. The membrane was incubated overnight at 4°C with primary rabbit anti-Ctr1 antibody (43 kDa; 1:2,000) in blocking solution diluted 1:5 in TBST. To detect the primary antibodies, membranes were incubated for 2 hr at room temperature in a solution containing horseradish peroxidase-conjugated secondary anti-rabbit antibody (1:3,000). The signals were visualized using enzyme chemiluminescent solutions. Membranes were rinsed in TBST and stripped in stripping buffer for 20 min then rinsed again. The blocking procedure was repeated. The primary antibody solution contained mouse anti-β-actin (42 kDa; 1:5,000) and the secondary antibody solution contained horseradish peroxidase-conjugated anti-mouse antibody (1:10,000). Each blot was performed in triplicate.

For α-synuclein and Iba1 blotting, the membrane was blocked in Li-Cor blocking solution (Li-Cor). The membrane was incubated overnight at 4°C in a primary antibody solution containing mouse anti-α-synuclein (14 kDa; 1:1,500) or rabbit anti-Iba1 (17

kDa; 1:1,000) and chicken anti-β-actin (42 kDa; 1:3,000) in TBST. To detect the primary antibodies, membranes were incubated for 2 hr at room temperature in TBST containing infrared-linked secondary antibodies donkey anti-mouse (Li-Cor, IR800; 1:20,000), donkey anti-rabbit (Li-Cor, IR800; 1:20,000) or donkey anti-chicken (Li-Cor, IR680; 1:20,000). The blots were imaged with the Odyssey infrared imaging system (Li-Cor) at 84 µm resolution with medium intensity and quantified with Image Studio software (version 3.1). Each blot was performed in triplicate.

4.3.6 qPCR Analysis of *Dmt1* and *Ctr1* mRNA

Total RNA was isolated from tissues using TRIzol reagent following the manufacturer's instructions. RNA samples were reverse-transcribed using the BioRad iScript cDNA synthesis kit (Hercules, CA). The iTaq Universal SYBR Green Supermix was used for qPCR analyses following the manufacturer's instructions.

Dmt1 cDNA was amplified using the following nucleotide sequences:

Forward primer: 5'-GAT TCC AGA CGA TGG TGC TT-3'

Reverse primer: 5'- GTG AAG GCC CAG AGT TTA CG -3'

Ctr1 cDNA was amplified using the following nucleotide sequences:

Forward primer: 5'-ACC TTT GCG CTG ACT CTC AT-3'

Reverse primer: 5'- TGA TCG ATC TCC ATG TGG TT -3'

β-actin was used as an internal control with the following sequences:

Forward primer: 5'- AGC CAT GTA CGT AGC CAT CC -3'

Reverse primer: 5'- CTC TCA GCT GTG GTG GTG AA -3'

Primers were designed using the Primer Express 3.0 software. All primers were obtained from Integrated DNA Technologies. Experimental conditions were optimized for annealing temperature, primer specificity, and amplification efficiency. The amplification was performed in the CFX Connect™ quantitative Real-Time PCR Detection (qPCR) system (BioRad, Hercules, CA) with an initial 3 min denaturation at 95°C followed by 40 cycles of 30 sec denaturation at 95°C, 10 sec gradient from 55.0 to 65.0°C and a 30 sec extension at 72°C. A dissociation curve was used to verify that the majority of fluorescence detected could be correlated to the labeling of specific PCR products, and to verify the absence of primer dimers and sample contamination. Each qPCR reaction was run in triplicate. Relative mRNA expression ratios between groups were calculated using the delta-delta cycle time (ΔΔCt) formulation; Ct is the threshold cycle time value. Ct values of *Dmt1* and *Ctr1* were normalized to the reference gene in the same sample. The relative ratio between control and treatment groups was then calculated and expressed as relative increases, setting the control as 100% following the method of Livak and Schmittgen (2001).

4.3.7 Biogenic Amine Quantification

Neurotransmitter analysis was conducted as previously described (O'Neal et al., 2014b; Wang et al., 2013). Briefly, OB and thalamus samples were sonicated in 0.5 ml 0.1N perchloric acid ($HClO_4$) on ice, at 50% power, pulsing for 45 s to precipitate proteins. Samples were then centrifuged at 16,400 *x g* for 35 min at 4°C. Supernatant was transferred to 0.22 µm Spin-X tube with nylon filter (Corning) and centrifuged at 1000 *x g* for 15 min at 4°C. Prepared samples were then stored at -80°C until HPLC analysis. A Dionex UltiMate 3000 (ThermoScientific; Germering, Germany) system

with a built in autosampler and a Coulochem III (Thermo Scientific) electrochemical detector were used for HPLC analysis of DA, its metabolites DOPAC and HVA, as well as 5-HT and its metabolite 5-HIAA, NE, GABA, glutamate, and taurine. The optimized monoamine method used an isocratic mobile phase (consisting of 0.08 M NaH_2PO_4, 10% methanol, 2.0 mM OSA, 0.025 mM EDTA, and 0.2 mM TEA, in 13 mΩ purified water, pH 2.4). Samples were injected and monoamines separated on a reverse phase C18 column (150 x 3.2mm, 3.0 μm particle size, MD-150, Thermo Scientific, Bannockburn, IL) protected by a guard column. Separation occurred at 32 °C at a flow rate of 0.6 ml/min. For GABA, glutamate, and taurine detection, samples were first derivatized with OPA (*o*-phthalaldehyde, methanol, and 2-mercaptoethanol) before injection onto the column. The isocratic mobile phase (pH 6.75) consisted of Na_2HPO_4 in 13 mΩ purified water with 22% methanol and 4% acetonitrile. Separation occurred at 35°C with a flow rate of 0.5 ml/min. For monoamine neurotransmitter and metabolite detection, the electrochemical potential of the detector was set at 250 mV, with a conditioning cell at -150 mV. For GABA, glutamate, and taurine detection, the electrochemical potential of the detector was set at 550 mV, with a conditioning cell at -150 mV. Neurotransmitter and metabolite levels in each sample were quantified by comparing sample values to a reference curve prepared by adding standards of a known concentration to perchloric acid. A sample chromatogram displaying the results for GABA, glutamate, and taurine is shown in **Figure 19**. Chromeleon 7.0 software was used for data acquisition and analysis. Neurotransmitter concentrations were expressed as ng/mg of protein as assessed by BCA protein assay (Smith et al., 1985) using bovine serum albumin as the standard (Bradford, 1976).

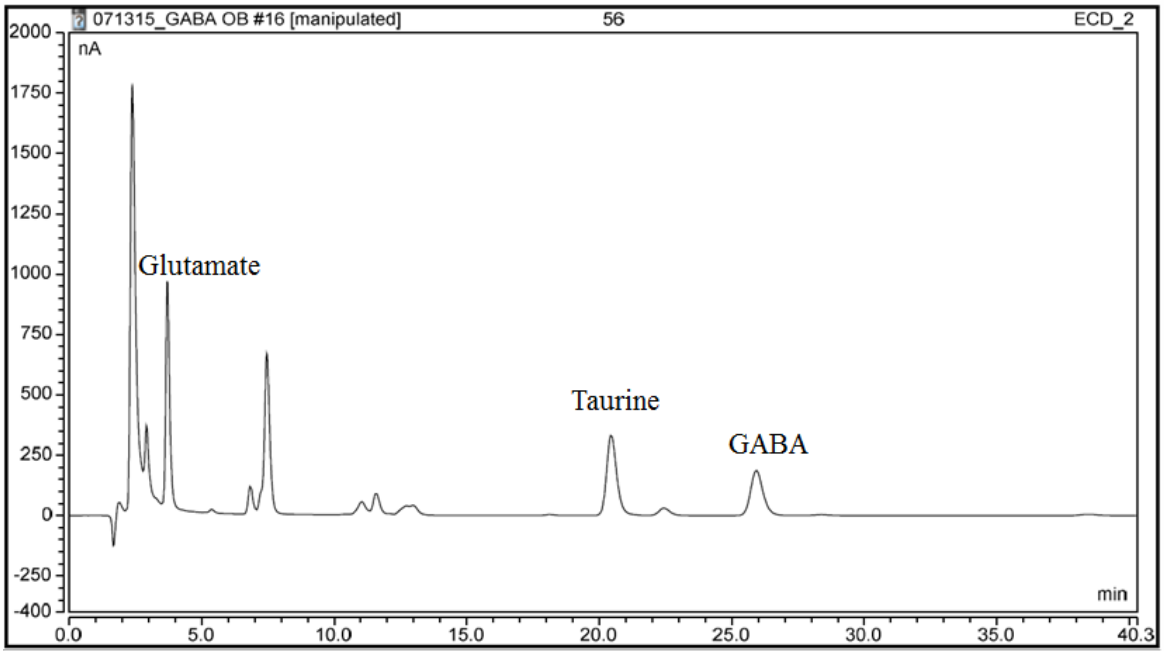

Figure 19. Sample HPLC Chromatogram. Analysis of olfactory bulb tissue from a control animal showing separated peaks identified as GABA, glutamate, and taurine. Electrochemical detector used for analysis of neurotransmitters.

4.3.8 BrdU/DCX/GFAP Triple Imaging in Brain Sections

Brains were transferred from 4% paraformaldehyde after 7 days to a 30% sucrose solution for 7 days to equilibrate tissue, preventing the formation of ice crystals during freezing. Frozen brains were cut (30 µm thickness) on a microtome and stored in cryoprotectant at -20°C. Every 6^{th} section (180 µm interval) throughout the SVZ and SGZ was used for IHC. During processing, sections were removed from cryoprotectant and floating slices were triple-rinsed in PBS x 10 min (rinsed). Sections were incubated in 2M HCl for 2 hr to denature DNA then rinsed. Denatured slices were blocked in PBS containing 0.5% Triton X-100 (v/v), 5% BSA, and 10% normal goat serum for 1.5 hr at room temperature and then rinsed. Rinsed sections were incubated overnight at 4°C with mouse anti-BrdU (1:400), rabbit anti-DCX (1:1,000), chicken anti-GFAP (1:1,000) primary antibody in blocking solution diluted 1:10 with PBS. The sections were rinsed and incubated for 2 hr at room temperature with goat anti-mouse (488 nm; 1:1,000), goat anti-rabbit (555 nm; 1:1,000), and goat anti-chicken (638 nm; 1:1,000) secondary antibody in dilute blocking solution. Labeled sections were rinsed for 15 min and mounted on charged slides then coverslipped in ProLong Gold antifade solution (Molecular Probes). Slides were protected from light and allowed to dry overnight at room temperature. BrdU, DCX and GFAP immunofluorescence were visualized in the same sections using a Nikon inverted confocal laser scanning microscope. Images of the SVZ and OB were taken from each slice at 40X (Nikon; Plan Apo, 4X/0.20 ∞ 0.17) and x100 (Nikon; Plan Apo, 10X/0.45 ∞ 0.17) magnifications. Images of the SVZ were also taken from each slice at x400 (Nikon; Plan Apo, 40X/0.95 ∞ 0.17) magnification. Images were scanned with the Nikon EZ-C1 (version 3.90) confocal imaging program. For each

image, the frame average of 16 images was obtained to improve the signal to noise ratio. Signal intensities were quantified using the NIS-Elements BR (Version 3.10) program. The software automatically detected regions of interest (ROIs) and calculated mean intensity values. A minimum of four to six slices per animal were imaged and the values averaged to produce one value per animal. The group averages were used for statistical analysis.

4.3.9 Statistical Analysis

All data are expressed as mean ± S.D. Statistical analyses of the differences between three treatment groups were carried out by one-way ANOVA. Where ANOVA analysis indicated significant differences between groups, specific differences were identified by post hoc analysis using Tukey's test. Analyses of differences between two treatment groups were carried out by Student's t test. Group differences were considered statistically significant for *p*-values less than 0.05. All analyses were conducted using SPSS (Version 21.0).

4.4 Results

4.4.1 Body and Relative Organ Weights Following Mn Exposure

Animals' body weights were recorded daily throughout the 15-day study. Control animals showed steady weight gain over the course of the study; final body weights were 272.6 ± 9.2 (mean ± S.D.) as compared to 188.8 ± 6.7 on study day 1. Comparatively, animals instilled with 0.2 mg/kg and 0.8 mg/kg (cumulative Mn dose ranged from 2.8-11.2 mg/kg) showed a 7.6% or 12.8% reduction, respectively, in final body weight

compared with control animals' final body weights. In previous experiments utilizing different Mn exposure routes, animals receiving intraperitoneal exposure showed 3.1-12.0% reduction in body weight gain (cumulative dose range 120-300 mg/kg) compared with controls (Chapter 3) and animals orally exposed (cumulative dose 1,500 mg/kg) showed a 5.3% reduction in body weight gain compared with controls (Chapter 2).

For animals instilled with Mn, relative organ weights of the spleen and pituitary gland were also calculated as:

$$\frac{organ\ weight}{final\ body\ weight}\ x\ 100$$

Relative organ weights were calculated as a crude estimate to determine if systemic toxicity or immune responses occurred as a result of intranasal Mn exposure. The spleen and pituitary glands were selected for examination because they play a role in immune function and their sizes may vary during an immune response. Additionally, the spleen and pituitary gland have readily distinguishable boundaries which facilitated collection at necropsy. Comparing the whole organ weights to the animals' final body weights revealed that relative organ weights of neither spleen, nor pituitary was significantly altered following Mn exposure (p=0.74 and p=0.63, respectively). Finally, whole brain weight was unchanged following intranasal Mn exposure (p=0.08).

4.4.2 Metal Concentrations in Brain and Body Tissues

AAS analysis of select tissues in the brain revealed that Mn concentrations were significantly increased following Mn instillation of either 0.2 or 0.8 mg/kg in all regions analyzed, except cerebellum (p=0.44; **Table 5**). As expected, following an intranasal

instillation, Mn concentrations in the brain were highest in the olfactory bulb (2.33 ± 1.86 µg/g). Interestingly, the SVZ had the second highest Mn concentration, which was significantly increased by 95.5% following Mn exposure (1.29 ± 0.45 µg/g for the 0.8 mg/kg dose group compared with the control group (0.66 ± 0.31 µg/g; $p < 0.01$).

Cu concentrations were differentially affected in brain regions following Mn exposure (**Table 6**). In the STR, Cu concentrations were significantly increased following Mn exposure (4.98 ± 0.56 µg/g compared with 2.57 ± 0.35 µg/g for controls; $p < 0.01$). In the SVZ, Cu concentrations were significantly reduced between 46.4%-86.7% following Mn exposure (5.17 ± 0.78 µg/g and 1.28 ± 0.04 µg/g for 0.2 mg/kg and 0.8 mg/kg, respectively, compared with 9.64 ± 2.81 µg/g in controls; $p < 0.01$). The SVZ was the only tissue examined in which Cu concentration was significantly reduced following Mn exposure. In the majority of tissues analyzed, including the olfactory bulb, hippocampus, frontal cortex, and cerebellum, Cu concentrations remained unchanged. It is also interesting to note that basal Cu concentration is highest in the SVZ, about 3.75-fold higher than in the STR or 3.4-fold higher than HP Cu concentrations. This confirmed the previous findings from synchrotron analysis of SVZ that the basal Cu concentration in the SVZ is 20-30 times higher than those in other brain regions (Pushkar et al., 2013).

Table 5. Tissue Mn Concentrations Were Analyzed by Atomic Absorption Spectroscopy Following Intranasal Mn Exposure. Data represent mean ± S.D. µg/g; n=4-10; *$p < 0.05$, **$p < 0.01$, ***$p < 0.001$ when compared with controls.

Mn Levels			
Tissue	control	0.2 mg/kg	0.8 mg/kg
SVZ	0.66 ± 0.31	1.31 ± 0.10**	1.29 ± 0.45**
Striatum	0.35 ± 0.05	1.07 ± 0.06**	1.10 ± 0.15**
Hippocampus	0.43 ± 0.06	--	0.77 ± 0.01***
Olfactory Bulb	0.64 ± 0.2	--	2.33 ± 1.86*
Frontal Cortex	0.42 ± 0.15	1.79 ± 0.26**	1.13 ± 0.33**
Choroid Plexus	0.57 ± 0.24	1.31 ± 0.23*	1.28 ± 0.44*
Pituitary	0.93 ± 0.12	--	4.15 ± 0.72***
Cerebellum	0.68 ± 0.16	--	1.09 ± 0.97
Other Tissue	0.33 ± 0.05	--	0.75 ± 0.10**
Lung	0.37 ± 0.13	--	0.50 ± 0.01
Femur	0.69 ± 0.10	1.68 ± 0.25**	2.40 ± 0.38**
Plasma	0.004 ± 0.001	--	0.010 ± 0.002**

Table 6. Tissue Cu Concentrations Were Analyzed by Atomic Absorption Spectroscopy Following Intranasal Mn Exposure. Data represent mean ± S.D. µg/g; n=4-10; *$p < 0.05$, **$p < 0.01$when compared with controls.

Cu Levels			
Tissue	control	0.2 mg/kg	0.8 mg/kg
SVZ	9.64 ± 2.81	5.17 ± 0.78**	1.28 ± 0.04**
Striatum	2.57 ± 0.35	2.51 ± 0.59	4.98 ± 0.56**
Hippocampus	2.81 ± 0.56	--	2.33 ± 0.19
Olfactory Bulb	2.34 ± 0.28	--	2.64 ± 0.44
Frontal Cortex	2.68 ± 0.31	2.39 ± 0.19	2.53 ± 0.22
Choroid Plexus	3.34 ± 2.95	3.06 ± 0.75	2.54 ± 0.44
Pituitary	0.54 ± 0.14	--	0.45 ± 0.03
Cerebellum	0.56 ± 0.4	--	0.56 ± 0.06
Other Tissue	0.21 ± 0.05	--	0.24 ± 0.01
Lung	0.50 ± 0.02	--	0.51 ± 0.02
Femur	0.59 ± 0.19	0.64 ± 0.09	0.67 ± 0.11
Plasma	0.19 ± 0.01	--	0.21 ± 0.002**

4.4.3 Immunohistological Findings from Triple Labeled Brain Slices

In control animals, low magnification (x40) confocal images of sagittal brain sections revealed the fluorescent BrdU signal was localized to the lateral walls in the lateral ventricles where the SVZ is located (**Figure 20**). The BrdU signal can also be observed in the delta SVZ (ΔSVZ) region, located at the superior aspect of the SVZ where the RMS begins, and anteriorly into the RMS as well. At this low magnification, labeling for DCX and GFAP was also visible. This region shows high levels of DCX expression.

As intranasal instillation of Mn significantly alters Mn and Cu levels in the SVZ, we hypothesized that Mn exposure would inhibit neurogenesis in the SVZ and ΔSVZ, the superior aspect of the SVZ leading directly to the RMS. To test this hypothesis, animals received twice daily injections of 50 mg/kg BrdU during the last four days of Mn exposure to pulse-label actively dividing cells in the SVZ. In contradiction to our original hypothesis, BrdU signals were clearly increased following Mn exposure (**Figure 20** top row). Quantification of the average fluorescence intensity confirms the signal was significantly increased by 25.1% after 0.2 mg/kg Mn exposure ($p < 0.05$; **Figure 21).**

An increase in BrdU signal indicates an increase in the proliferation of new cells in this neurogenic niche. These cells are capable of differentiating to neuroblasts or producing new glial cells to maintain the pool of astrocytic stem cells (ASCs), the true neural stem cells in the region. For a complete understanding of Mn-induced neurotoxicity, it is necessary to understand how Mn exposure affects these differentiation processes, potentially resulting in altered neuronal and glial populations. To test the effects of Mn exposure on cell differentiation in the SVZ, brain slices from each exposure

group were triple-labeled for BrdU, DCX (to identify neuroblasts), and GFAP (to identify ASCs). Triple-labeling revealed that BrdU expressing cells in the SVZ also expressed DCX or GFAP, indicating that both neuroblasts and ASCs were actively proliferating in the SVZ. Quantification of the dual-fluorescence signals in sagittal slices revealed significant 27.0% increases in expression of both DCX and GFAP ($p < 0.01$) following 0.2 mg/kg Mn exposure (**Figure 21**). These same changes were not observed following 0.8 mg/kg Mn exposure. This indicated that Mn exposure not only increased the proliferation of cells, but also differentiation of the cells to either neuroblasts (DCX^+) or ASCs ($GFAP^+$).

In the ΔSVZ region, DCX was significantly increased following 0.8 mg/kg Mn exposure (58.8%; $p < 0.01$). GFAP remained unchanged in the ΔSVZ region ($p = 0.334$).

Combining the fluorescence intensities for the SVZ and ΔSVZ at low magnification (x40) revealed significant increases of 28.9%, 29.2%, and 8.9% for BrdU, DCX, and GFAP respectively ($p < 0.01$) following 0.2 mg/kg Mn exposure.

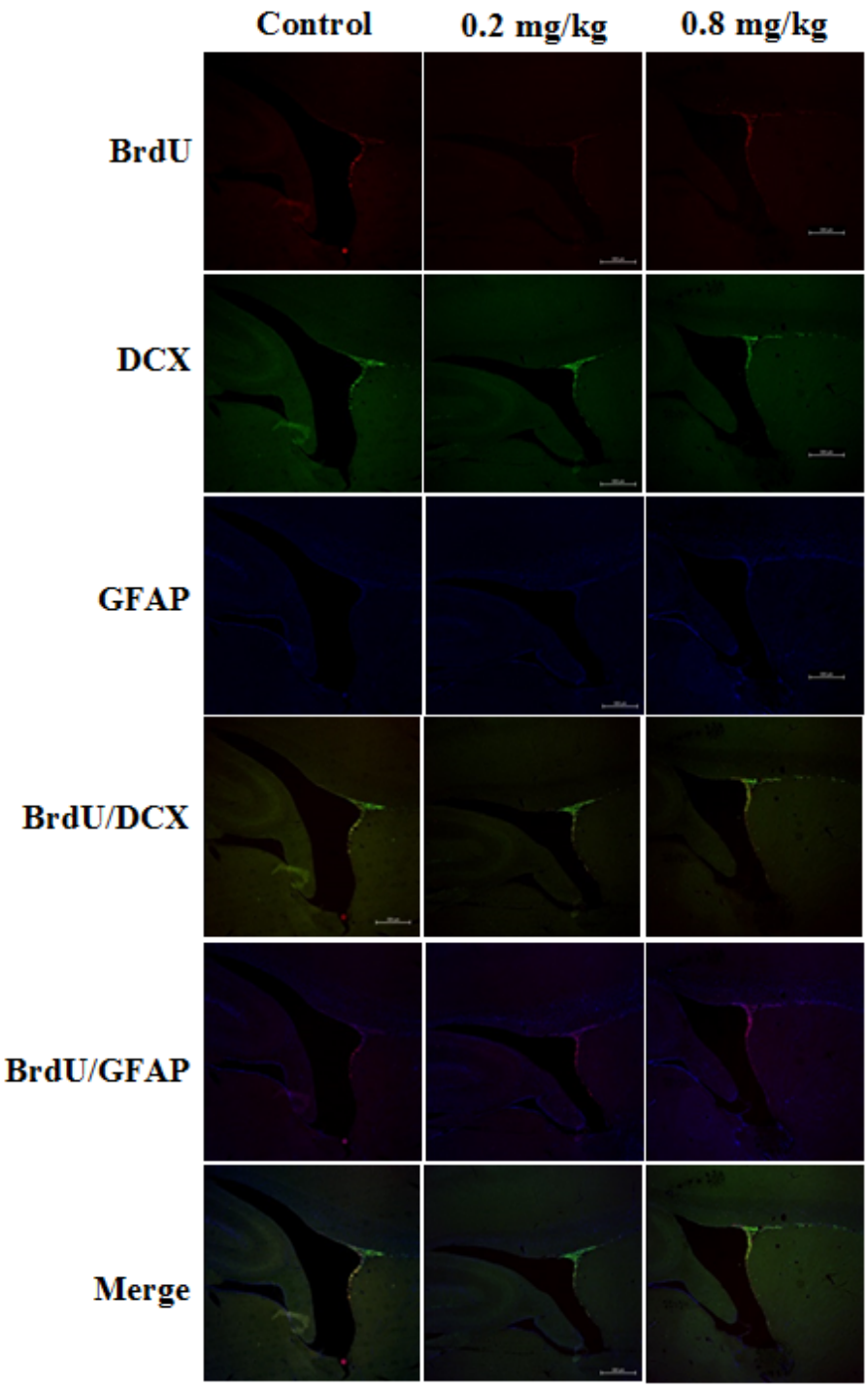

Figure 20. Immunohistochemical triple labeling for BrdU, DCX, and GFAP in the SVZ at low magnification. Rats received twice daily injections of 50 mg/kg BrdU during the last four days of the study to pulse-label actively dividing cells in the SVZ. Representative images from each treatment group show labeling of BrdU (red), DCX (green), GFAP (blue), BrdU/DCX, BrdU/GFAP, and merge at low magnification (x40).

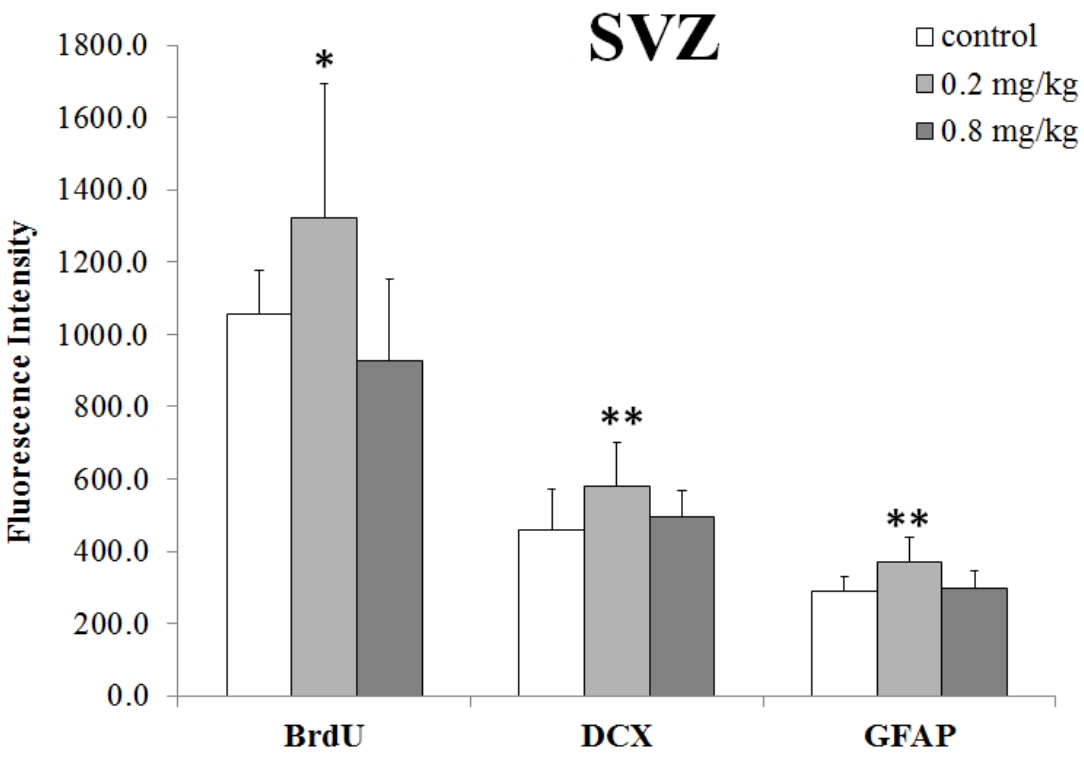

Figure 21. Quantification of IHC triple labeling in the SVZ for BrdU, DCX, and GFAP at low magnification (x40). Bar graph shows the fluorescence intensity for each label in the SVZ. Data represent mean ± S.D., n = 4; * $p < 0.05$, ** $p < 0.01$ as compared with controls.

The trend in increasing expression of BrdU and DCX after Mn exposure observed at low magnification (x40) continued for the high magnification images (x100 and x400, **Figure 22**). At x100 magnification, BrdU label was significantly increased by 83.1%, and DCX label was significantly increased by 78.4% ($p < 0.01$) following 0.2 mg/kg Mn exposure. At x400 magnification, BrdU expression was significantly increased following both 0.2 and 0.8 mg/kg Mn exposure, 54.4% and 37.7%, respectively as compared with control ($p < 0.01$; **Figure 23**). Thus, Mn-exposure appeared to disturb the processes of both cell proliferation and differentiation critical for normal adult neurogenesis.

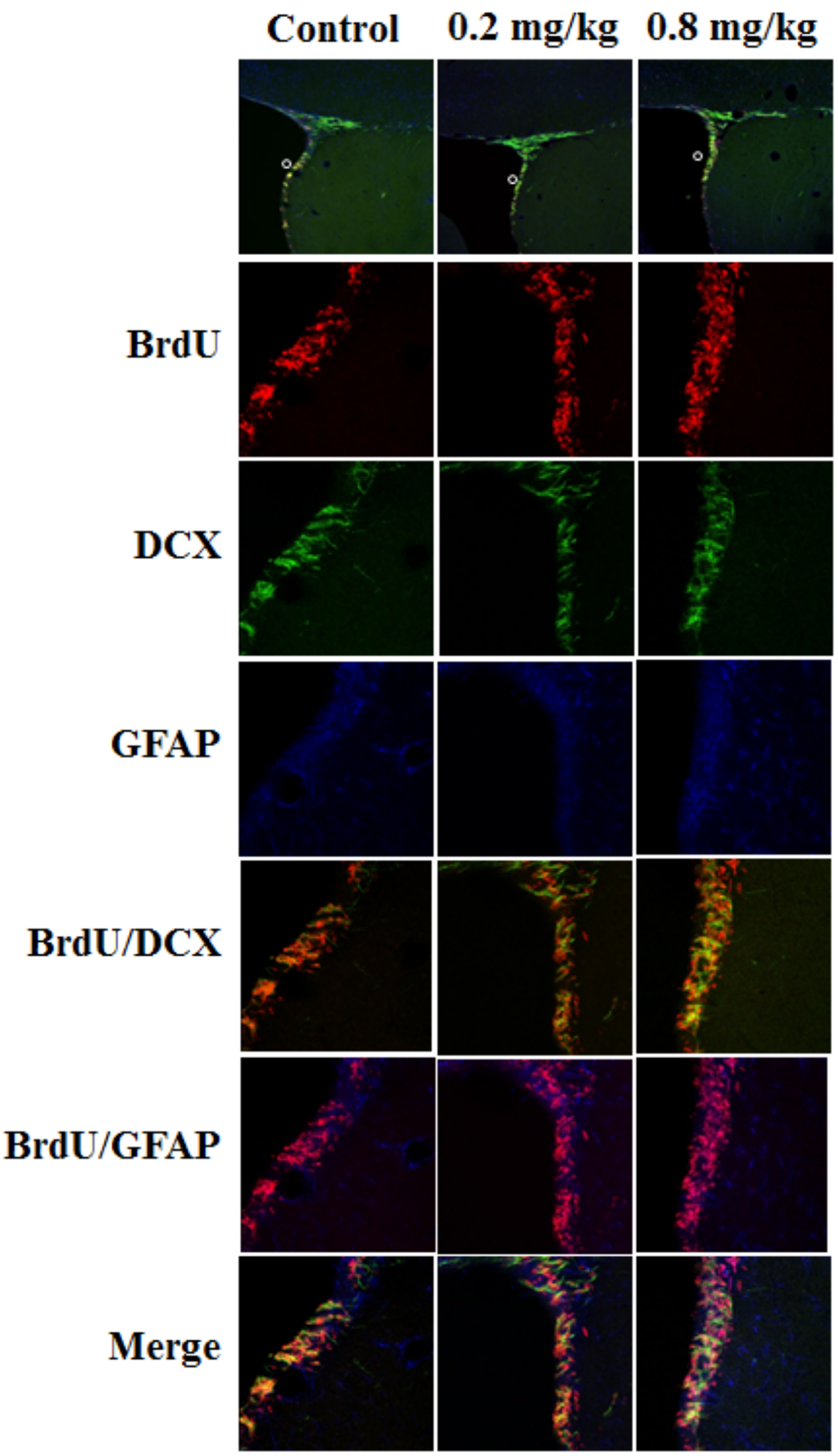

Figure 22. Immunohistochemical triple labeling for BrdU, DCX, and GFAP in the SVZ at high magnification. Representative images from each treatment group are shown. The circle in the x100 magnification (top row) indicates the approximate area of the SVZ enlarged in the x400 magnification images below of BrdU (red), DCX (green), GFAP (blue), BrdU/DCX, BrdU/GFAP, and merge.

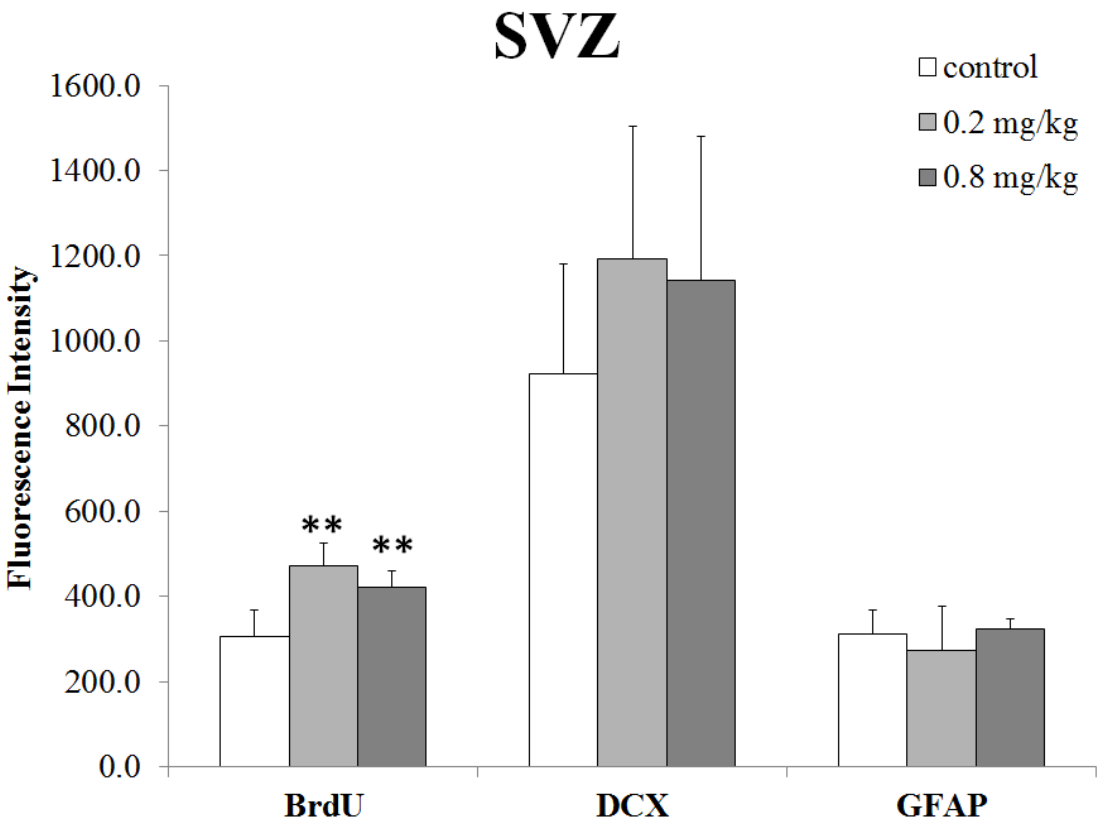

Figure 23. Quantification of IHC staining in the SVZ for BrdU, DCX, and GFAP at high magnification (x400). Bar graph showing fluorescence intensity for each label in the SVZ. Data represent mean ± S.D., n = 4; ** $p < 0.01$ compared with controls.

At higher magnification of the ΔSVZ region, we observed BrdU signal co-localized with both the DCX and GFAP signals; this was particularly evident when comparing the BrdU/DCX and BrdU/GFAP combined images (**Figure 24**). Quantification of ΔSVZ images at high magnification (x100) similarly revealed a 53.5% significant increase in BrdU expression following 0.8 mg/kg Mn exposure ($p < 0.05$) (**Figure 25**). DCX and GFAP expression were non-significantly increased following Mn exposure ($p = 0.08$ and 0.06, respectively). Increasing magnification to x400 in the ΔSVZ showed significantly increased BrdU expression following both 0.2 and 0.8 mg/kg Mn exposure (71.7% and 74.6%, respectively) compared with controls ($p < 0.05$). Additionally, DCX expression significantly increased by 91.8% in the ΔSVZ following 0.8 mg/kg Mn exposure ($p < 0.05$).

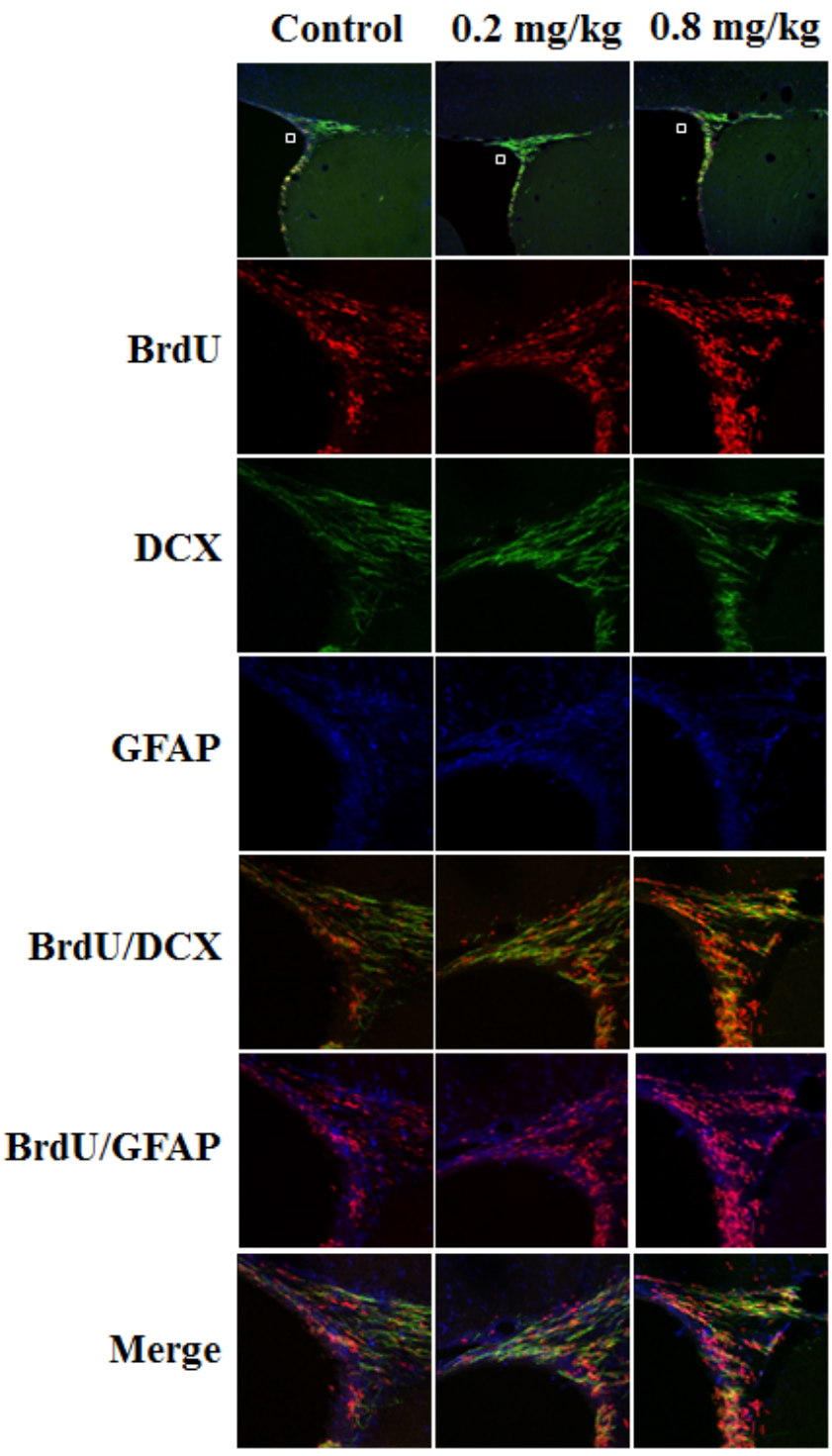

Figure 24. Immunohistochemical triple labeling for BrdU, DCX, and GFAP in the ΔSVZ at high magnification. Representative images from each treatment group are shown. The square in the x100 magnification (top row) indicates the approximate area of the ΔSVZ enlarged in the x400 magnification images below of BrdU (red), DCX (green), GFAP (blue), BrdU/DCX, BrdU/GFAP, and merge.

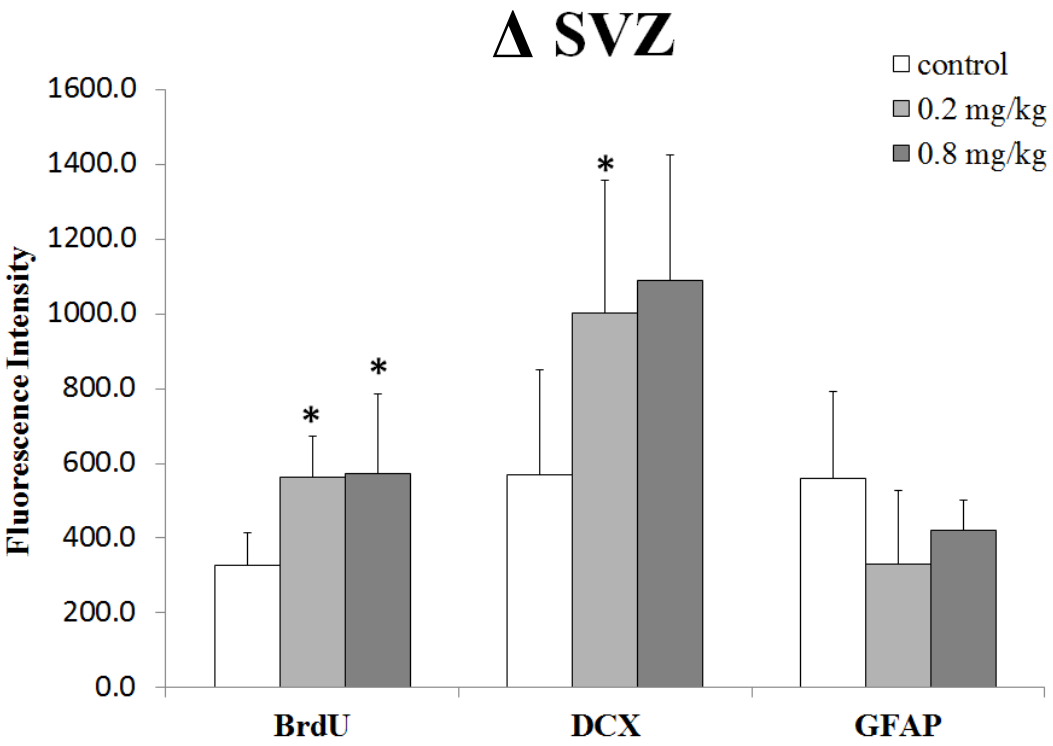

Figure 25. Quantification of IHC staining in the ΔSVZ region for BrdU, DCX, and GFAP at high magnification (x400). Bar graph showing fluorescence intensity for each label in the ΔSVZ. Data represent mean ± S.D., n = 4; * $p < 0.05$ compared with controls.

Newly proliferated $BrdU^+$ cells may begin to migrate along the RMS to their final destination in the olfactory bulb. Cells that survive in the olfactory bulb are capable of migrating further to the glomerular layer or the granule layer. Therefore, we assessed the changes within these two layers of the olfactory bulb with or without Mn exposure. This examination is of particular importance in that intranasal manganese exposure resulted in the highest concentration of Mn in the olfactory bulb. High magnification images (x100) of the olfactory bulb (**Figure 26**) showed BrdU expression in the glomerular layer was significantly increased by 58.9% following 0.2 mg/kg intranasal Mn exposure ($p < 0.01$; **Figure 27**). Additionally within the glomerular layer, DCX expression was significantly increased by 51.9% following 0.2 mg/kg Mn exposure ($p < 0.01$).

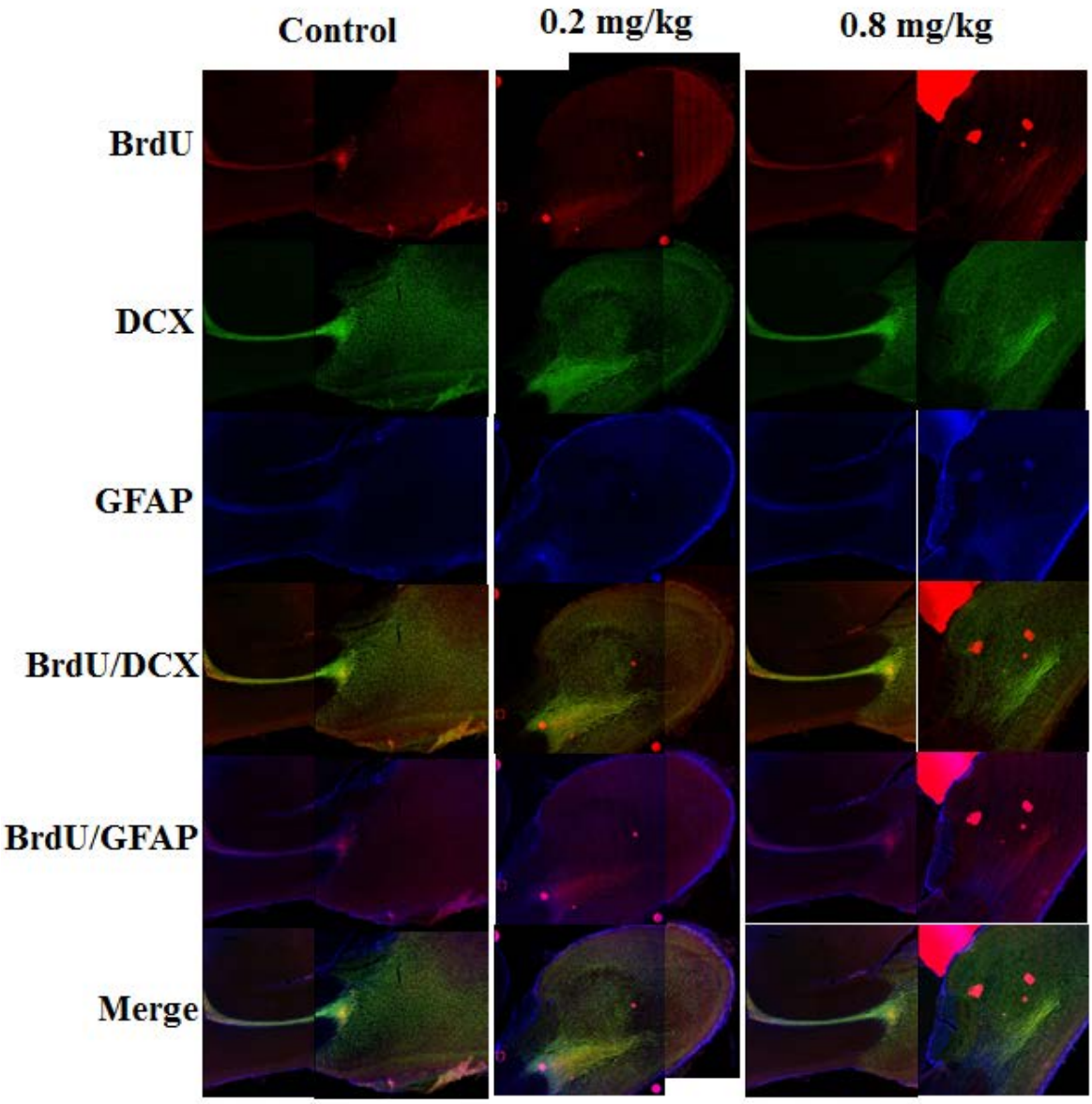

Figure 26. Immunohistochemical triple labeling for BrdU, DCX, and GFAP in the olfactory bulb at high magnification (x100). Representative images from each treatment group are shown. The square indicates the glomerular cell layer of the olfactory bulb and the circle indicates the granule cell layer of the olfactory bulb labeled for BrdU (red), DCX (green), GFAP (blue), BrdU/DCX, BrdU/GFAP, and merge.

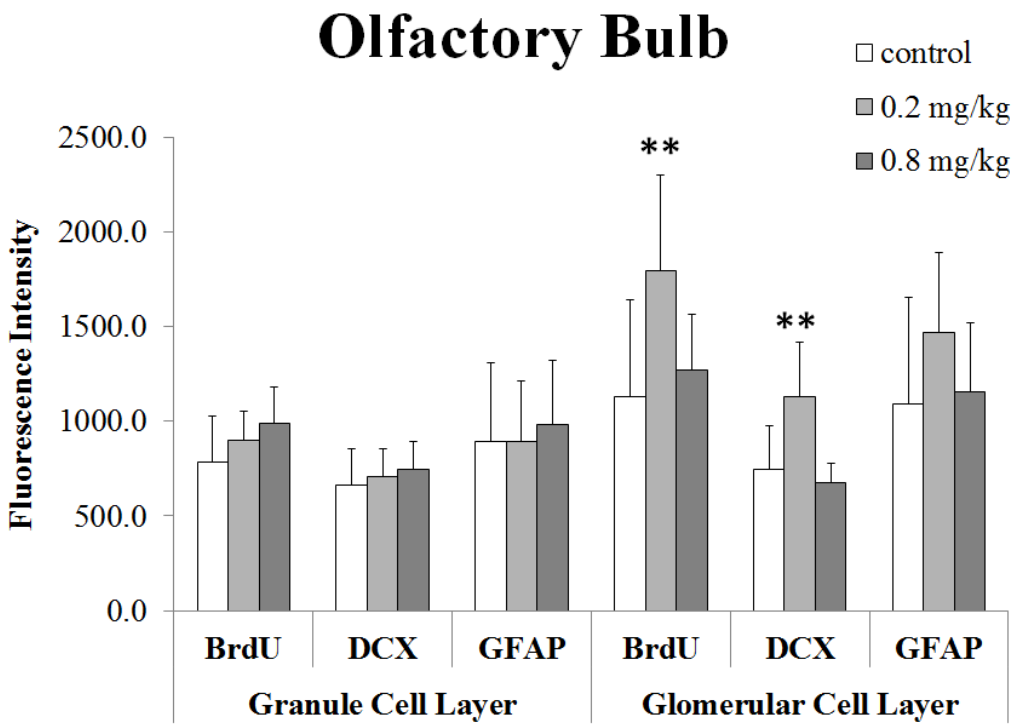

Figure 27. **Quantification of IHC staining in the olfactory bulb for BrdU, DCX, and GFAP at high magnification (x100).** Bar graph showing the fluorescence intensity for each label in the granule and glomerular cell layers. Data represent mean ± S.D., n = 4; ** $p < 0.01$ compared with controls.

4.4.4 *Dmt1* and *Ctr1* mRNA and Protein Expression Following Intranasal Mn Exposure

Altered metal levels in the brain have differential effects on brain function in neurodegenerative disease, and specifically in the SVZ, altered metal levels affect the processes of cell proliferation and differentiation critical for normal adult neurogenesis. A complete understanding of the factors affecting neurogenesis could potentially lead to improved therapies for neurodegenerative disease, stroke, and brain injury. Therefore, it is of utmost importance that we begin to explain the mechanisms responsible for altered metal homeostasis in the SVZ. Altered metal levels could be due to the changes in proteins participating in regulation of cellular metal homeostasis. Two metal transporters known to be involved in Mn and Cu homeostasis, i.e., divalent metal transporter-1 (*Dmt1*) and Cu transporter 1 (*Ctr1*), were selected as candidates for further investigation. In previous studies, we have shown that Mn accumulation in the SVZ induces a 13% increase in *Dmt1* following intraperitoneal exposure (Fu et al., 2015). However, following IN Mn exposure, qPCR results in this study revealed that neither *Dmt1* nor *Ctr1*mRNA expression was significantly altered in SVZ, OB, STR, or HP (p values ranging from 0.28-0.67). Of note, increasing expression of *Dmt1* in the STR was close to, but did not reach statistical significance ($p = 0.07$).

By using Western blotting techniques, the total protein expression was also analyzed in these same tissues. Although it appeared that CTR1 protein expression was increased in the SVZ, but decreased in the STR following Mn exposure, quantification of Western blots did not reveal significant differences between groups in all tissues examined. The most striking result from these studies was the discovery that there was limited expression of CTR1 protein in both the OB and HP (**Figure 28**).

After intranasal Mn exposure, the highest levels of Mn in the brain were found in the OB. We investigated potential changes in α-synuclein and Iba1 in the OB following Mn exposure because some of the earliest symptoms of Parkinson's disease are observed in this brain region. According to the Braak hypothesis of Parkinson's disease pathology, olfactory structures are among the first to display pathological changes, and olfactory deficits are a common early symptom of Parkinson's disease (Braak et al., 2003; Berendse et al., 2011). Additionally, increased α-synuclein aggregation is a hallmark Parkinson's disease. Mn exposure is known to induce oxidative stress and inflammation which are important pathways in Mn-induced neurotoxicity; therefore, expression of Iba1, a marker of activated microglia, was analyzed in the olfactory bulb. Through these studies, it was revealed that olfactory α-synuclein was not significantly altered following IN Mn exposure ($p = 0.22$). Although it appeared Iba1 expression was significantly increased following Mn exposure, the increase did not reach statistical significance ($p = 0.06$). Noticeably, the proteins in these blots were poorly resolved and the signals overlapped, particularly for the β-actin signal, which made them unsuitable for quantification. Although the quality of the Western Blot results leaves much to be desired, the trend towards increasing expression of olfactory Iba1 was consistent for 6 blots.

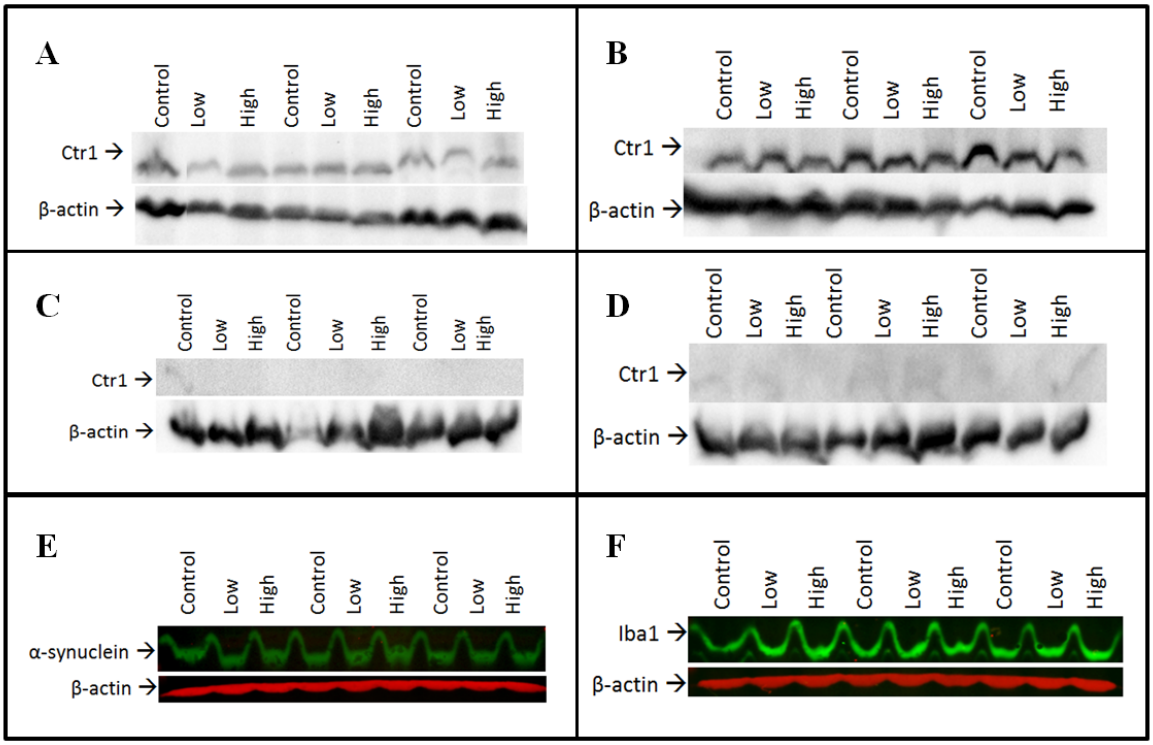

Figure 28. Western blots showing CTR1, α-synuclein, and Iba1 protein expression following intranasal Mn exposure. CTR1 protein levels detected in SVZ (A), STR (B), HP (C), and OB (D) using horseradish peroxidase-linked secondary antibodies. α – synuclein detected in OB (E), and Iba1 detected in OB (F) using Odyssey infrared imaging system. Each well contains approximately, 50 µg protein, n=3 per group. Each blot analyzed in triplicate (at a minimum).

4.4.5 HPLC Evaluation of Biogenic Amines in Olfactory Bulb and Thalamus

These studies followed the dose regimen detailed by Blecharz-Klin et al. (2013) who investigated neurochemical alterations following the IN Mn exposure. These authors showed only modest changes in any neurotransmitter system with the most striking result being a significant decrease in DA concentrations in the hippocampus. They also showed a significant increase in norepinephrine in the cortex and a significant decrease in serotonin in the cortex, hippocampus and striatum. Magnetic resonance spectroscopy studies of the human population exposed to Mn consistently reveal group differences in GABA expression in the thalamus (Dydak et al, 2011). Blecharz-Klin et al. (2013) did not investigate changes in GABA, nor did they investigate changes in the thalamus. Therefore, in the present study, GABA concentrations in the thalamus and olfactory bulb were investigated using HPLC. Changes in monoamine levels, including dopamine and serotonin and their metabolites were also evaluated in these brain regions.

Although the concentrations of GABA in the thalamus and OB were not significantly altered, it was interesting to note that thalamic GABA levels appeared to be reduced following Mn exposure ($p = 0.32$). Glutamate was not significantly altered in either the thalamus or olfactory bulb ($p = 0.1$-0.32). Lastly, monoamine data was not significantly altered following intranasal Mn exposure in either the OB or thalamus. DA concentrations in the thalamus appeared to be reduced following Mn exposure, but the variability was too large to provide conclusive results (n=3-4; $p = 0.095$).

4.5 Discussion

Previous work from our lab has shown that Mn exposure following intraperitoneal injection leads to significant accumulation in the SVZ and significantly altered Cu levels in this region. Cu levels are normally high in the SVZ, an area with known neurogenic function, even in adulthood. We hypothesized that the high basal Cu concentrations in the SVZ were necessary for normal adult neurogenesis in this niche. The effects on adult neurogenesis resulting from altered metal homeostasis following intranasal Mn exposure were unknown in this area. The AAS data presented here demonstrated that intranasal instillation of Mn led to significant accumulation of Mn in the SVZ and correspondingly, a significant decrease in SVZ Cu concentrations was observed. The IHC data revealed a significant increase in the expression of BrdU in the SVZ, ΔSVZ, and glomerular cell layer of the olfactory bulb following intranasal Mn exposure. Additionally, expression of DCX in these regions was also significantly increased following Mn exposure. GFAP expression was significantly increased only in the SVZ, the finding was not surprising because GFAP labels astrocytic stem cells, the true stem cells of the SVZ niche. These cells do not migrate, but proliferate in the SVZ niche, maintaining a pool of undifferentiated progenitor cells. GFAP expression did not change in the ΔSVZ which could indicate that the superior aspect of the SVZ does not maintain a pool of neural stem cells. Recently, we showed $BrdU^+$ cells mainly expressed DCX, with fewer $BrdU^+$ cells expressing GFAP following intraperitoneal Mn exposure (Fu et al., 2015). Our similar findings here suggest that Mn exposure mainly affected proliferating neuroblasts originating in the SVZ.

The application of the intranasal instillation route of Mn exposure is novel to the study of adult neurogenesis. There are several advantages of intranasal instillation over other traditional exposure routes, including, but not limited to: a more biologically relevant dose route with greater bioavailability (Tjälve et al., 1996) following direct transport into the CNS (Dorman et al., 2004), smaller cumulative doses, and shorter study durations because Mn can bypass the blood-brain barrier (Thompson et al., 2007). Although neurochemistry was unaffected in the current study, modest changes in dopamine and serotonin and their metabolites have been observed following this dose administration (Blecharz-Klin et al., 2012). Additionally, we observed highly significant changes in both Mn and Cu concentrations in the brain following this route of exposure that are similar in magnitude to changes observed after intraperitoneal exposure. This is striking because the cumulative doses used in this study are less than 10% those used in intraperitoneal studies to achieve the same results. This finding suggests that Mn exposure by inhalation may be more harmful than other routes of exposure. Interestingly, changes in animals' body weights and relative organ weights which are indicators of general toxicity (Oszlanczi et al., 2010) were not significantly different between intranasal and intraperitoneal exposures, suggesting that the intranasal route is no more toxic than is intraperitoneal exposure, with regard to systemic toxicity.

After intranasal instillation, Mn levels were highest in the OB, suggesting Mn first entered the brain at the OB and followed retrograde transport to more posteriorly located brain structures, such as the SVZ and STR. Mn levels were unchanged at the cerebellum, which was anticipated given the expected rate of Mn transport. It is estimated to take 6 weeks for Mn to reach the cerebellum by this exposure route (Dorman et al., 2002),

whereas our study lasted for only two weeks. The same group of researchers has also shown that Mn concentrations in the OB remain elevated for up to 45 days following exposure (Dorman et al., 2004), suggesting there is great potential for Mn exposure to continue following dose cessation after this route of exposure.

Because of the SVZ's close proximity to the STR, it was important to confirm two discreet tissues were collected correctly at necropsy. Previous research from our lab has shown that tissue collected as SVZ shows amplification of nestin, a marker of proliferating cells following qPCR analysis. If this tissue was not the SVZ, there would be no amplification of this gene. Likewise, in the current study, Mn concentrations at each dose level were significantly different between the SVZ and the STR (control $p < 0.01$, 0.2 mg/kg $p < 0.001$, and 0.8 mg/kg $p < 0.05$). Additionally, differences in the Cu concentrations following Mn exposure also verified that the SVZ and striatal tissues were distinct; Cu concentrations were significantly reduced in the SVZ, while they were significantly increased in the STR.

Our observations raise several interesting questions: 1) what is the significance of the high Cu concentrations in the neurogenic niche; what is the function with regard to adult neurogenesis? 2) Are high Cu concentrations required for normal adult neurogenesis? 3) Is the mechanism responsible for accumulating high Cu levels in the SVZ altered following Mn exposure?

We have shown that basal Cu levels are extraordinarily high in the SVZ and they significantly decreased following Mn exposure. Kikuchihara et al. (2015) also showed a significant reduction of Cu concentration in the subventricular zone (SGZ) following Mn exposure. It is unknown if the basal Cu levels in the SGZ are significantly higher than

those in surrounding tissues because we cannot dissect out the SGZ at this time. It is also unknown if Mn exposure affects the Cu level in the SGZ. It would be possible in future studies to dissect out the entire dentate gyrus from the HP to check metal concentrations using AAS or use synchrotron analysis to detect Cu levels within the SGZ specifically. The results of the current study and the results from work in the SGZ by Kikuchihara's group suggest that Cu homeostasis is important in adult neurogenesis (Kikuchihara et al., 2015). Since a Cu imbalance is implicated in a variety of neurodegenerative diseases, it is possible that Cu dyshomeostasis is the beginning of a decline in proper brain repair mechanisms following Mn exposure. This deserves immediate investigation. Our results provide direct evidence that adult neurogenesis and gliogenesis are stimulated following intranasal Mn exposure.

CHAPTER 5: SUMMARY AND FUTURE DIRECTIONS

5.1 Summary

The transition metal Mn is the 12th most abundant element on earth (Nadaska et al., 2012). It is found in every cell in the body and is required for normal development and function of every cell in the body (Aschner et al., 2007; Crossgrove and Zheng, 2004; Guilarte, 2010). However, overexposure to this metal is toxic to various organ systems. The central nervous system is the primary target of Mn toxicity, with Mn accumulation in the globus pallidus producing signs and symptoms similar but not identical to idiopathic Parkinson's disease, including bradykinesia, memory deficits, and kinetic tremor (Bowman et al., 2011; Jiang et al., 2006; Racette et al., 2005). Overexposure to Mn primarily results from inhalation of high concentrations of Mn in the air in occupational settings such as welding, smelting, and dry-battery production (Cowan et al., 2009a,b; Keen and Lönnerdal, 1995; Racette et al., 2012). Regulatory standards are designed to protect workers from toxic exposures; however, researchers studying these populations have routinely shown Mn exposures above regulatory standards occur. More alarming still is the fact that low-level occupational exposure, with air Mn concentrations at or below occupational standards can also be detrimental. Neurochemical, neurobehavioral,

and neuroendocrine changes may occur before structural damage occurs, and are linked to pathogenic conditions (Alessio et al., 1989; Cowan et al., 2009a,b; Dydak et al., 2011; Lucchini and Zimmerman, 2009; Mutti et al., 1996).

Research on Mn neurotoxicity has often investigated changes in neurotransmitter expression and function, and studies suggest that dopaminergic neurons and their terminals are lesioned similar to Parkinson's disease following Mn exposure, but the results from other studies is often contradictory and the effect of Mn exposure on neurotransmitters remains uncertain.

It is known that symptoms of Mn-induced toxicity continue to progress even though further exposure has stopped, but it is unknown whether release of Mn from storage organs including bone could account for continual disease progression.

Lastly, it is unknown what the effect of Mn exposure is on the SVZ, a region with rich neurogenic potential; the SVZ in the lateral ventricles houses actively proliferating neural stem cells. These cells can differentiate and migrate anteriorly to the olfactory bulb. The olfactory bulb is the first brain region metals and other contaminants come into contact with following direct transport into the brain by way of olfactory neurons. The effect of olfactory Mn transport on either the olfactory bulb or the SVZ also remains unknown.

The studies in this doctoral dissertation were designed to address several of these research challenges in the field of Mn neurotoxicological research.

5.1.1 Chapter 2 Summary

Bone is a major storage organ for Mn, sequestering more than 40% of the total Mn in the body. The toxicokinetics of Mn in bone tissue, particularly the rate of accumulation, time to steady-state concentration, and half-life of Mn in bone remained unknown. Mn and Cu concentrations in bone tissues from rats orally exposed to Mn were evaluated at various times both during ongoing administration of Mn and following cessation of Mn exposure. We showed a rapid accumulation of Mn in bone followed by a much slower elimination from bone. We calculated the half-life of Mn in rat bone and for the first time were able to estimate the half-life of Mn in human bone to be approximately 8.6 years. We showed that Mn reaches steady-state concentrations after only 6 weeks. Lastly, the results of our work showed that Mn concentrations in bone were well correlated with concentrations in brain, indicating that bone is an accurate biomarker of Mn exposure and Mn accumulation in brain. The significance of this work was immediately apparent—it has helped provide support for use of bone as a biomarker of Mn exposure in the human population.

5.1.2 Chapter 3 Summary

Motor symptoms resulting from Mn toxicity resemble idiopathic Parkinson's disease. However, animal studies suggest that dopaminergic neurons selectively lesioned in Parkinson's disease remain intact after Mn intoxication (Guilarte, 2010). Therefore, some other change must be responsible for behavioral observations and motor function. Reports of Mn exposure altering neurotransmitter and metabolite levels have been

published (Gwiazda et al., 2007; Racette et al., 2012a), but the findings are often contradictory and widely debated. We investigated regional changes in dopamine and other neurotransmitters, including serotonin, norepinephrine, and GABA in rats subchronically exposed to Mn by intraperitoneal injection to attempt to explain differences in brain regions implicated in Parkinson's disease. We also used three dose levels to uncover a possible dose-response relationship. We showed significantly increased levels of DA and its metabolites in the striatum, as well as increased dopamine turnover in other brain regions affected by Parkinson's disease. Additionally, GABA levels were significantly higher in the hippocampus. No structural abnormalities were identifiable in any region evaluated. In conclusion, the results from this study showed that Mn exposure had more pronounced effects on neurotransmitter expression in the striatum rather than the substantia nigra following Mn exposure. We also showed that Mn exposure did have a dose-dependent effect on locomotor behavior in rats.

5.1.3 Chapter 4 Summary

Excess exposure to Mn in the human population predominantly occurs following inhalation. Mn accumulates in the olfactory bulb and can be transported to deeper brain structures, possibly including the subventricular zone, an area with known neurogenic capacity. The effect of Mn exposure in this region was unknown. Following a two-week intranasal Mn exposure in rats and pulse-labeling of BrdU at the end of the study, brain sections were evaluated for changes in cell proliferation and differentiation in the SVZ. The results of our work showed significant accumulation of Mn and a significant

reduction in Cu concentrations in the SVZ following Mn exposure. This altered metal homeostasis was found to be coupled with altered cell proliferation and differentiation. Following Mn exposure, there were significantly more $BrdU^+$ cells in the SVZ compared with controls. Additionally, there were more cells expressing markers for neuroblasts (DCX^+) and astrocytic stem cells ($GFAP^+$). Interestingly, we noted significantly increased expression of both BrdU and DCX, but not GFAP in the glomerular layer of the olfactory bulb. This is important because it shows for the first time that intranasal Mn exposure directly interacts with neurogenesis, potentially affecting neuronal repair mechanisms.

5.2 Limitations

The studies in this dissertation have several limitations. First, the dose, exposure route and duration are different for each study. The method selected for each study design was appropriate, but the differences between studies limited the ability to directly compare the results. Therefore, it is difficult to draw conclusions between studies (i.e. between the studies of bone accumulation and neurogenesis). Second, the sample sizes for neurochemistry and immunohistochemistry were limited. While the statistical power was sufficient to detect group differences, any important individual differences (for example cell death) may not have been captured. Lastly, changes in neurochemistry and neurogenesis due to Mn exposure are expected to be dynamic. The studies in this dissertation were designed to assess changes in these specific endpoints following Mn exposure. Because samples were collected at one point in time, in both cases 24 hr after dose cessation, it is possible that important differences were not captured. For instance,

perhaps neurochemistry is most significantly affected after the initial Mn exposure as opposed to 24 hr after cessation. It would have been beneficial to have collected samples at more than one point in time. Similarly, in studies of adult neurogenesis, without collecting samples over time, it is impossible to draw conclusions about how Mn exposure affects cell survival or migration.

5.3 Future Directions

The research in this dissertation has established that toxic Mn exposure can alter neurochemistry in regions important in neurodegenerative disease but there was no significant effect on dopaminergic cell loss. While our neurochemistry data from these studies did not result in any definitive dose-response relationship in neurotransmitter expression, we did show dose-dependent decrease in locomotor behaviors. The open field test may not be sensitive enough to detect the extent of behavioral changes resulting from Mn toxicity, nor does it allow for detecting changes in learning and memory following Mn exposure. Changes we observed in the hippocampus neurotransmission suggest changes in learning and memory following Mn exposure are possible and should be investigated. The Morris water maze is the common test used to determine differences in learning and memory and may be suitable here. To detect differences in motor function, the rotarod test coupled with a stride analysis test may be more suitable than the open field test.

We have also showed that Mn exposure had significant effects on toxicokinetics of Mn storage in and elimination from bone. The levels of Mn in bone were significantly correlated with levels in brain, making bone a highly useful biomarker of Mn exposure.

To facilitate development of bone as a suitable biomarker and development of a technique for measuring Mn in bone, it would be helpful to know the contribution of other tissues, including skin, muscle, and bone marrow, that could potentially interfere with collecting accurate measurements of a patient's bone Mn concentrations. We have preliminary data suggesting neither muscle nor bone marrow contain substantial amounts of Mn, but this should be verified, and skin (including fur from animals) should be evaluated as well.

Lastly, intranasal Mn exposure has been demonstrated to be an effective route of exposure for the study of Mn neurotoxicity and adult neurogenesis. The primary route of exposure in humans is by inhalation. By this route, a large percentage of Mn is taken into the CNS directly at the olfactory mucosa while a smaller fraction is inhaled or swallowed and passes into the blood. Circulation permits additional uptake of Mn into the CNS from the blood through the brain barrier systems. The method of intranasally instilling Mn directly at the olfactory mucosa maximizes the amount of Mn directly entering the CNS and minimizes the amount of Mn available to enter into systemic circulation.

Mn accumulation in other brain regions leads to altered neurochemistry. Changes in neurochemistry may cause subtle neuronal injuries. It is worthwhile to investigate changes in neurochemistry in the SVZ and see if these subtle changes may trigger adult neurogenesis processes in the SVZ, leading to increased proliferation and migration of DCX^+ cells to the OB for the purpose of neuronal repair. Additionally, it would be interesting to investigate levels of glutamate in the frontal cortex of intranasally instilled animals as changes in frontal cortex glutamate have been seen in MRS experiments with Mn exposed workers.

The answers to the following questions are currently unknown: 1) why are basal Cu levels are so high in the SVZ, 2) how does Mn accumulate in this region, and 3) how does Mn accumulation subsequently disrupt Cu homeostasis in the SVZ. It is important for a complete understanding of Mn neurotoxicity in relationship to neurodegenerative disease pathology that each of these questions be addressed. The present studies began to address how Mn accumulates and how Cu levels are altered following Mn exposure, but the results were inconclusive and the methods did not consider all possible transporters which could be participating in altered metal homeostasis. An analysis of the repertoire of metal transporters involved in Mn and Cu homeostasis should be undertaken to fully explain these changes.

Overall, it can be concluded from the data presented in these studies that neurotoxic Mn exposure causes subclinical alterations in neurochemistry, metal concentrations and homeostasis, and animal behavior. These changes have not led to any detectable structural damage within the time frame investigated in these studies and the results of this work do not suggest that structural damage is imminent. However, some of the changes observed are themselves toxic (i.e., increased levels of DA), and are capable of affecting other biological processes. Therefore, it seems likely that Mn exposure may ultimately lead to structural damage. This deserves further investigation.

LIST OF REFERENCES

LIST OF REFERENCES

Alessio L, Apostoli P, Ferioli A, Lombardi S (1989). Interference of manganese on neuroendocrinal system in exposed workers. Preliminary report. *Biol Trace Elem Res.* 21:249-253.

Alvarez-Buylla A, Garcia-Verdugo JM (2002). Neurogenesis in adult subventricular zone. *The Journal of Neuroscience* 22(**3**):629-634.

Andersen ME, Dorman DC, Clewell HJ, Taylor MD, Nong A (2010). Multi-dose-route, multi-species pharmacokinetic models for manganese and their use in risk assessment. *Journal Of Toxicology And Environmental Health Part A* 73(**2**):217–234. doi:10.1080/15287390903340849

Andersen ME, Gearhart JM, Clewell HJ, 3rd. (1999). Pharmacokinetic data needs to support risk assessments for inhaled and ingested manganese. *NeuroToxicology* 20:161-171.

Apostoli P, Lucchini R, Alessio L (2000). Are current biomarkers suitable for the assessment of manganese exposure in individual workers? *Am J Ind Med* 37:283-290.

Arora M, Bradman A, Austin C, Vedar M, Holland N, Eskenazi B, Smith DR (2012). Determining fetal manganese exposure from mantle dentine of deciduous teeth. *Environ Sci Technol.* 46(**9**):5118–25.

Aschner JL, Aschner M (2005). Nutritional aspects of manganese homeostasis. *Mol Aspects Med.* 26:353-362.

Aschner, M., Erikson, K. M., Herrero Hernández, E., Hernández, E. H., & Tjalkens, R. (2009). Manganese and its role in Parkinson's disease: from transport to neuropathology. *Neuromolecular medicine*, *11*(4), 252–266. doi:10.1007/s12017-009-8083-0

Aschner M, Gannon M (1994). Manganese (Mn) transport across the rat blood-brain barrier: saturable and transferrin-dependent transport mechanisms. *Brain Research Bulletin* 33(**3**):345-349.

Aschner M, Guilarte TR, Schneider JS, Zheng W (2007). Manganese: recent advances in understanding its transport and neurotoxicity. *Toxicology and Applied Pharmacology* 221:131-147.

Aschner M, Vrana KE, Zheng W (1999). Manganese uptake and distribution in the central nervous system (CNS). *Neurotoxicology* 20:173–180.

Aslam, Pejovic-Milic A, Chettle DR, McNeill FE (2008). Quantification of manganese in human hand bones: a feasibility study. *Phys. Med. Biol.* 53 4081–4092.

ATSDR (2012). Toxicological Profile for Manganese. Atlanta, GA: U.S. Department of Health and Human Services, Public Health Service

Au C, Benedetto A, Aschner M (2008). Manganese transport in eukaryotes: the role of DMT1. *Neurotoxicology* 29:569-576.

Baker MG, Simpson CD, Sheppard L, Stover B, Morton J, Cocker J, Seixas N (2015). Variance components of short-term biomarkers of manganese exposure in an inception cohort of welding trainees. *Journal of Trace Elements in Medicine and Biology* 29:123-129.

Bancroft GN, Sikavitsas VI, van den Dolder J, Sheffield TL, Ambrose CG, Jansen JA, Mikos AG (2002). Fluid flow increases mineralized matrix deposition in 3D perfusion culture of marrow stromal osteoblasts in a dose-dependent manner. *PNAS* 99(**20**):12600-12605.

Barbeau A, Inoué N, Cloutier T (1976). Role of manganese in dystonia. *Adv Neurol* 14:339-352.

Barnham KJ, and Bush AI (2008). Metals in Alzheimer's and Parkinson's diseases. *Curr. Opin. Chem. Biol.* 12(**2**):222-228.

Bellusci M, La Barbera A, Padella F, Mancuso M, Pasquo A, Grollino MG, Leter G, Nardi E, Cremisini C, Giardullo P, Pacchierotti F (2014). Biodistribution and acute toxicity of a nanofluid containing manganese iron oxide nanoparticles produced by a mechanochemical process. *Int J Nanomedicine* 9:1919-1929.

Berendse HW, Roos DS, Raijmakers P, Doty RL (2011). Motor and non-motor correlates of olfactory dysfunction in Parkinson's disease. *J Neurol Sci* 310(**1-2**):21-24. doi: 10.1016/j.jns.2011.06.020.

Blecharz-Klin, K., Piechal, A., Joniec-Maciejak, I., Pyrzanowska, J., & Widy-Tyszkiewicz, E. (2012). Effect of intranasal manganese administration on neurotransmission and spatial learning in rats. *Toxicology and applied pharmacology*, *265*(1):1–9. doi:10.1016/j.taap.2012.09.015

Bocca B, Madeddu R, Asara Y, Tolu P, Marchal JA, Forte G (2011). Assessment of reference ranges for blood Cu, Mn, Se and Zn in a selected Italian population. *J Trace Elem Med Biol.* 25:19-26.

Bouchard MF, Laforest F, Vandelac L, Bellinger D, Mergler D (2007). Hair manganese and hyperactive behaviors: pilot study of school-age children exposed through tap water. *Environmental Health Perspectives* 115:122-127.

Bouchard MF, Sauve S, Barbeau B, Legrand M, Brodeur ME, Bouffard T, Limoges E, Bellinger DC, Mergler D (2011). Intellectual impairment in school-age children exposed to manganese from drinking water. *Environmental Health Perspectives* 119:138-143.

Bowler RM, Gocheva V, Harris M, Ngo L, Abdelouahab N, Wilkinson J, Doty RL, Park R, Roels HA (2011). Prospective study on neurotoxic effects in manganese-exposed bridge construction welders. *NeuroToxicology* 32(**5**):596-605.

Bowman AB, Kwakye GF, Hernández EH, Aschner M. (2011). Role of manganese in neurodegenerative diseases. *Journal of Trace Elements in Medicine and Biology* 25(**4**):191–203. doi:10.1016/j.jtemb.2011.08.144

Braak H, Del Tredici K, Rub U, de Vos RAI, Jansen Steur ENH, Braak E (2003). Staging of brain pathology related to sporadic Parkinson's disease. *Neurobiology of Aging* 24(**2**):197-211.

Bradford MA (1976). A rapid and sensitive method for the quantitation of microgram quantities of protein utilizing the principle of protein-dye binding. *Analytical Biochemistry* 72:248-254.

Butcher DJ, Zybin A, Bolshov MA, Niemax K (1999). Speciation of methylcyclopentadienyl manganese tricarbonyl by high-performance liquid chromatography-diode laser atomic absorption spectrometry. *Analytical Chemistry* 71:5379-5385.

Cahill DF, Bercegeay MS, Haggerty RC, Gerding JE, Gray LE (1980). Age-related retention and distribution of ingested Mn3O4 in the rat. *Toxicol Appl Pharmacol.* 53:83-91.

Calabresi P, Ammassari-Teule M, Gubellini P, Sancesario G, Morello M, Centonze D, Marfia GA, et al. (2001). A synaptic mechanism underlying the behavioral abnormalities induced by manganese intoxication. *Neurobiology of disease* 8(**3**):419–32.

Cannon JR, Geghman KD, Tapias V, Sew T, Dail MK, Li C, Greenamyre JT (2013). Expression of human E46K-mutated a-synuclein in BAC-transgenic rats replicates early-stage Parkinson's disease features and enhances vulnerability to mitochondrial impairment. *Experimental Neurology* 240:44-56. doi:10.1016/j.expneurol.2012.11.007; PMID: 23153578

Chandra SV, Shukla GS (1981). Concentrations of striatal catecholamines in rats given manganese chloride through drinking water. *Journal of Neurochemistry* 36(**2**):683–687. Retrieved from http://www.ncbi.nlm.nih.gov/pubmed/7463083

Chandra SV, Shukla GS, Murthy RC (1979). Effect of stress on the response of rat brain to manganese. *Toxicology and Applied Pharmacology* 47(**3**):603–608.

Chandra SV, Shukla GS, Saxena DK (1979). Manganese-induced behavioral dysfunction and its neurochemical mechanism in growing mice. *Journal of Neurochemistry* 33(**6**):1217–21.

Chandra SV, Shukla GS, Srivastawa RS, Singh H, Gupta VP (1981). An exploratory study of manganese exposure to welders. *Clin Toxicol* 18:407-418.

Charash B, Placek E, Sos TA, Kligfield P (1982). Dose-related effects of manganese on the canine electrocardiogram. *J. Electrocardiol*. 15:149-152.

Chen JY, Tsao G, Zhao Q, Zheng W (2001). Differential cytotoxicity of Mn(II) and Mn(III): special reference to mitochondrial [Fe-S] containing enzymes. *Toxicology and Applied Pharmacology* 175:160-168.

Chua AC, Morgan EH (1997). Manganese metabolism is impaired in the Belgrade laboratory rat. *J Comp Physiol B* 167(**5**):361-369.

Chung SE, Cheong HK, Ha EH, Kim BN, Ha M, Kim Y, Hong YC, Park H, Oh SY (2015). Maternal blood manganese and early neurodevelopment: the mothers and children's environmental health (MOCEH) study. *Environmental Health Perspectives* 123(**7**):717-722.

Clark NA, Teschke K, Rideout K, Copes R (2007). Trace element levels in adults from the west coast of Canada and associations with age, gender, diet, activities, and levels of other trace elements. *Chemosphere* 70:155-164.

Collipp PJ, Chen SY, Maitinsky S (1983). Manganese in infant formulas and learning disability. *Ann Nutr Metab.* 27:488-494.

Cooper, W. C. (1984) The Health Implications of Increased Manganese in the Environment Resulting from the Combustion of Fuel Additives: A Review of the Literature. *Journal of Toxicology and Environmental Health* 14(**1**):23-46.

Cotzias GC, Papavasiliou PS, Mena I, Tang LC, Miller ST (1974). Manganese and Catecholamines. *Advances in Neurology* 5:235-243.

Couper J (1837). On the effects of black oxide of manganese when inhaled into the lungs. *Brit Ann Med Pharm, Vital Stat Gen Sci.* 1:41-42.

Cowan DM, Fan Q, Zou Y, Shi X, Chen J, Aschner M, Rosenthal FS, Zheng W (2009a). Manganese exposure among smelting workers: blood manganese-iron ratio as a novel tool for manganese exposure assessment. *Biomarkers* 14:3-16.

Cowan DM, Zheng W, Zou Y, Shi X, Chen J, Rosenthal FS, Fan Q (2009b). Manganese exposure among smelting workers: Relationship between blood manganese-iron ratio and early onset neurobehavioral alterations. *NeuroToxicology* 30:1214-1222.

Crawford S, Davis K, Saddler C, Joseph J, Catapane EJ, Carroll MA (2011). The ability of PAS, acetylsalicylic acid and calcium disodium EDTA to protect against the toxic effects of manganese on mitochondrial respiration in gill of crassostrea virginica. *In Vivo* 33:7-14.

Crossgrove JS, Zheng W (2004). Manganese toxicity upon overexposure. *NMR Biomedicine* 17:544-553.

Crossgrove JS, Yokel RA (2005). Manganese distribution across the blood-brain barrier IV. Evidence for brain influx through store-operated calcium channels. *NeuroToxicology* 26:297-307.

Crossgrove JS, Allen DD, Bukaveckas BL, Rhineheimer SS, Yokel RA (2003). Manganese distribution across the blood-brain barrier. I. Evidence for carrier-mediated influx of manganese citrate as well as manganese and manganese transferrin. *NeuroToxicology* 24(**1**):3-13.

Curtis MA, Faull RLM, Eriksson PS (2007). The effect of neurodegenerative diseases on the subventricular zone. *Nat. Rev. Neuroscience* 8(**9**):712-723.

DeSimone LA, Hamilton PA, Gilliom RJ (2009). The quality of our nation's waters—Quality of water from domestic wells in principal aquifiers of the United States, 1991-2004—Overview of major findings. U.S. Geological Survey Circular 1332. p48.

DeWitt MR, Chen P, Aschner M (2013). Manganese efflux in Parkinsonism: insights from newly characterized SLC30A10 mutations. *Biochem Biophys Res Commun*. 432(**1**):1-4.

Dobson AW, Erikson KM, Aschner M. (2004). Manganese neurotoxicity. *Annals of the New York Academy of Sciences* 1012:115–128. doi:10.1196/annals.1306.009

Doetsch F, Caille I, Lim DA, Garcia-Verdugo JM, Alvarez-Buylla A (1999). Subventricular zone astrocytes are neural stem cells in the adult mammalian brain. *Cell* 97:703-716.

Dorman DC, Brenneman KA, McElveen AM, Lynch SE, Roberts KC, Wong BA (2002). Olfactory transport: a direct route of delivery of inhaled manganese phosphate to the rat brain. *Journal of Toxicology and Environmental Health, Part A* 65:1493-1511.

Dorman DC, McManus BE, Parkinson CU, Manuel CA, McElveen AM, Everitt JI (2004). Nasal toxicity of manganese sulfate and manganese phosphate in young male rats following subchronic (13-week) inhalation exposure. *Inhalation Toxicology* 16:481-488.

Dorman DC, McElveen AM, Marshall MW, Parkinson CU, Arden James R, Struve MF, et al. (2005). Maternal-fetal distribution of manganese in the rat following inhalation exposure to manganese sulfate. *NeuroToxicology* 26:625-632.

Dydak U, Jiang YM, Long LL, Zhu H, Chen J, Li WM, Edden RA, Hu S, Fu X, Long Z, Mo XA, Meier D, Harezlak J, Aschner M, Murdoch JB, Zheng W (2011). In vivo measurement of brain GABA concentrations by magnetic resonance spectroscopy in smelters occupationally exposed to manganese. *Environmental Health Perspectives* 2:219-224.

Eastman RR, Jursa TP, Benedetti C, Lucchini RG, Smith DR (2013). Hair as a biomarker of environmental manganese exposure. *Environ Sci Technol.* 47(**3**):1629-37.

EPA. Mn (CASRN 7439-96-5) Integrated Risk Information System.

Ericson JE, Crinella FM, Clarke-Stewart KA, Allhusen VD, Chan T, Robertson RT (2007). Prenatal manganese levels linked to childhood behavioral disinhibition. *Neurotoxicol Teratol.* 29(**2**):181-187.

Fitsanakis VA, Zhang N, Anderson JG, Erikson KM, Avison MJ, Gore JC, Aschner M (2008). Measuring brain manganese and iron accumulation in rats following 14 weeks of low-dose manganese treatment using atomic absorption spectroscopy and magnetic resonance imaging. *Toxicological Sciences* 103(**1**):116–124. doi:10.1093/toxsci/kfn019

Frisbie SH, Ortega R, Maynard DM, Sarkar B (2002). The concentrations of arsenic and other toxic elements in Bangladesh's drinking water. *Environmental Health Perspectives* 110(**11**):1147-1153.

Frumkin H, Solomon G (1997). Manganese in the U.S. gasoline supply. *American Journal of Industrial Medicine* 31:107-115.

Fu S, O'Neal S, Hong L, Jiang W, Zheng W (2015). Elevated adult neurogenesis in brain subventricular zone following in vivo manganese exposure: roles of copper and DMT1. *Toxicological Sciences* 143(**2**):482-498.

Fujioka M, Taoka T, Matsuo Y, Mishima K, Ogoshi K, Kondo Y, Tsuda M, Fujiwara M, Asano T, Sakaki T, Miyasaki A, Park D, and Siesjö BK (2003). Magnetic resonance imaging shows delayed ischemic striatal neurodegeneration. *Ann Neurol* 54(**6**):732-47.

Fujishiro H, Yano Y, Takada Y, Tanihara M, Himeno S (2012). Roles of ZIP8, ZIP14, and DMT1 in transport of cadmium and manganese in mouse kidney proximal tubule cells. *Metallomics* 4(**7**):700-708.

Furchner JE, Richmond CR, Drake GA (1966). Comparative metabolism of radionuclides in mammals. 3. Retention of manganese-54 in the mouse, rat, monkey and dog. *Health Phys* 12:1415-1423.

Gao X, Chen J (2013). Moderate traumatic brain injury promotes neural precursor proliferation without increasing neurogenesis in the adult hippocampus. *Exp. Neurol.* 239:38-48.

Garzon-Muvdi T, Quinones-Hinojosa A (2010). Neural stem cell niches and homing: recruitment and integration into functional tissues. *ILAR* 51(**1**):3-23.

Genter MB, Newman NC, Shertzer HG, Ali SF, Bolon B (2012). Distribution and systemic effects of intranasally administered 25nm silver nanoparticles in adult mice. *Toxicologic Pathology* 40:1004-1013.

Gianutsos G, Morrow GR, Morris JB (1997). Accumulation of manganese in rat brain following intranasal administration. *Fundamental and Applied Toxicology* 37:102-105.

Gibaldi M, Perrier, D (1982). *Pharmacokinetics*. pp. 84–109, 433–444. Marcel Dekker, New York.

Gibbons RA, Dixon SN, Hallis K, Russell AM, Sansom BF, Symonds HW (1976). Manganese metabolism in cows and goats. *Biochimica et Biophysica Acta (BBA)-General Subjects* 444(**1**):1-10.

Guilarte TR (2010). Manganese and Parkinson's disease: a critical review and new findings. *Environmental Health Perspectives* 118(**8**):1071–1080.

Guilarte TR, Chen MK, McGlothan JL, Verina T, Wong, DF, Zhou, Y (2006). Nigrostriatal Dopamine System Dysfunction and Subtle Motor Deficits in Manganese-Exposed Non-Human Primates. *Experimental Neurology 202*:381-390.

Guilarte TR, Gonzales KK (2015). Manganese-Induced Parkinsonism Is Not Idiopathic Parkinson's Disease: Environmental and Genetic Evidence. Toxicological Sciences 146(2):204-212.

Grashow R, Zhang J, Fang SC, Weisskopf MG, Christiani DC, Cavallari JM (2014). Toenail metal concentration as a biomarker of occupational welding fume exposure. *J Occup Environ Hyg.* 11(**6**):397-405.

Grunecker B, Kltwasser SF, Zappe AC, Bedenk BT, Bicker Y, Spoormaker VI, Wotjak CT, Czisch M (2013). Regional specificity of manganese accumulation and clearance in the mouse brain: implications for manganese-enhanced MRI. *NMR Biomed*. 26:542-556.

Gwiazda R, Lucchini R, Smith D (2007). Adequacy and consistency of animal studies to evaluate the neurotoxicity of chronic low-level manganese exposure in humans. *J Toxicol Environ Health A.* 70(**7**):594-605.

Hafeman D, Factor-Litvak P, Cheng Z, van Geen A, Ahsan H (2007). Association between manganese exposure through drinking water and infant mortality in Bangladesh. *Environ Health Perspect*. 115(**7**):1107-1112.

Harris WR, Chen Y (1994). Electron paramagnetic resonance and difference ultraviolet studies of Mn2+ binding to serum transferrin. *J Inorg Biochem.* 54(**1**):1–19.

Hastings TG, Zigmond MJ (1994). Identification of catechol-protein conjugates in neostriatal slices incubated with [3H]dopamine: impact of ascorbic acid and glutathione. *Journal of Neurochemistry* 63:1126-1132. PMID:8051554

He L, Girijashanker K, Dalton TP, Reed J, Li H, Soleimani M, Nebert DW (2006). ZIP8, member of the solute-carrier-39 (SLC39) metal-transporter family: characterization of transporter properties. *Molecular Pharmacology* 70(**1**):171-180.

Hong L, Jiang W, Zheng W, Zeng S. HPLC analysis of para-aminosalicylic acid and its metabolite in plasma, cerebrospinal fluid and brain tissues (2011). *Journal of Pharmaceutical and Biomedical Analysis* 54:1101-1109.

Hong L, Xu C, O'Neal S, Bi HC, Huang M, Zheng W, Zeng S (2014). Roles of P-glycoprotein and multidrug resistance protein in transporting para-aminosalicylic acid and its N-acetylated metabolite in mice brain. *Acta Pharmacol Sin*. 35(**12**):1577-1585.

Hong JS, Hung CR, Seth PK, Mason G, Bondy SC (1984). Effect of Manganese Treatment on the Levels of Neurotransmitters, Hormones, and Neuropeptides: Modulation by Stress. *Environmental Research* 34(**2**):242-249.

Huang CC, Chu NS, Lu CS, Wang JD, Tsai JL, Tseng JL, Wolters EC, Calne DB (1989). Chronic manganese intoxication. *Arch Neurol* 46:1104-1106.

Husain M, Khanna VK, Roy A, Tandon R, Pradeep S, Set PK (2001). Platelet Dopamine Receptors and Oxidative Stress Parameters as Markers of Manganese Toxicity. *Human & Experimental Toxicology* 20(**12**):631-636.

ICRP. 1972. Report of the task group on reference man. Publication no.23, international commission on radiological protection, New York.

Inoue N and Makita Y (1996). Neurological aspects in human exposures to manganese. In: Toxicology of Metals. L. W. Chang, Ed. CRC Press, Boca Raton. pp415-421.

Jiang YM, Mo XA, Du FQ, Fu X, Zhu XY, Gao HY, Xie JL, Liao FL, Pira E, and Zheng W (2006). Effective Treatment of Manganese-Induced Occupational Parkinsonism with PAS-Na: A Case of 17-Year Follow-Up Study. *J. Occup. Env. Med.* 48:644-649.

Jiang YM, Zheng W, Long LL, Zhao WJ, Li XG, Mo XA, Lu JP, Fu X, Li WM, Liu SF, Long QY, Huang JL, and Pira E (2007). Brain magnetic resonance imaging and manganese concentrations in red blood cells of smelting workers: Search for biomarkers of manganese exposure. *NeuroToxicology* 28:126-135.

Jiang Y, Zheng W (2005). Cardiovascular toxicities upon manganese exposure. *Cardiovascular Toxicology* 5:345-354.

Kalia K, Jiang W, Zheng W (2008). Manganese accumulates primarily in nuclei of cultured brain cells. *NeuroToxicology* 29:466-470.

Kanayama Y, Tsuji T, Enomoto S, Amano R (2005). Multitracer screening: brain delivery of trace elements by eight different administration methods. *Biometals* 18:553-565.

Kannurpatti SS, Joshi PG, Joshi NB (2000). Calcium sequestering ability of mitochondria modulates influx of calcium through glutamate receptor channel. *Neurochem Res.* 25(**12**):1527-1536.

Keen CL, Lönnerdal B (1995). Toxicity of essential and beneficial metal ions. Manganese. In Handbook of Metal-Ligand Interactions in Biological Fluids, Berthon G, ed. Marcel Dekker, Inc.: New York, NY. pp683-688.

Khan K, Wasserman GA, Liu X, Ahmed E, Parvez F, Slavkovich V, Levy D, Mey J, van Geen A, Graziano JH, Factor-Litvak P (2012). Manganese exposure from drinking water and children's academic achievement. *Neurotoxicology* 33:91-97.

Khan K, Factor-Litvak P, Wasserman GA, Liu X, Ahmed E, Parvez F, Slavkovich V, Levy D, Mey J, van Geen A, Graziano JH (2013). Manganese exposure from drinking water and children's classroom behavior in Bangladesh. *Environmental Health Perspectives* 119:1501-1506.

Kikuchihara Y, Abe H, Tanaka T, Kato M, Wang L, Ikarashi Y, Yoshida T, Shibutani M (2015). Relationship between brain accumulation of manganese and aberration of hippocampal adult neurogenesis after oral exposure to manganese chloride in mice. *Toxicology* 33(**1**):24-34.

Klaassen CD (1976). Biliary excretion of metals. *Drug Metab Rev.* 5(**2**):165-196.

Kobayashi K, Kuroda J, Shibata N, Hasegawa T, Seko Y, Satoh M, Tohyama C, Takano H, Imura N, Sakabe K, Fujishiro H, Himeno S (2007). Induction of metallothionein by manganese is completely dependent on interleukin-6 production. *J Pharmacol Exp Ther*. 320(**2**):721-727.

Kondakis XG, Makris N, Leotsinidis M, Prinou M, Papapetropoulos T (1989). Possible health effects of high manganese concentration in drinking water. *Arch Environ Health*. 44(**3**):175-178.

Korczynski RE (2000). Occupational health concerns in the welding industry. *Appl Occup Environ Hyg*. 5:936-945.

Krebs N, Langkammer C, Goessler W, Ropele S, Fazekas F, Yen K, Scheurer E (2014). Assessment of trace elements in human brain using inductively coupled plasma mass spectrometry. *J Trace Elem Med Biol.* 28(**1**):1-7.

Kunar MJ, Couceyro PR, Lambert PD (1999). Catecholamines. In G.J. Siegel, B.W. Agranoff, R.W. Albers, S.K. Fisher, & M.D. Uhler (Eds.), *Basic Neurochemistry Molecular, Cellular, and Medical Aspects* (pp. 243-261). Philadelphia, PA: Lippincott-Raven.

Laohaudomchok W, Lin X, Herrick RF, Fang SC, Cavallari JM, Christiani DC, Weisskopf MG (2011). Toenail, blood and urine as biomarkers of manganese exposure. *J Occup Environ Med.* 53(**5**):506-510.

Leavens TL, Rao D, Anderson ME, Dorman DC (2007). Evaluating transport of manganese from olfactory mucosa to striatum by pharmacokinetic modeling. *Toxicological Sciences* 97:265-278.

Lebda MA, El-Neweshy MS, El-Sayed YS (2012). *NeuroToxicology* 33(**1**):98-104.

Lee JW, Lee CK, Moon CS, Choi IJ, Lee KJ, Yi SM, Jang BK, Yoon BJ, Kim DS, Peak D, Sul D, Oh E, Im H, Kang HS, Kim JH, Lee JT, Kim K, Park KL, Ahn R, Park SH, Kim SC, Park CH, Lee JH (2012). Korea National Survey for Environmental Pollutants in the Human Body 2008: Heavy metals in the blood or urine of the Korean population. *Int J Hyg Environ Health.* 215:449-457.

Leyva-Illades D, Chen P, Zogzas CE, Hutchens S, Mercado JM, Swaim CD, Morrisett RA, Bowman AB, Aschner M, Mukhopadhyay S (2014). SLC30A10 is a cell surface-localized manganese efflux transporter, and parkinsonism-causing mutations block its intracellular trafficking and efflux activity. *J Neurosci.* 34(**42**):14079-95.

Liu Y, Koltic D, Byrne P, Wang H, Zheng W, Nie LH (2013). Development of a transportable neutron activation analysis system to quantify manganese in bone in vivo: feasibility and methodology. *Physiol. Meas.* 34:1593-1609.

Liu YZ, Byrne P, Wang HY, Koltick D, Zheng W, Nie L (2014). A compact DD neutron generator-based NAA system to quantify manganese (Mn) in bone in vivo. *Physiol Meas.* 35:1899-1911.

Long Z, Li XR, Xu J, Edden RA, Qin WP, Long LL, Murdoch JB, Zheng W, Jiang YM, Dydak U (2014). Thalamic GABA predicts fine motor performance in manganese-exposed smelter workers. *PLoS ONE* 9(**2**):e88220.

Long LL, Li XR, Huang ZK, Jian YM, Fu SX, Zheng W (2009). Relationship between changes in brain MRI and 1H-MRS, severity of chronic liver damage, and recovery after liver transplantation. *Exp Biol Med*. 234:1075-1085.

Lu L, Zhang LL, Li GJ, Guo W, Liang W, Zheng W (2005). Serum concentrations of manganese and iron as the potential biomarkers for manganese exposure in welders. *NeuroToxicology* 26(**2**): 257-265.

Lucaciu CM, Dragu C, Copaescu L, Morariu VV (1997). Manganese transport through human erythrocyte membranes. An EPR study. *Biochim Biophys Acta* 1328(**2**):90–8.

Lucchini RG, Albini E, Benedetti L, Borghesi S, Coccaglio R, Malara EC, et al. (2007). High prevalence of parkinsonian disorders associated to manganese exposure in the vicinities of ferroalloy industries. *Am J Ind Med* 50:788-800.

Lucchini R, Zimmerman N (2009). Lifetime cumulative exposure as a threat for neurodegeneration: need for prevention strategies on a global scale. *NeuroToxicology* 30:1144-1148.

Lucchini RG, Dorman DC, Elder A, Veronesi B (2012). Neurological impacts from inhalation of pollutants and the nose-brain connection. *NeuroToxicology* 33:838-841.

Lucchini RG, Guazzetti S, Zoni S, Donna F, Peter S, Zacco A, Salmistraro M, Bontempi E, Zimmerman NJ, Smith DR (2012). Tremor, olfactory and motor changes in Italian adolescents exposed to historical ferromanganese emission. *NeuroToxicology* 33:687-696.

Lytle CM, Smith BN, McKinnon CZ (1995). Manganese accumulation along Utah roadways: a possible indication of motor vehicle exhaust pollution. *The Science of the Total Environment* 162:105-109.

Madejczyk MS, Ballatori N (2012). The iron transporter ferroportin can also function as a manganese exporter. *Biochim Biophys Acta* 1818(**3**):651-657.

Marchal G, Ni Y, Zhang X, Yu J, Lodemann KP, Baert AL (1993). Mn-DPDP enhanced MRI in experimental bile duct obstruction. *J Comput Assist Tomogr*. 17:290-296.

Mates JM, Segura JA, Alonso FJ, Marquez J (2010). Roles of dioxins and heavy metals in cancer and neurological diseases using ROS-mediated mechanisms. *Free Radical Biol. Med.* 49(**9**):1328-1341.

McMillian, D.E. (1999). A Brief History of the Neurobehavioral Toxicity of Manganese: Some Unanswered Questions. *NeuroToxicology* 20(**2-3**):499-508.

Mena I, Horiuchi K, Burke K, Cotzias GC (1969). Chronic manganese poisoning. Individual susceptibility and absorption of iron. *Neurology* 19:1000-1006.

Menezes-Filho JA, Paes CR, Pontes AM, Moreira JC, Sarcinelli PN, Mergler D (2009). High levels of hair manganese in children living in the vicinity of a ferro-manganese alloy production plant. *Neurotoxicology* 30(**6**):1207-13.

Mergler D, Baldwin M, Belanger S, Larribe F, Beuter A, Bowler R, Panisset M, Edwards R, De Geoffroy A, Sassine M-P, Hudnell K (1999). Manganese Neurotoxicity, a Continuum of Dysfunction: Results from a Community Based Study. *NeuroToxicology* 20(**2-3**):327-342.

Michalke B, Fernsebner K (2014). New insights into manganese toxicity and speciation. *Journal of Trace Elements in Medicine and Biology* 28:106-116.

Morello M, Canini A, Mattioli P, Sorge RP, Alimonti A, Bocca B, Forte G, Martorana A, Bernardi G, Sancesario G (2008). Sub-cellular localization of manganese in the basal ganglia of normal and manganese-treated rats an electron spectroscopy imaging and electron energy-loss spectroscopy study. *NeuroToxicology* 29:60-72.

Mutti A, Bergamaschi E, Alinovi R, Lucchini R, Vettori MV, Franchini I (1996). Serum prolactin in subjects occupationally exposed to manganese. *Ann Clin Lab Sci.* 26(**1**):10-7.

Nachtman JP, Tubben RE, Commissaris RL (1986). Behavioral Effects of Chronic Manganese Administration in Rats: Locomotor Activity Studies. *Neurobehavioral Toxicology and Teratology* 8(**6**):711-715.

Nadaska G, Lesny J, Michalik I (2012) Environmental Aspect of Manganese Chemistry. 1-16. http://heja.szif.hu/ENV/ENV_100702-A/env100702a.pdf

Newland MC, Cox C, Hamada R, Oberdorster G, Weiss B (1987). The clearance of manganese chloride in the primate. *Fundam Appl Toxicol* 9:314-328.

Newland C (1999). Animal models of manganese's neurotoxicity. *NeuroToxicology* 20(**2-3**):415-432.

Omokhodion FO, Howard JM (1994). Trace elements in the sweat of acclimatized persons. *Clin Chim Acta*. 231(**1**):23-28.

O'Neal SL, Hong L, Fu S, Jiang W, Jones A, Nie LH, Zheng W (2014a). Manganese accumulation in bone following chronic exposure in rats: steady-state concentration and half-life in bone. *Toxicology Letters* 229(**1**):90-100.

O'Neal SL, Lee J-W, Zheng W, Cannon JR (2014b). Subacute manganese exposure in rats is a neurochemical model of early manganese toxicity. *NeuroToxicology* 44:303-313.

Ono K, Komai K, Yamada M (2002). Myoclonic involuntary movement associated with chronic manganese poisoning. *J Neurol Sci.* 199(**1-2**):93-96.

Ordoñez-Librado JL, Gutierrez-Valdez AL, Colín-Barenque L, Anaya-Martínez V, Díaz-Bech P, Avila-Costa MR (2008). Inhalation of divalent and trivalent manganese mixture induces a Parkinson's disease model: immunocytochemical and behavioral evidences. *Neuroscience* 155(**1**):7–16. doi:10.1016/j.neuroscience.2008.05.012

OSHA (2013). Manganese Fume (as Mn). *Chemical Sampling Information*. United States Department of Labor, April 2013. Retrieved from https://www.osha.gov/dts/chemicalsampling/data/CH_250200.html

Oszlanczi G, Vezer T, Sarkozi L, Horvath E, Szabo A, Horovath E, Konya Z, Papp A (2010). Metal deposition and functional neurotoxicity in rats after 3-6 week nasal exposure by two physicochemical forms of Mn. *Enviornmental Toxicology and Pharmacology* 30:121-126.

Ou CY, Huang ML, Jiang YM, Luo HL, Deng XF, Wang C, Wang F, Huang XW (2011). Effect of Sodium-Paraminosalicylic Acid on Concentrations of Amino Acid Neurotransmitters in Basal Ganglia of Manganese-Exposed Rats. *Zhonghua Yu Fang Yi Xue Za Zhi* 45(**5**):422-425.

Oulhote Y, Mergler D, Bouchard MF (2014). Sex- and age-differences in blood manganese levels in the U.S. general population: national health and nutritional examination survey 2011-2012. *Environ health.* 13:87. doi: 10.1186/1476-069X-13-87.

Pejovic-Milic A, Aslam, Chettle DR, Oudyk J, Pysklywec MW, Haines T (2009). Bone manganese as a biomarker of manganese exposure: a feasibility study. *Am J. Ind. Med.* 52:742-750.

Post JE (1999). Manganese oxide minerals: crystal structures and economic and environmental significance. *Proc Natl Acad Sci USA* 96:3447-3454.

Pushkar Y, Robison GA, Sullivan G, Fu SX, Kohne M, Jiang W, Rohr S, Lai B, Marcus MA, Zakharova T, Zheng W (2013). Aging results in copper accumulations in subventricular astrocytes. *Aging Cell* 12:823-832.

Racette BA, Aschner M, Guilarte TR, Dydak U, Criswell SR, Zheng W (2012a). Pathophysiology of manganese-associated neurotoxicity. *NeuroToxicology* 33:881-886.

Racette BA, Criswell SR, Lundin JI, Hobson A, Seixas N, Kotzbauer PT, Evanoff BA, Perlmutter JS, Zhang J, Sheppard L, Checkoway H (2012). Increased risk of parkinsonism associated with welding exposure. *NeuroToxicology* 33(**5**):1356-1361.

Racette BA, McGee-Minnich L, Moerlein SM, Mink JW, Videen TO, Perlmutter JS (2001). Welding-related Parkinsonism, clinical features, treatment, and pathophysiology. *Neurology* 56:8–13.

Racette BA, Tabbal SD, Jennings D, Good L, Perlmutter JS, Evanoff B (2005). Prevalence of Parkinsonism and relationship to exposure in a large sample of Alabama welders. *Neurology* 64:230–235.

Rahil-Khazen R, Bolann BJ, Myking A, Ulvik RJ (2002). Multi-element analysis of trace element levels in human autopsy tissues by using inductively coupled atomic emission spectrometry technique (ICP-AES). *J. Trace Elem. Med. Biol.* 16(**1**):15-25.

Reaney SH, Kwik-Uribe CL, Smith DR (2002). Manganese oxidation state and its implications for toxicity. *Chem. Res. Toxicol.* 15(**9**):1119–1126.

Riojas-Rodriguez H, Solis-Vivanco R, Schilmann A, Montes S, Rodriguez S, Rios C, Rodriguez-Agudelo Y (2010) Intellectual function in Mexican children living in a mining area and environmentally exposed to manganese. *Environ Health Perspect.* 118(**10**):1465-70.

Robison G, Zakharova T, Fu S, Jiang W, Fulper R, Barrea R, Marcus MA, Zheng W, Pushkar Y (2012). X-Ray fluorescence imaging: a new tool for studying manganese neurotoxicity. *PloS ONE* 7(**11**):e48899. doi: 10.1371/journal.pone.0048899.

Robison G, Zakharova T, Fu S, Jiang W, Fulper R, Barrea R, Zheng W, Pushkar Y (2013). X-ray fluorescence imaging of the hippocampal formation after manganese exposure. *Metallomics* 5:1554-1565.

Rodier J (1955). Manganese poisoning in Moroccan miners. *British Journal of Industrial Medicine* 12:21–35.

Roth JA (2009). Are there common biochemical and molecular mechanisms controlling manganism and parkisonism. *Neuromolecular medicine* 11(**4**):281–296. doi:10.1007/s12017-009-8088-8

Rutchik JS, Zheng W, Jiang YM, Mo XE (2012a). How Does an Occupational Neurologist Assess Welders and Steelworkers for a Manganese-Induced Movement Disorder? An International Team's Experiences in Guangxi, China, Part I. *J Occ Env Med.* 54(**11**):1432-1434.

Rutchik JS, Zheng W, Jiang YM, Mo XE (2012b). How Does an Occupational Neurologist Assess Welders and Steelworkers for a Manganese-Induced Movement Disorder? An International Team's Experiences in Guangxi, China, Part II. *J Occ Env Med.* 54(**12**):1562-1564.

Sarkar S, Schmued L (2011). The Fluoro-Jade Dyes: Novel, Sensitive, and Reliable Fluorochromes for the Histochemical Localization of Degenerating Neurons. In B. Bolon & M. T. Butt (Eds.), *Fundamental Neuropathology for Pathologists and Toxicologists Principles and Techniques* (pp. 171–179). Hoboken, NJ: Wiley & Sons, Inc.

Schmitt C, Strazielle N, Richaud P, Bouron A, Ghersi-Egea JF (2011). Active transport at the blood-CSF barrier contributes to manganese influx in the brain. *J Neurochem* 117:747-756.

Schneider JS, Decamp E, Clark K, Bouquio C, Syversen T, Guilarte TR (2009). Effects of chronic manganese exposure on working memory in non-human primates. *Brain research* 1258:86–95. doi:10.1016/j.brainres.2008.12.035

Schroeder HA, Balassa JJ, Tipton IH (1966). Essential trace metals in man: manganese. A study in homeostasis. *J. Chronic Disease* 19:545-571.

Schwarting RK, Huston JP (1996). Unilateral 6-hydroxydopamine lesions of meso-striatal dopamine neurons and their physiological sequelae. *Progress in Neurobiology* 49(**3**):215-266. PMID:8878304

Seaborn CD, Nielsen FH (2002). Dietary silicon and arginine affect mineral element composition of rat femur and vertebra. *Biol Trace Elem Res* 89:239-250.

Sengupta P (2011). A scientific review of age determination for a laboratory rat: how old is it in comparison with human age? *Biomed Int.* 2:81-89.

Serrat MA, Reno PL, McCollum MA, Meindl RS, Lovejoy CO (2007). Variation in mammalian proximal femoral development: Comparative analysis of two distinct ossification patterns. *J. Anat.* 210:249-258.

Sheng Y, Butler GE, Schumacher M, Cascio D, Cabelli DE, Valentine JS (2012). Six-coordinate manganese (3+) in catalysis by yeast manganese superoxide dismutase. *Proc Natl Acad Sci USA* 109(**36**):14314-9.

Sierra P, Loranger S, Kennedy G, Zayed J (1995). Occupational and environmental exposure of automobile mechanics and nonautomotive workers to airborne manganese arising from the combustion of methylcyclopentadienyl manganese tricarbonyl (MMT). *Am Ind Hyg Assoc J.* 56:713-716.

Sikk K, Haldre S, Aquilonius S-M, Taba P (2011). Manganese-induced Parkinsonism due to ephedrone abuse. *Parkinson's Disease* 20(**6**):915-920.

Smith D, Gwiazda R, Bowler R, Roels H, Park R, Taicher C, Lucchini R (2007). Biomarkers of Mn exposure in humans. *Am J Ind Med*. 50:801-811.

Smith PK, Krohn RI, Hermanson GT, Mallia AK, Gartner FH, Provenzano MD, Fujimoto EK, Goeke NM, Olson BJ, Klenk DC (1985). Measurement of protein using bicinchoninic acid. *Analytical Biochemistry* 150:76-85.

Spangler AH, Spangler JG (2009). Groundwater manganese and infant mortality rate by county in North Carolina: an ecological analysis. *Ecohealth* 6:596-600.

Squitti R, Gorgone G, Panetta V, Lucchini R, Bucossi S, Albini E, Alessio L, Alberici A, Melgari JM, Benussi L, Binetti G, Rossini PM, Draicchio F (2009). Implications of metal exposure and liver function in Parkinsonian patients resident in the vicinities of ferroalloy plants. *J Neural Transm.* 116:1281-1287.

Sriram K, Lin GX, Jefferson AM, Roberts JR, Andrews RN, Kashon ML, Antonini JM (2012). Manganese accumulation in nail clippings as a biomarker of welding fume exposure and neurotoxicity. *Toxicology* 291(**1–3**):73–82.

Stastny D, Vogel RS, Picciano MF (1984). Manganese intake and serum manganese intake of human milk-fed and formula-fed infants. *Am J Clin Nutr.* 39:872-878.

Subramanian KS, Meranger JC (1985). Graphite furnace atomic absorption spectrometry with nitric acid deproteinization for determination of manganese in human plasma. *Science of the Total Environment* 57(**13**):2478-81.

Tapias V, Cannon JR, Greenamyre JT (2014). Pomegranate juic exacerbates oxidative stress and nigrostriatal degeneration in Parkinson's disease. *Neurobiology of Aging* 35(**5**):1162-1176. PMID:24315037

Thompson K, Molina RM, Donaghey T, Schwob JE, Brain JD, Wessling-Resnick M (2007). Olfactory uptake of manganese requires DMT1 and is enhanced by anemia. *The FASEB Journal* 21:223-230.

Tjälve H, Henriksson J, Tallkvist J, Larsson BS, Lindquist NG (1996). Uptake of manganese and cadmium from the nasal mucosa into the CNS via olfactory pathways in rats. *Pharmacology and Toxicology* 79:347-356.

Tøndevold E, Eliasen P (1982). Blood flow rates in canine cortical and cancellous bone measured with 99Tcm-labeled human albumin microspheres. *Acta Orthop. Scand.* 53:7-11.

Tran TT, Chowanadisai W, Crinella FM, Chicz-DeMet A, Lönnerdal B (2002). Effect of high dietary manganese intake of neonatal rats on tissue mineral accumulation, striatal dopamine levels, and neurodevelopmental status. *NeuroToxicology* 23:635-643.

Tuschl K, Mills PB, Clayton PT (2013). Manganese and the brain. *International Review of Neurobiology* 110:277-312.

Vander EL, Colet JM, Muller RN (1997). Spectroscopic and metabolic effects of MnCl2 and MnDPDP on the isolated and perfused rat heart. *Invest Radiol*. 32:581-588.

Vezér T, Kurunczi A, Naray M, Papp A, Nagymajtenyi L. (2007). Behavioral Effects of Subchronic Inorganic Manganese Exposure in Rats. *American Journal of Industrial Medicine* 50:841–852. doi:10.1002/ajim.20485

Viana GF, de Carvalho CF, Nunes LS, Rodrigues JL, Ribeiro NS, de Almeida DA, Ferreira JR, Abreu N, Menezes-Filho JA (2014). Noninvasive biomarkers of manganese exposure and neuropsychological effects in environmentally exposed adults in Brazil. *Toxicol Letters* 231(**2**):169-178.

Vigeh M, Yokoyama K, Ramezanzadeh F, Dahaghin M, Sakai T, Morita Y, Kitamura F, Sato H, Kobayashi Y (2006). Lead and other trace metals in preeclampsia: a case-control study in Tehran, Iran. *Environ Res*. 100:268-275.

Vorhees CV, Graham DL, Amo-Kroohs RM, Braun AA, Grace CE, Schaefer TL, Skelton MR, Erikson KM, Aschner M, Williams MT (2015). Effects of developmental manganese, stress, and the combination of both on monoamines, growth, and corticosterone. *Toxicol Rep*. 1:1046-1061.

Wang DX, Du XQ, Zheng W (2008). Alteration of saliva and serum concentrations of manganese, copper, zinc, cadmium and lead among career welders. *Toxicol Letters* 176:40-47.

Wang X, Li GJ, Zheng W (2006). Upregulation of DMT1 expression in choroidal epithelia of the blood-CSF barrier following manganese exposure in vitro. *Brain Research* 30:1-10.

Wang DX, Zhou WM, Wang SZ, Zheng W (1998). Occupational exposure to manganese in welders and associated neurodegenerative diseases in China. *Toxicol Sci.* 42(suppl):24.

Wang JD, Huang CC, Hwang YH, Chiang JR, Lin JM, Chen JS (1989). Manganese induced parkinsonism: an outbreak due to an un-repaired ventilation control system in a ferromanganese smelter. *Br J Ind Med.* 46:856-859.

Wang Y, Lee JW, Oh G, Grady SR, McIntosh JM, Brunzell DH, Cannon JR, Drenan RM (2013). Enhanced Synthesis and Release of Dopamine in Transgenic Mice with Gain-of-Function α6* nAChRs. *Journal of Neurochemistry* 129(**2**):315-327. doi:10.1111/jnc.12616

Wang L, Ohishi T, Shiraki A, Morita R, Akane H, Ikarashi Y, Mitsumori K, Shibutani M (2012). Developmental exposure to manganese chloride induces sustained aberration of neurogenesis in the hippocampal dentate gyrus of mice. *Toxicol. Sci.* 127(**2**):508–521.

Yazbeck C, Moreau T, Sahuquillo J, Takser L, Huel G (2006). Effect of maternal manganese blood levels on erythrocyte calcium-pump activity in newborns. *Sci Total Environ* 354:28-34.

Yokel RA (2009). Manganese flux across the blood brain barrier. *NeuroMolecular Medicine* 11:297-310.

Yoon H, Kim DS, Lee GH, Kim JY, Kim DH, Kim KW, Chae SW, You WH, Lee YC, Park SJ, Kim HY and Chae HJ (2009). Protective effects of sodium para-amino salicylate on manganese-induced neuronal death: the involvement of reactive oxygen species. *J Pharm Pharmacol* 61:1563-1569.

Zaichick S, Zaichick V, Karandashev VK, Moskvina IR(2011). The effect of age and gender on 59 trace-element contents in human rib bone investigated by inductively coupled plasma mass spectrometry. *Biological Trace Element Research* 143:41-57.

Zaverucha-do-Valle C, Gubert F, Mesentier-Louro L, Scemes E, Pitossi F, Santiago MF, Mendez-Otero R. (2013). Resident Neural Stem Cells. In R. Coeli dos Santos Goldenberg and A.C. Campos de Carvalho (Eds.), *Resident Stem Cells and Regnerative Therapy*. (pp. 69-88). Oxford, United Kingdom: Academic Press.

Zhang LL, Lu L, Pan YJ, Ding CG, Xu DY, Huang CF, Pan XF, Zheng W (2015). Baseline blood levels of manganese, lead, cadmium, copper, and zinc in residents of Beijing suburb. *Environ Res.* 140:10-17.

Zheng, W (2001). Neurotoxicology of the brain barrier system: New implications. *J Toxicol-Clin Toxicol.* 39(**7**):711-719.

Zheng W (2005). Blood-CSF barrier in iron regulation and manganese-induced Parkinsonism. In: The Blood-Cerebrospinal Barrier, Zheng W and Chodobski A, Ed., CRC Press, New York. pp.413-436.

Zheng W, Ren S, Graziano JH (1998). Manganese inhibits mitochondrial aconitase: A mechanism of manganese neurotoxicity. *Brain Res.* 799:334-342.

Zheng W, Fu SX, Dydak U, Cowan DM (2011). Biomarkers of manganese intoxication. *NeuroToxicology* 32(**1**):1-8.

Zheng W, Jiang YM, Zhang YS, Jiang W, Wang X, Cowan DM (2009). Chelation therapy of manganese intoxication by para-aminosalicylic acid (PAS) in Sprague-Dawley rats. *NeuroToxicology* 30:240-248.

Zheng W, Kim H, Zhao Q (2000). Comparative toxicokinetics of manganese chloride and methylcyclopentadienyl manganese tricarbonyl in male Sprague-Dawley rats. *Toxicol Sci.* 54:295-301.

Zheng W, Jiang YM, Zhang YS, Jiang W, Wang X, Cowan DM (2009). Chelation therapy of manganese intoxication by para-aminosalicylic acid (PAS) in Sprague-Dawley rats. *NeuroToxicology* 30:240-248.

Zheng W, Aschner M and Ghersi-Egea JF (2003). Brain barrier systems: a new frontier in metal neurotoxicological research. Invited Review, Toxicol. Appl. Pharmacol. 192:1-11.

Zheng W and Monnot AD (2012).Regulation of brain iron and copper homeostasis by brain barrier systems: Implication in neurodegenerative diseases. *Pharmacol Ther*. 133:177-188.

Zheng W, Zhao Q, Slavkovich V, Aschner M, Graziano JH (1999). Alteration of Iron Homeostasis Following Chronic Exposure to Manganese in Rats. *Brain Research* 833:125-132.

Zhu J, Gale EM, Atanasova I, Rietz TA, Caravan P (2014). Hexameric Mn(II) dendrimer as MRI contrast agent. *Chemistry* 20:14507-14513.

Zoni S, Bonetti G, Lucchini R (2012). Olfactory functions at the intersection between environmental exposure to manganese and Parkinsonism. *J Trace Elem Med Bio.* 26:179-182.

VITA

VITA

Stefanie O'Neal

EDUCATION & TRAINING

Graduate:		**Discipline & Advisor**
2011-	Purdue University, West Lafayette, IN PhD Candidate	Toxicology Wei Zheng, PhD

Undergraduate:

2002-06	Indiana University, Bloomington, IN B.S., Psychology B.A., Biology

PROFESSIONAL AFFILIATIONS

Academy of Surgical Research, *member*
American Association for Laboratory Animal Science, *ALAT certified*
Animal Behavior Management Alliance, *junior member*
Society of Toxicology, *Student Member*

RESEARCH EXPERIENCE

School of Health Sciences, Purdue University Toxicology PhD Program
Graduate Research Assistant to Dr. Wei Zheng May 2012—present

Biomedical Engineering department, Purdue University
Graduate Research Assistant to Dr. Kevin Otto, rotation experience Mar-May 2012

Biology department, Purdue University Oct-Jan 2011
Graduate Research Assistant to Dr. Ignacio Camarillo, rotation experience

Medicinal Chemistry and Molecular Pharmacology department, Purdue University
Graduate Research Assistant to Dr. Eric Barker, rotation experience Aug-Oct 2011

Harlan Laboratories, Inc.
Sr. level surgical technician, group leader 2009-2011
Research technician, study coordinator 2006-2009

Biology department, Indiana University
Undergraduate Research Assistant to Gregory Demas Aug 2005- May 2006

Psychology department, Indiana University & Indianapolis Zoo Aug 2004- May 2006
Undergraduate Research Assistant to Dr. William Timberlake & Dr. Eduardo Fernande

HONORS & AWARDS

Wayne V. Kessler Graduate Student Award	Spring 2015
PULSe Outstanding Graduate Researcher	Spring 2015
Society of Toxicology Graduate Student Travel Award	Fall 2014
Compton Graduate Travel Award	Fall 2014
PULSe Travel Award	Fall 2014
Teaching Academy 2013-2014 Graduate Teaching Award	Spring 2014
Purdue Engagement Grant to fund Next Generation Scholars	Spring 2014
PULSe Travel Award	Fall 2013
Committee for Education of Teaching Assistants (CETA) Teaching Award	Spring 2013
PULSe & Women in Science Program Travel Award	Fall 2012
Certificate of Appreciation for participation in Science in Schools	2011-2012

SEMINARS

1. Intranasal Manganese Exposure Activates Adult Neurogenesis in the Subventricular Zone. Ohio Valley Society of Toxicology, Cincinnati, OH. June 2015.
2. Environmental Causes of Neurodegenerative Parkinsonian Disorder: Manganese Exposure and Mode of Action. PULSe Student Seminar, West Lafayette, IN. April 2015.
3. Half-Life of Manganese (Mn) in Murine Bone Following Oral Exposure, HSCI 69600 seminar, West Lafayette, IN, March, 2014.
4. Establishment of a Rodent Model of Manganese-Induced Parkinsonian Disorder, PULSe Student Seminar, West Lafayette, IN, September, 2013.
5. Polar bear stereotypic and general activity under fixed and variable time schedules, 19th Annual Tri-State Conference on Learning and Behavior, Indianapolis, IN, 2006.

PUBLICATIONS

1. O'Neal SL, Zheng W (2015). Manganese Toxicity Upon Overexposure: A Decade in Review. *Current Environmental Health Reports* 2(**3**):315-328.
2. Fu S, O'Neal SL, Hong L, Jiang W, Zheng W (2015). Elevated Adult Neurogenesis in Brain Subventricular Zone Following In Vivo Manganese Exposure: Roles of Copper and DMT1. *Toxicological Sciences* 143(2):482-498.
3. Hong L, Xu C, O'Neal SL, Bi HC, Huang M, Zheng W, Zeng S (2014). Roles of P-glycoprotein and multidrug resistance protein in transporting para-aminosalicylic acid and its N-acetylated metabolite in mice brain. *Acta Pharmacologica Sinica* 35(**12**): 1577-85.

4. O'Neal SL, Lee JW, Zheng W, Cannon JR (2014). Subchronic manganese exposure in rats is a neurochemical model of early manganese toxicity. *NeuroToxicology* 44:303-313.
5. O'Neal SL, Hong L, Fu S, Jiang W, Jones A, Nie LH, Zheng W(2014). Manganese accumulation in bone following chronic exposure in rats: Steady-state concentration and half-life in bone. *Toxicology Letters* 229:93-100.
6. Mason, A. O., Grieves, T. J., Scotti, M.-A. L., Levine, J., *Frommeyer, S.*, Ketterson, E. D., Demas, G. E., Kriegsfeld, L. J., (2007). Suppression of kisspeptin expression and gonadotropic axis sensitivity following exposure to inhibitory day lengths in female Siberian hamsters. *Hormones and Behavior*, 492-498.

ABSTRACTS & CONFERENCE PROCEEDINGS

1. Zheng W, Fu X, O'Neal SL (2015). Manganese-Copper Interaction: Effects on Adult Neurogenesis and Stem Cell Migration. Toxicologist 144(1):2369. 54th Annual Society of Toxicology conference, San Diego, CA March 22-26, 2015.
2. Jones A, O'Neal SL, Zheng W (2015) Intranasal Mn exposure Leads to a Significant Accumulation of Mn in Bone. Toxicologist 144(1):330. 54th Annual Society of Toxicology conference, San Diego, CA March 22-26, 2015.
3. O'Neal, SL, Fu S, Zheng W. (2015) Activated Adult Neurogenesis in the Subventricular Zone Following Intranasal Manganese Exposure in Rats. Toxicologist 144(1):962. 54th Annual Society of Toxicology conference, San Diego, CA March 22-26, 2015.
4. O'Neal, S.L., Zheng, W. (2014) Absorbance and Distribution Characteristics of Manganese: A Comparison of Three Dose Routes. Ohio Valley Society of Toxicology Meeting 2014 [Health and Human Sciences Fall Research Day, October 29, 2014]
5. O'Neal, S.L., Lee, J., Cannon, J.R., Zheng, W. (2014) Altered Neurotransmitter Levels in Rats Exposed to Manganese: Relevance to Dopaminergic Dysfunction and Neurodegeneration. Toxicologist 138(1):1361. 53rd National Society of Toxicology conference, Phoenix, AZ March 22-27, 2014 [Health and Disease: Science, Culture, and Policy Research Poster Session March 31, 2014 West Lafayette, IN]
6. Zheng W, O'Neal SL, Hong L, and Jones AJ (2014). Half-life of manganese (Mn) in murine bone following oral exposure. Toxicologist 138(1):1362. 53rd Annual Society of Toxicology conference, Phoenix, AZ March 22-27, 2014
7. O'Neal, S.L., Cannon, J.R., Zheng, W. (Sep/Oct 2013) Altered Neurotransmitter Levels in Rats Subchronically Exposed to Manganese: Relevance to Dopaminergic Dysfunction and Neurodegeneration. Poster presented at Ohio Valley Society of Toxicology Regional Meeting in Louisville, KY on September 23, 2013. [Indianapolis Society for Neuroscience October 18, 2013]
8. Zheng W, Hong L, O'Neal S, and Jiang W (2013). Bone as the storage site of manganese (Mn) exposure: Relationship to Mn levels in brain. J Trace Elem Med Biol 27S1: 24. 10th International Society of Trace Elements Research in Humans conference, Tokyo, Nov 18-22, 2013

9. Hong L, O'Neal SL, Nie L, Zheng W (2013). Bone manganese (Mn) concentrations in Sprague-Dawley rats following subchronic manganese
10. exposure. Toxicologist 132(1):1864. 52nd National Society of Toxicology conference, San Antonio, TX March 10-14, 2013.
11. O'Neal, S.L., Hong L, Zheng W. (Feb/April 2013) Accumulation of Manganese (Mn) in Rat Brain Ventricular Region Following In Vivo Subchronic Mn Exposure: Effect on Copper (Cu) Status. Toxicologist 132(1): 1520. 52nd National Society of Toxicology conference, San Antonio, TX March 10-14, 2013. [WISP, February 20, 2013] [Purdue Interdisciplinary Graduate Program Spring Reception April 1, 2013].
12. Hong L, O'Neal S, Nie L, and Zheng W (2013). Bone manganese (Mn) concentrations in Sprague–Dawley rats following subchronic manganese exposure. Toxicologist 132(1):1864.
13. O'Neal, S.L., Hong L., Zheng W. (2012) Manganese is Sequestered in Rat Bone. Poster presented at PULSe First Year Student Poster Session.

14. O'Neal, S. (2010). HydroGel is an Adequate Source of Hydration for Surgically Modified Rat Models. Poster presented at the Academy of Surgical Research Conference in Clearwater Beach, FL.

LEADERSHIP EXPERIENCE

Purdue University Graduate Student Government

Academic and Professional Development Committee—Chair	2012-2013
Academic and Professional Development Committee—Recorder	2011-2012

Department of Health Sciences Graduate Student Government

Vice President	2012-2013
Treasurer	2013-2014
President	2014-2015

TEACHING EXPERIENCE

Responsibilities include attending classes, taking attendance, preparing lecture materials, holding office hours, holding weekly review sessions, proctoring exams, grading assignments, reports and exams, individual tutoring and calculating course grades.

Teaching Assistant to Lisa Hilliard,
Medical Terminology HSCI 13100
Introduction to Medical Laboratory Sciences HSCI 13000
Immunology for Medical Laboratory Sciences HSCI 33300

Teaching Assistant to Dr. Wei Zheng,
Toxicology HSCI 56000

Teaching Assistant to Dr. Frank Rosenthal,
Introduction to the Health Science Professions HSCI 10100

Industrial Hygiene Engineering Control HSCI 34600
Principles of Public Health Science HSCI 20100
Teaching Assistant to Dr. Neil Zimmerman,
Applied Industrial Hygiene HSCI 44600
Introduction to Environmental and Occupational Health Sciences HSCI 34500

Teaching Assistant to Dr. Craig E. Nelson,
Freshman Intensive Seminars, Indiana University

MENTORING EXPERIENCE

Supervising Honors Undergraduate Researchers in the School of Health Sciences
Alexander Jones: Pharmacokinetics of manganese exposure in bone
Vivien Lai: Aberrant migration of neural stem cells after manganese exposure
Erin Kay: Effects of manganese exposure in adult subgranular zone of the dentate gyrus

PROFESSIONAL SERVICE

Reviewer for Professional Journals
NeuroToxicology, Chemical Research in Toxicology, Biological Trace Element Research

Society of Toxicology
Metals Specialty Section- Elected Graduate Student Representative
Rapid Response Task Force- Appointed Graduate Student Representative
Graduate Student Leadership Council- Communications subcommittee member

CONFERENCES ATTENDED

Ohio Valley Society of Toxicology Student Meeting—Cincinnati, OH	2015
Society of Toxicology 54rd Annual Meeting—San Diego, CA	2015
Ohio Valley Society of Toxicology Annual Meeting—Dayton, OH	2014
Ohio Valley Society of Toxicology Student Meeting—Louisville, KY	2014
Society of Toxicology 53rd Annual Meeting—Phoenix, AZ	2014
Alzheimer's Disease Research Symposium—Indianapolis, IN	2013
Society for Neuroscience Regional Meeting—Indianapolis, IN	2013
Ohio Valley Society of Toxicology Regional Meeting—Louisville, KY	2013
Ohio Valley Society of Toxicology Student Meeting—Cincinnati, OH	2013
Society of Toxicology 52nd Annual Meeting—San Antonio, TX	2013
Parkinson's Disease Research Symposium—Indianapolis, IN	2012
Academy of Surgical Research—Clearwater Beach, FL	2010
American Association for Laboratory Animal Science—Indianapolis, IN	2008
Animal Behavior Management Alliance—Houston, TX	2005

PUBLICATIONS

PUBLICATIONS

1. O'Neal SL, Zheng W (2015). Manganese Toxicity Upon Overexposure: A Decade in Review. *Current Environmental Health Reports* 2(**3**):315-328.

2. Fu S, O'Neal SL, Hong L, Jiang W, Zheng W (2015). Elevated Adult Neurogenesis in Brain Subventricular Zone Following In Vivo Manganese Exposure: Roles of Copper and DMT1. *Toxicological Sciences* 143(**2**):482-498.

3. Hong L, Xu C, O'Neal SL, Bi HC, Huang M, Zheng W, Zeng S (2014). Roles of P-glycoprotein and multidrug resistance protein in transporting para-aminosalicylic acid and its N-acetylated metabolite in mice brain. *Acta Pharmacologica Sinica* 35(**12**): 1577-85.

4. O'Neal SL, Lee JW, Zheng W, Cannon JR (2014). Subchronic manganese exposure in rats is a neurochemical model of early manganese toxicity. *NeuroToxicology* 44:303-313.

5. O'Neal SL, Hong L, Fu S, Jiang W, Jones A, Nie LH, Zheng W(2014). Manganese accumulation in bone following chronic exposure in rats: Steady-state concentration and half-life in bone. *Toxicology Letters* 229:93-100.

6. Mason AO, Grieves TJ, Scotti M-A, Levine J, *Frommeyer S*, Ketterson ED, Demas GE, Kriegsfeld LJ (2007). Suppression of kisspeptin expression and gonadotropic axis sensitivity following exposure to inhibitory day lengths in female Siberian hamsters. *Hormones and Behavior* 492-498.